

Quantum complexity in gravity, quantum field theory, and quantum information science

Stefano Baiguera^{a,b}, Vijay Balasubramanian^{c,d,e,f}, Pawel Caputa^{g,h,i}, Shira Chapman^j, Jonas Haferkamp^k, Michal P. Heller^l, Nicole Yunger Halpern^{m,n}

^a*INFN Sezione di Perugia, Via A. Pascoli, 06123 Perugia, Italy*

^b*Dipartimento di Matematica e Fisica, UCSC, Via della Garzetta 48, 25133 Brescia, Italy*

^c*David Rittenhouse Laboratory, University of Pennsylvania, 209 S. 33rd Street, Philadelphia, PA 19104, USA*

^d*Santa Fe Institute, 1399 Hyde Park Road, Santa Fe, NM 87501, USA*

^e*Theoretische Natuurkunde, Vrije Universiteit Brussel, Pleinlaan 2, B-1050 Brussels, Belgium*

^f*Rudolf Peierls Centre for Theoretical Physics, University of Oxford, Oxford OX1 3PU, UK*

^g*The Oscar Klein Centre and Department of Physics, Stockholm University, AlbaNova, 106 91 Stockholm, Sweden*

^h*Yukawa Institute for Theoretical Physics, Kyoto University, Kitashirakawa Oiwakecho, Sakyo-ku, Kyoto 606-8502, Japan*

ⁱ*Faculty of Physics, University of Warsaw, Pasteura 5, 02-093 Warsaw, Poland*

^j*Department of Physics, Ben-Gurion University of the Negev, Beer-Sheva 84105, Israel*

^k*School of Engineering and Applied Sciences, Harvard University, Cambridge, MA 02318, USA*

^l*Department of Physics and Astronomy, Ghent University, 9000 Gent, Belgium*

^m*Joint Center for Quantum Information and Computer Science, NIST/University of Maryland, College Park, Maryland 20742, USA*

ⁿ*Institute for Physical Science and Technology, University of Maryland, College Park, MD 20742, USA*

Abstract

Quantum complexity quantifies the difficulty of preparing a state, or implementing a unitary, using limited resources. Over the past decade, quantum-complexity research has surged. Applications range from quantum computation to condensed matter and quantum gravity. Different communities apply different tools to quantum complexity, as well as define complexity differently. This review bridges the disciplines' approaches. We cover multiple definitions of complexity, as well as their key properties and applications. In quantum information, random quantum circuits proved to be an invaluable tool in extracting properties of the complexity growth of discrete quantum circuits. In quantum many-body systems and quantum field theory (QFT), complexity is defined geometrically through geodesics. Complexity can be defined also in terms of state or operator spreading and tensor-network concepts. In addition to reviewing these approaches, we outline applications to simple quantum systems, quantum many-body models and QFTs, including conformal field theories (CFTs). Finally, we detail the relationship between complexity and gravitational observables within the anti-de Sitter-space (AdS)/CFT correspondence. This review thereby integrates recent quantum-complexity advances across fields.

Email addresses: stefano.baiguera@pg.infn.it (Stefano Baiguera), vijay@physics.upenn.edu (Vijay Balasubramanian), pawel.caputa@fysik.su.se (Pawel Caputa), schapman@bgu.ac.il (Shira Chapman), jhaferkamp@seas.harvard.edu (Jonas Haferkamp), michal.p.heller@ugent.be (Michal P. Heller), nicoleyh@umd.edu (Nicole Yunger Halpern)

Contents

1	Preface	3
2	Key notions	5
3	Dialogue	8
4	Definition and time evolution of quantum complexity	12
4.1	Time evolution of complexity, according to counting arguments about quantum circuits	12
4.2	Complexity saturation as a late-time stage of quantum many-body equilibration . . .	16
4.3	Growth of complexity under random circuits	18
4.4	Linear growth of exact circuit complexity	19
4.5	Linear growth of approximate circuit complexity	20
4.6	Barriers to proving that quantum complexity grows superpolynomially under long-time evolutions	22
5	Paradigms for complexity I: Nielsen complexity	24
5.1	Definition of Nielsen complexity	25
5.2	Geometric features of Nielsen complexity	26
5.3	Constraints on the cost function from expected time dynamics	28
5.4	Relation between Nielsen complexity and entanglement: binding complexity	29
5.5	Complexity in quantum field theories	31
6	Paradigms for complexity II: Krylov and spread complexities	39
6.1	Spread complexity of evolving states	39
6.2	Krylov complexity of evolving operators	45
6.3	Applications	47
6.4	Open problems and directions	55
7	Quantum complexity and space-time: a more concerted approach	58
7.1	Holographic complexity proposals	59
7.2	Time-dependent properties of the holographic proposals	61
7.3	Time-independent properties of the holographic proposals	64
7.4	Generalizations of the holographic proposals	65
7.5	Quantitative matches between the boundary complexity and the bulk observables .	69
7.6	Computational pseudorandomness and the holographic dictionary	74
8	Paradigms for complexity III: tensor-network-inspired definitions of complexity	76
8.1	Complexity from path-integral optimization	76
8.2	Holographic path-integral optimization	79
9	Quantum complexity in quantum information theory and many-body physics	81
9.1	Operationalism and resource theory	81
9.2	Circuit complexity and topological order	83
9.3	Bounding complexity growth with entanglement	84

9.4 Bounding complexity via concentration	85
10 Epilogue	87
Appendix A Guide to acronyms	90

1. Preface

This review’s main goal is to facilitate new, and consolidate existing, bridges between communities whose members study quantum complexity. The communities use different conceptual approaches, mathematical tools, and levels of rigor. Other reviews cover some of the topics discussed below [1–3]. However, we offer two novel perspectives. First, our diverse backgrounds enable us to cover extensive ground at the intersection of gravity, quantum information theory, quantum field theory (QFT), and quantum many-body systems. Second, this review reflects the state of the art in this fast-moving field in early 2025.

We begin with a historical overview. Quantum complexity originated in the field of quantum computation. The concept served as a mathematical tool in the optimization of unitary transformations’ implementations. This optimization has concerned users of early quantum computers, which have limited resources. Since 2009, *tensor networks* have bridged quantum computation to holographic studies [4]. Tensor networks are graphical structures, similar to quantum circuits, that can efficiently represent certain quantum states classically. Holography is a duality between gravitational physics in a bulk geometry and a quantum system on the geometry’s boundary. Tensor networks helped establish quantum complexity’s relevance to gravitational physics. Via the holographic correspondence, quantum-complexity studies expanded into QFT and the Sachdev-Ye-Kitaev (SYK) model. In parallel, researchers developed complexity-related quantities for characterizing operator growth (how operators evolve in the Heisenberg picture) under many-body quantum chaos. Finally, starting in 2021, physicists have proven several conjectured properties of complexity measures, enabling a more precise formulation of the holographic correspondence.

Figure 1 depicts the review’s structure. A reader might traverse it via any of (at least) four paths, indicated by arrows in the figure. A common thread unites each path’s components. All paths begin in Sec. 2, a glossary for key concepts. A reader may study this section more or less thoroughly, depending on their background, and return to the section later as necessary. Let us now outline the paths consecutively.

We start with the leftmost arrow in Fig. 1. It points to Section 3, a dialogue inspired by Galilei’s famous discourse on cosmology. Our dialogue resembles a discussion at a conference: not all terms are sharply defined, and different speakers present different perspectives. Later sections provide greater rigor and more detail. The dialogue terminates the first, briefest path through the review.

The second path focuses on quantum-information-theoretic features of quantum complexity (see the second-leftmost sequence of arrows in Fig. 1). This path includes the definition of circuit complexity in Sec. 4. Section 9 presents applications of complexity to quantum information theory and many-body physics.

The third path’s protagonist is the evolution of complexity under Hamiltonian dynamics (see the second-rightmost sequence of arrows in Fig. 1). Section 4 describes how complexity grows under Hamiltonian evolution, using counting arguments, and under random circuits. The complexity’s time evolution inspired the definitions of geometrical observables in gravitational physics, as

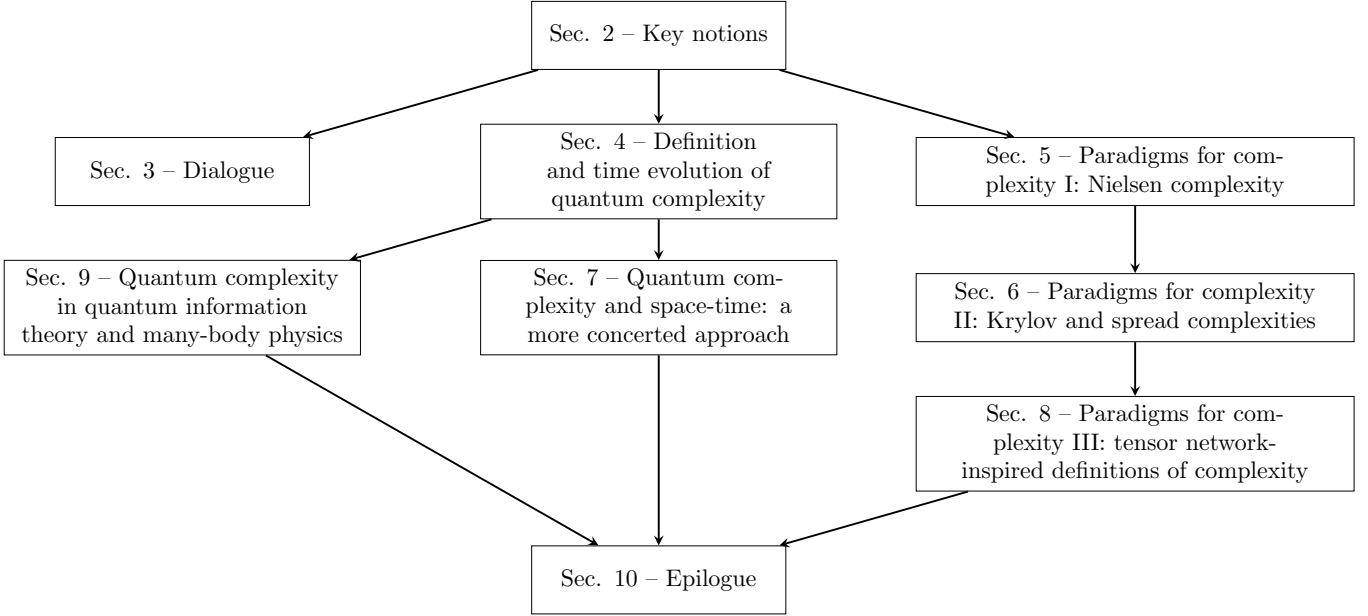


Figure 1: Structure of the review.

discussed in Sec. 7.

The right-hand side of Fig. 1 illustrates the fourth path through the review. It focuses on quantum-complexity definitions suited to continuous-time evolution. Sections 5, 6 and 8 introduce Nielsen’s complexity, the Krylov complexity, and complexity quantities inspired by tensor networks. All these measures elucidate thermalization, chaos, quantum-circuit optimization, and more.

Apart from the first path, all paths end in Sec. 10. There, we summarize the main results and open problems. Like Sec. 3, Sec. 10 contains a dialogue, for accessibility and the reader’s amusement. Appendix A contains a guide to the acronyms in this paper.

Some paths intersect at certain topics. For example, the *holographic duality* proposes that each quantum-complexity measure has an analogue in a gravitational system: a geometric observable. This intertwining surfaces in Sections 5–8.

2. Key notions

This review covers developments across disciplines, from high-energy physics and gravity through many-body physics to quantum information science. These disciplines feature different vocabularies. Here, we survey key notions from across the disciplines, to assist readers from all backgrounds with our multifaceted material.

1. **AdS/CFT correspondence:** A duality between (i) gravity in asymptotically anti-de Sitter (AdS) spacetime and (ii) a conformal field theory (CFT), typically a gauge theory, on the spacetime's timelike boundary.
2. **Black hole:** A region of spacetime where gravity is so strong that no matter or light can escape. Mathematically, a black hole is represented by a solution to Einstein's equations (or to another gravitational theory's equations of motion). A black hole contains a singularity, where certain scalar functions of the curvature diverge.
3. **Duality:** An equivalence between two seemingly distinct descriptions of the same physics. The two descriptions related by a duality are often called *sides*.
4. **Entanglement:** A nonlocal relationship achievable between quantum particles. The relationship can lead to correlations (between outcomes of measurements of the particles) stronger than any achievable classically. An entangled state stores information inaccessible via local measurements. The *entanglement entropy*, among other measures, quantifies the entanglement between two systems.
5. **Event horizon:** A null hypersurface beyond which no matter or light can escape.
6. **Fast scrambler:** A quantum system that quickly distributes quantum information across all of its degrees of freedom. Generic out-of-time-ordered correlators (OTOCs, see the corresponding key notion) of a fast scrambler decay exponentially quickly, with the greatest possible exponent, during a certain time frame. Let N denote the number of degrees of freedom; and t , time. A generic (possibly regularized) OTOC of a fast scrambler scales as

$$\text{OTOC}(t) \sim (\text{const.}) - \frac{(\text{const.})}{N} e^{\lambda_{\text{OTOC}} t} + \mathcal{O}(N^{-2}). \quad (1)$$

The Lyapunov-like exponent λ_{OTOC} is well-defined only in a semiclassical regime, where one can expand the OTOC in a small parameter (\hbar or $1/N$, for instance). At the *scrambling time* $t_* \sim \lambda_{\text{OTOC}}^{-1} \log(N)$, the first two terms in (1) equal each other: information about a local perturbation [W in Eq. (3)] has scrambled throughout the system; $W(t)$ and V have an order-1 commutator. A system's scrambling time is as low as possible if the Lyapunov-like exponent is as large as possible: $\lambda_{\text{OTOC}} = 2\pi/\beta$ [5]. Systems that achieve this condition are called fast scramblers. Black holes and the large- N SYK model are believed to be examples.

7. **Holography:** A duality stating that gravitational physics in a bulk region is equivalent to a quantum theory on the region's boundary. Often, a holographer aims to identify a map between a bulk quantity and a boundary quantity. Identifying such a map, one *matches* the two quantities.
8. **Jackiw-Teitelboim (JT) gravity:** A two-dimensional gravitational theory with a coupling to a dilaton (a real scalar field Φ) [6]. Let G_N denote Newton's constant; \mathcal{M} , a d -dimensional smooth manifold; g , the metric's determinant; R , the Ricci scalar; L , the AdS radius; K , the

extrinsic curvature of the induced metric on the manifold’s boundary, $\partial\mathcal{M}$; and h , the determinant of that induced metric. The JT-gravity action, excluding topological contributions, has the form

$$S_{\text{JT}}[g, \Phi] := \frac{1}{16\pi G_{\text{N}}} \int_{\mathcal{M}} d^d x \sqrt{-g} \Phi \left(R + \frac{2}{L^2} \right) + \frac{1}{8\pi G_{\text{N}}} \int_{\partial\mathcal{M}} d^{d-1} x \sqrt{-h} \Phi \left(K - \frac{1}{L} \right). \quad (2)$$

The AdS/CFT duality interrelates (i) JT gravity in asymptotically AdS spacetime and (ii) the SYK model’s low-energy regime.

9. **Kolmogorov complexity:** The length of the shortest computer program that produces a given output.
10. **Out-of-time-order correlator (OTOC):** A correlation function intended to measure the spread of many-body entanglement across, and to signal chaos of, quantum systems. Let S denote a quantum many-body system. Let W and V denote local operators that are unitary or Hermitian, depending on the context, and that act on far-apart subsystems of S . $W(t)$ follows from evolving W , in the Heisenberg picture, under the system’s dynamics. Let ρ denote a state of S . The OTOC has the form [5]¹

$$F(t) = \text{Tr} \left(W^\dagger(t) V^\dagger W(t) V \rho \right). \quad (3)$$

The OTOC quantifies the failure of $W(t)$ to commute with V . Relatedly, the OTOC quantifies how much a local perturbation V affects a far-away operator W later. Often, when referring to an OTOC, a text actually refers implicitly to the OTOC’s real part.

11. **Quantum chaos:** The definition of quantum chaos is a subject of debate. According to an early definition, a quantum-chaotic system has a semiclassical limit that is classically chaotic. Since then, quantum chaos has been defined in terms of nonintegrability, energy-level statistics, out-of-time-ordered correlators, and spectral form factors [7–9].
12. **Quantum circuit:** A sequence of quantum gates. In a conventional circuit diagram, time runs from left to right. Time is discretized into slices, or *layers*. Multiple gates can act during each layer (if they commute with each other and if, at most, one gate acts on each qubit). The number of layers is the circuit’s *depth*.
13. **Quantum complexity:** The least number of quantum logic gates, selected from a chosen set, in any circuit that (i) implements a target unitary or (ii) prepares a target state from a simple initial state. High-energy theorists sometimes call quantum complexity *quantum computational complexity*, which can have a different meaning in computer science. In sections that provide explicit analytic bounds, we will emphasize the difference between the exact circuit complexity $\mathcal{C}_0(U)$ of a unitary U , measuring the minimal number of gates to effect U exactly, and the approximate circuit complexity $\mathcal{C}_\delta(U)$, the minimal number of gates to approximate U up to an error of δ . When this distinction is not central to the material presented, we drop the subscript.
14. **Quantum gate:** An elementary unitary operation that acts on a quantum system, usually a

¹The OTOC often diverges in QFT. One therefore *regularizes* the OTOC: one removes the ρ from the trace’s argument. Instead, most commonly, one places a $\rho^{1/4}$ after each remaining factor. Alternative regularization prescriptions differ in the power of ρ and in the operators’ ordering.

set of qubits. A k -local quantum gate acts on just k qubits. Example 1-qubit gates include the Hadamard gates; and example 2-qubit gates include the controlled-NOT, or CNOT, gate [10].

15. **Random state:** A quantum state selected from a Hilbert space, typically according to the *Haar measure*, the unique unitarily invariant measure. One can think of a (Haar-)random state as “uniformly randomly” selected.
16. **Sachdev-Ye-Kitaev (SYK) model:** An exactly solvable model of N Majorana fermions ψ_i , where $i \in \{1, \dots, N\}$. Let $J_{i_1 i_2 \dots i_q}$ denote the strength of a random coupling among an even number q of fermions. The SYK Hamiltonian has the form

$$H_{\text{SYK}} := i^{q/2} \sum_{1 \leq i_1 < i_2 < \dots < i_q \leq N} J_{i_1 i_2 \dots i_q} \psi_{i_1} \psi_{i_2} \dots \psi_{i_q}. \quad (4)$$

The SYK model admits simplifications when taking $N \rightarrow \infty$ and $q \rightarrow \infty$ keeping the ratio $\lambda_{\text{SYK}} = 2q^2/N$ fixed, which is often referred to as double scaled SYK (DSSYK).

17. **Tensor networks:** A tensor network is a graphical representation of a quantum state [11]. The network consists of basic units, called *tensors*, that are multilinear maps. A tensor’s inputs and outputs, labeled by indices, represent quantum degrees of freedom. To evaluate a tensor network, one *contracts* the tensors, summing over indices. Tensor networks are useful, e.g., in variational studies of ground states. Also, using tensor networks, one can bound entanglement entropies in a simple, graphical manner.

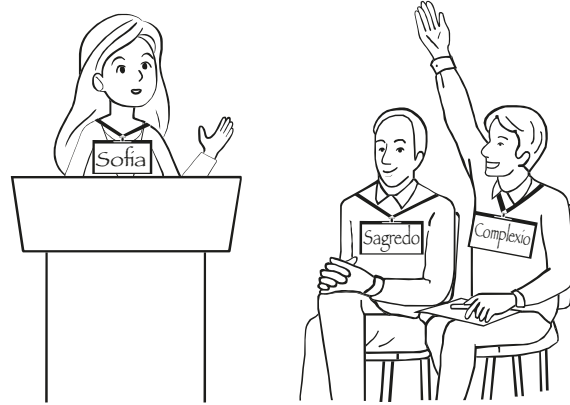
An important type of tensor network is the *multiscale entanglement renormalization ansatz* (MERA) [12]. MERA efficiently approximates scale-invariant quantum systems’ ground states. A continuous version (cMERA) has been proposed to approximate free CFTs’ ground states well [13].

18. **Thermofield-double state:** Consider a quantum system governed by a Hamiltonian H with eigenvalues E_n and eigenstates $|n\rangle$. Denote by Z_β the partition function at an inverse temperature β . Two copies of the system can jointly be in the thermofield-double state

$$|\text{TFD}\rangle := \frac{1}{\sqrt{Z_\beta}} \sum_n e^{-\frac{\beta E_n}{2}} |n\rangle |n\rangle. \quad (5)$$

Each copy is in a finite-temperature canonical (thermal) reduced state.

19. **Universal gate set:** A set of quantum gates such that, using gates drawn from the set, one can approximately effect every unitary operator arbitrarily precisely.



3. Dialogue

To the discerning reader

The dialogue below is inspired by Galilei’s *Dialogue Concerning the Two Chief World Systems* and is similar to discussions one hears during conferences. We imagine a conversation among three participants: *Sofia* represents our view of complexity. *Complexio* acts as an interested audience member aiming to clarify the literature, albeit sometimes with technical questions. *Sagredo* mediates between the others.

Sagredo: Finally, we resolved to meet today to clarify the past decade’s central developments in complexity.

Complexio: Sofia, can you clarify the definition of quantum complexity?

Sofia: Quantum complexity is defined in terms of a gate set and a reference state. You can think of the set as containing the gates implementable by some experimentalist. The reference state should be simple, or computationally easy to prepare. Common reference states include tensor products, especially a product of $|0\rangle$ s. A state’s quantum complexity is the least number of gates, drawn from that set, in any circuit that prepares the state from the reference.

Complexio: I have heard computer scientists invoke *computational complexity* when discussing a classical or quantum algorithm. Is computer scientists’ computational complexity the same as quantum complexity—which I believe is also called *quantum computational complexity*, confusingly?

Sofia: The two concepts are easily conflated. Let us use just the term *quantum complexity*, rather than *quantum computational complexity*, to avoid confusion with computer scientists’ terminology. Computational complexity is a concept applied in both classical and quantum computer science. It is the number of steps in an algorithm. In contrast, quantum complexity is the least number of steps in *any* algorithm that prepares a target state or implements a target unitary.

Complexio: Why should I care about quantum complexity?

Sofia: Complexity has diverse applications. One can use it to characterize quantum systems’ dynamics and thermalization, solve optimization problems, capture chaotic properties, describe quantum information scrambling. . . Shall I continue?

Sagredo: These applications sound interesting, but complexity seems intangible. In most cases, it is difficult or impossible to compute.

Sofia: Fair objection. Nevertheless, heuristic arguments reveal how a state’s quantum complexity changes under generic state evolution. Also, bounding complexity is easier than calculating it, and bounds suffice for many purposes.

Sagredo: Sofia, even finding bounds—other than the simple bounds known already—seems nontrivial. How can we make progress?

Sofia: At least two approaches can improve current bounds on complexity. One approach centers on random unitary circuits, which form a toy model for chaotic dynamics. Invoking random unitary circuits, we can apply differential topology and algebraic geometry to manifolds formed by unitaries. Also, when considering random unitary circuits, we can apply unitary designs—probability distributions that cannot be distinguished from the Haar measure in polynomial time.

The second approach centers on Nielsen’s notion of complexity. Suppose we want to perform some unitary on n qubits. Each of many circuits implements that unitary. The unitary group $SU(2^n)$, equipped with a continuous norm, forms a differential manifold. Nielsen casts the optimal circuit as a path on the manifold. The geodesic’s length bounds the unitary’s quantum complexity [10, 14]. This bound is often imprecise, but it may be useful.

Sagredo: I have heard of other notions of complexity, such as Kolmogorov complexity. Can you define them?

Sofia: Certainly! Kolmogorov complexity is the length of the shortest computer program that produces a target output [15]. Another notion, Krylov complexity, quantifies operator growth—an operator’s spreading, under evolution in the Heisenberg picture, across the space of operators [16]. Similarly, spread complexity quantifies a state’s expansion across the state space under evolution [17].

Complexio: Does Krylov or spread complexity offer any advantage over the other notions of complexity?

Sofia: Both have interesting physical applications and are relatively simple to calculate. Reference [16] introduced Krylov complexity to distinguish chaotic from integrable dynamics of finite-size quantum many-body systems that lack semiclassical limits. Spread complexity relates to spectral form factors, which characterize many-body quantum-systems’ energy spectra [17]. Moreover, to calculate the Krylov or spread complexity, one must diagonalize (or tridiagonalize) only the Hamiltonian’s projection onto a small subspace. Therefore, one can calculate these complexities relatively easily.

Complexio: Interesting story. However, quantum complexity still seems... complex. Complicated. I wish there were a simple way to understand and apply it.

Sagredo: I have heard that the holography duality is an equivalence between gravitational physics in a bulk geometry and a quantum theory defined on its boundary. Holographic duals usually simplify difficult quantum problems. Does quantum complexity have a holographic interpretation?

Sofia: We hope so! Quantum complexity has been proposed to have an Einstein-Rosen bridge’s (ERB’s) volume as a holographic dual. An ERB is a spacetime region that connects a maximally extended Schwarzschild black hole’s two boundaries. In the holographic context, the black hole lives in AdS spacetime and is dual to the thermofield-double state of a CFT on the spacetime’s boundary. The ERB’s volume was proposed to be a holographic dual to the boundary state’s quantum complexity [18, 19]. More-complicated geometric quantities were conjectured to be dual to quantum complexity, too [20–24].

Complexio: Why should I expect the volume to be related to the boundary state’s complexity? Does any evidence support the conjecture?

Sofia: Yes. The geometric quantities behave similarly to the complexity of a quantum state evolving under random dynamics. One important behavior is linear growth until late times, achievable by geometric quantities in a semiclassical gravitational setting. Another behavior is the switchback effect, in which a perturbation delays growth.

More evidence emerges from a class of two-dimensional bulk models. There, a notion of wormhole length was formulated nonperturbatively. This length saturates at times exponentially long in the black hole’s entropy [25]. This behavior mirrors the saturation of complexity, under random dynamics, at times exponentially long in the system size. Moreover, in [26, 27], the authors show that a state’s spread complexity parallels a wormhole’s volume, at least in a two-dimensional gravitational setting.

Complexio: Are you sure that we are invoking the correct type of complexity? How do you know if we should use Nielsen, Krylov, or another complexity?

Sofia: The map I just mentioned—between a wormhole’s volume and spread complexity—hints that spread complexity is appropriate. Yet Refs. [28–34] point to other notions of complexity. We are not yet certain.

Complexio: The community sounds awfully uncertain about complexity in holographic contexts. Why bother working on the topic?

Sofia: First, the gravitational and quantum settings would merit analysis even in the absence of any duality. We want to understand black holes’ interiors and to optimize quantum circuits. Complexity has facilitated these goals. Second, we do hope to replace the many conjectures with a smaller number of theorems.

Complexio: The community seems to me to be far from theorems. To support a bulk-boundary map for Nielsen’s complexity, people constructed toy examples involving free QFTs. Yet free QFTs are not known to be dual to any gravitational systems. Rather, certain strongly coupled QFTs are. So how can the toy examples support the map?

Sofia: We expect some qualitative properties of QFTs not to depend on the QFT’s coupling strength. An example is the structure of the UV divergence of a QFT state’s complexity.² The UV divergence of the entanglement entropy offers another example.

Sagredo: Indeed, entanglement entropy provides a striking example of a holographic mapping that passed non-trivial consistency checks. The dual to a boundary QFT state’s entanglement entropy is the area of a minimal surface in the geometry dual to that state. The dual objects have been identified clearly in this example for various states.

Complexio: In contrast, according to the “complexity=anything” prescription, complexity parallels each of infinitely many gravitational quantities [23, 24, 35]. Every such quantity exhibits linear growth and the switchback effect. I can pick any conjecture I like, and all of them define a geometrical dual to quantum complexity. Does this multiplicity make sense? Is the cornucopia of holographic conjectures useful?

Sofia: The multiplicity does offer an upshot. As we discussed, quantum state complexity depends on a gate set and a reference state. We are free to choose each. This freedom mirrors the ambiguity in the complexity’s gravitational dual.

Still, I understand Complexio’s concern: some symmetries or other properties could restrict the

²The complexity contains multiple terms, which scale differently with the UV cutoff. Therefore, some people call “the structure of the UV divergence” “the UV divergences.”

gravitational dual to one geometric object, and we could be blind to those properties. One might overcome such blindness, or confirm a lack thereof, as follows. First, show that the complexity has exactly as many degrees of freedom as the gravitational analogue. Building on this result, identify a precise map between the complexity's degrees of freedom and the gravitational analogues. Alternatively, one could use bulk symplectic forms to relate boundary quantities to circuit complexity [36].

Complexio: Most of the holographic-complexity studies we just discussed were performed in the context of the AdS/CFT correspondence. Why have recent complexity trends focused on de Sitter spacetime? I thought that de Sitter spacetime's holographic properties were less understood than AdS spacetime's.

Sofia: You are right; de Sitter holography is poorly understood. Nevertheless, it holds promise for understanding quantum gravity in expanding universes similar to ours. After all, we do not live in AdS spacetime. If a holographic complexity conjecture for de Sitter spacetime is correct, it could elucidate the spacetime's quantum dual.

Complexio: You mentioned earlier that the definition of quantum state complexity has ambiguities, depending on a gate set and a reference state. Does any guiding principle direct these choices?

Sofia: Yes: certain operations may be easier to implement, and certain states may be easier to prepare, than others in experiments. I can illustrate with two examples. First, a superconducting qubit's native Hamiltonian is conventionally set proportional to σ_z . Consequently, adding a σ_z to the native Hamiltonian costs more control resources than adding a σ_x or a σ_y [37]. We should penalize difficult-to-implement generators. Distributed computing offers a second example of difficult operations: imagine performing a computation using multiple small quantum computers. The information processing remains highly coherent if one computer performs most of the computations. Any nonlocal operator, which acts on multiple nodes, deserves a large complexity penalty.

Complexio: Interesting. I am excited to read whether we can simulate gravitational physics on a tabletop, using a quantum computer.

Sagredo: And let this be the final conclusion of our long discussion. Above all, I shall impatiently read this review, to learn more about recent developments in complexity.

4. Definition and time evolution of quantum complexity

A quantum circuit consists of gates. A gate is an elementary unitary operation that acts simultaneously on some (typically small) number of qubits (or other qudits— d -level quantum systems). One can implement every n -qubit unitary arbitrarily precisely, by selecting gates from a universal set [10]. *Quantum complexity* is heuristically defined as the minimum number of gates needed to perform a certain task. Examples include mapping an initial state to a final one. Experimentally implementing a gate costs a finite amount of time. Therefore, some quantum-complexity measures reflect the duration of the optimal algorithm for performing a task.

In this section, we present the characteristic features of the quantum complexity’s time evolution under a chaotic Hamiltonian. They can be summarized as follows:

- Complexity grows linearly for a time exponential in the system’s size. It saturates at an approximately constant value until a doubly exponential time. After that, Poincaré recurrences return the complexity to near-minimal values.
- The complexity exhibits a switchback effect: a small perturbation delays its linear growth by a scrambling time.

One can predict the linear growth and switchback effect from simple counting arguments in a circuit model, Sec. 4.1 shows. Section 4.2 discusses the complexity’s saturation in the context of quantum many-body equilibration. In Sec. 4.3, we introduce *random* circuits as simple models for chaotic dynamics. In addition, random quantum circuits mimic the properties of the Haar measure with increasing depth. This phenomenon can be exploited to make many of the heuristic arguments about the growth of complexity rigorous for random quantum circuits. In Sec. 4.4 and Sec. 4.5 we present two recent rigorous arguments that prove a linear growth of quantum complexity for an exponentially long time. In Sec. 4.6 we revisit the problem of proving linear growth of quantum circuit complexity for exponentially long time for the time-evolution of time-independent local Hamiltonians from the perspective of computational complexity theory. This perspective will show that significant progress in theoretical computer science is necessary to even prove superpolynomial lower bounds on the quantum complexity in this setting.

4.1. Time evolution of complexity, according to counting arguments about quantum circuits

Consider a fast-scrambling quantum system evolving under a unitary $U(t) := e^{-iHt}$. How does this unitary’s complexity evolve in time? We answer this question with a simple counting argument [1, 2, 38, 39].

To show how, we consider a system of $K \gg 1$ qubits.³ Suppose that the Hamiltonian H is fast-scrambling: information about initially localized perturbations spreads across the system in many-body entanglement quickly (in a time logarithmic in the system size [40, 41]). Also, suppose that H is 2-local, effecting just 2-body interactions.⁴ By discretizing time, we can regard the evolution as formed from two-qubit gates. At each time step, all the qubits are paired, and each pair undergoes a gate (Fig. 2).

³We mention qubit for concreteness, but the argument extends to higher-dimensional qudits.

⁴The 2 is not essential; only the interactions’ k -locality is, for some $k \ll K$.

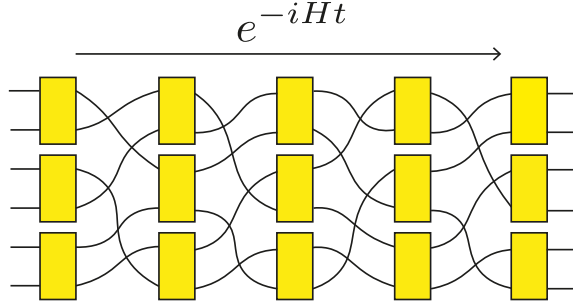


Figure 2: Illustration of the circuit that models unitary evolution following from a generic 2-local Hamiltonian.

What is the minimal number of gates needed to simulate evolution under H for some time t ? If t is, at most, exponentially large in K , the optimal circuit is believed to follow from discretizing the evolution under H . In other words, the discretized time evolution circuit likely does not contain gates that cancel each other, since the system is a fast scrambler. Of course, such cancellations would prevent the circuit from being the shortest. Hence the complexity of a fast scrambler's $U(t)$ evolves linearly in the number n of circuit layers:

$$\mathcal{C} = Kn/2. \tag{6}$$

This is easily turned into an equation for the complexity evolution as a function of time, since $n = t/\ell$ with ℓ the characteristic time scale for the application of a layer in the circuit⁵. A precise mathematical derivation of Eq. (6) can be made in the context of random circuits (Sec. 4.4).

For how long does the unitary's complexity grow linearly? Another counting argument answers this question, as shown in [10, Sec. 4.5.4] and [42, Sec. 8]. Until now, we have reasoned about digitally simulating evolution under the 2-local H . Consider, instead, an arbitrary finite, universal set of 2-qubit gates. Consider the set of all depth- n circuits formed from those gates. Each circuit implements some unitary. The complexity of $U(t)$ quits growing linearly once the aforementioned circuits have explored most of the volume of the group $SU(2^K)$.⁶ This exploration is achieved by a time $t \sim \mathcal{O}(2^{2K})$. At this time, the complexity reaches a maximal value $\mathcal{C}_{\max} \sim \mathcal{O}(2^{2K})$. The complexity is expected to then fluctuate around its maximal value. After a time $\sim 2^{2K}$, the complexity is expected to return to near-minimal value, in a Poincaré recurrence. Figure 3 depicts these expected features of the complexity's evolution.

In the previous two paragraphs, we supposed that gates would not cancel each other. If a circuit does contain gates that cancel, we call the cancellation a *shortcut*: the circuit implements the same unitary as a shorter circuit that lacks the cancelled gates. The no-shortcut assumption also enables us to answer the question *how does complexity react to a perturbation?*

Consider, again, the qubit system introduced above. Denote by W a one-qubit unitary pertur-

⁵In Sec. 4.5 we introduce T for a similar quantity: the number of layers in a 1D random quantum circuit in a brickwork layout.

⁶This claim and the ones to follow are based on populating the group manifold with δ size balls, where δ is the tolerance. The following claims therefore hold when studying approximate circuit complexity \mathcal{C}_δ , see section 2. The exact derivation is reviewed in [2].

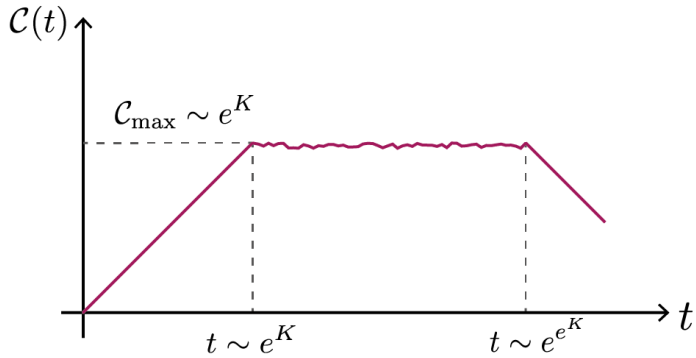


Figure 3: Illustration of the time evolution of complexity for a generic 2-local fast-scrambling Hamiltonian.

bation. Its *precursor operator* is

$$W(t) := U(t)WU(-t). \quad (7)$$

Using this precursor, we test how the system would behave if the perturbation W acted an amount t of time earlier. What is the complexity of $W(t)$? If W is the identity operator, then the precursor's complexity vanishes always: gates used to implement $U(t)$ always cancel gates used to implement $U(-t)$.

Gates cancel less if W is nontrivial. Consider Fig. 4, a circuit that implements the precursor $W(t)$. The gates leftward of the W represent the optimal construction of $U(t)$. That construction's first gate does not commute with the perturbation W . Therefore, gate 1 contributes to the complexity of $W(t)$. In contrast, gate 2 commutes with the perturbation. Therefore, the gate cancels between the circuit implementations of $U(t)$ and $U(-t)$. Hence gate 2 does not contribute to the complexity of $W(t)$. Like gate 2, gate 3 commutes W . However, gate 3 does not (generally) commute with gate 1, since both act on the same qubits. Therefore, gate 3 likely contributes to the complexity of $W(t)$.

If a perturbation has influenced a given qubit (if the qubit is in the perturbation's light cone) by a given time, we call that qubit *infected*. The number of infected qubits—the qubit *epidemic*—grows with the circuit depth. Once all qubits are infected, we expect gates not to cancel any longer. The epidemic crests at a time that we call the *scrambling time*, t_* . After this time, the complexity grows at twice the rate specified in Eq. (6).

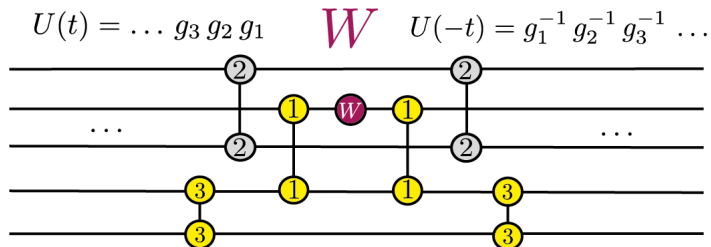


Figure 4: Circuit implementation of the precursor operator $W(t)$. Yellow gates are necessary for implementing $W(t)$. Gray gates are not necessary and cancel out, failing to appear in the optimal circuit.

Again using counting arguments, we answer two questions:

1. How many qubits are infected at a given circuit layer?
2. What is the precursor's complexity?

To answer these questions, we review and establish notation. As before, ℓ denotes a circuit layer's time duration. s denotes the number of qubits infected after a time t , or after $n = t/\ell$ circuit layers.

Let us answer question 1. At any given layer, the s infected qubits interact to some extent with the $K - s$ uninfected qubits. These interactions change the number of infected qubits by an amount Δs . We expect on probabilistic grounds⁷

$$\Delta s = s \frac{K - s}{K - 1}. \quad (8)$$

We can turn this finite-difference equation into a differential equation for ds/dt : recall that the number of circuit layers is $n = t/\ell$. Therefore, $\Delta n = 1$, so $\Delta s = \frac{\Delta s}{\Delta n} = \ell \frac{\Delta s}{\Delta t}$. The infinitesimal version thereof is $\ell \frac{ds}{dt} = s \frac{K-s}{K-1}$, by the right-hand side of Eq. (8). We solve the differential equation, invoking the boundary condition $s(0) = 1$ and neglecting small corrections of relative order $1/K$:

$$s(t) = K \frac{e^{(t-t_*)/\ell}}{1 + e^{(t-t_*)/\ell}}, \quad (9)$$

where we have introduced the scrambling time $t_* = \ell \log K$.

Now, we can answer question 2, calculating the precursor's complexity. The complexity—the number of gates—follows from how each infected qubit probably infects another qubit, via a gate, at each circuit layer n' . Layer n' thereby appears to increase $W(t')$'s complexity by one-half the number $s(t')$ of qubits infected by (up until the end of) layer n' . However, if a gate appears on the left-hand side of $W(t')$ in Fig. 4, then the gate appears also on the right-hand side. Therefore, layer n' actually increases $W(t)$'s complexity by $s(t')$. To count the gates, therefore, we sum the number of qubits infected by the first time step, the number infected by the next time step, the number infected by the next time step, and so on, until the final circuit layer n . We convert this sum into an integral over the time t :

$$\mathcal{C}(t) = \frac{1}{\ell} \int_0^t s(t') dt'. \quad (10)$$

We substitute in from Eq. (9) and integrate:

$$\mathcal{C}(t) = K \log(1 + e^{(t-t_*)/\ell}) = \begin{cases} K e^{(t-t_*)/\ell} & t \ll t_* \\ K(t - t_*)/\ell & t \gg t_* \end{cases}. \quad (11)$$

Initially, the complexity grows exponentially, as $e^{t/\ell}$. Yet the complexity is small throughout this stage, due to the $e^{-t_*/\ell}$ and the scrambling time's large size. Once t is large enough, we say that the perturbation has *scrambled*. Afterward, the complexity grows linearly, at twice the rate at which the unitary's complexity grows [because $W(t)$ contains two unitaries]. Figure 5 illustrates

⁷At a given layer, all qubits are paired. The number of newly infected qubits is proportional to the number of previously uninfected qubits, times the probability that they are paired with infected qubits. A qubit can't be paired with itself; hence the $K - 1$.

the delay in the complexity’s linear growth—the *switchback effect*—encoded in the $-t_*$ in the second line of Eq. (11). Holographic complexity proposals reproduce the switchback effect and the complexity’s initial exponential growth [see Sec. 7.2, particularly the discussion around Eq. (112)]. This reproduction originally motivated the complexity conjectures discussed in Sec. 7. It is an interesting question for future research to investigate whether more formal arguments on random circuits can be used to reproduce the switchback effect. The discussion above focused on a simple perturbation of one qubit at one instant, as well as on 2-qubit gates. These assumptions can be relaxed [1, 2, 19, 38, 39, 43].

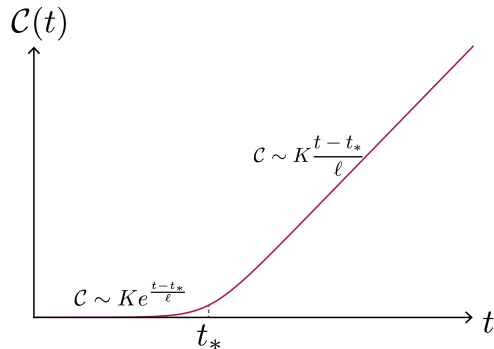


Figure 5: Precursor’s expected complexity, as a function of time. The switchback effect is the delay, until $t \approx t_*$, in the complexity’s linear growth.

4.2. Complexity saturation as a late-time stage of quantum many-body equilibration

The second law of thermodynamics suggests that state complexity should grow under generic dynamics. Of course, the second law concerns entropy, not complexity, and originally described classical systems. Yet complexity seems like it ought to obey the second law’s spirit [44]. It does, serving as the final stage of quantum many-body equilibration.

To elaborate, we first review equilibration and thermalization. We say that a system has *equilibrated* under two necessary conditions: (i) Large-scale quantities, such as temperature and volume, remain constant. (ii) No net flow of anything, such as energy or particles, enters or leaves the system. We define as follows the *thermalization* of a system that exchanges only heat with a temperature- T environment. Suppose that the system is classical, and consider measuring its energy. Let $p(E)$ denote the probability of obtaining the outcome E . The system thermalizes as $p(E) \rightarrow e^{-E/(k_B T)}/Z_{\text{class}}$. Boltzmann’s constant is k_B , the partition function $Z_{\text{class}} := \int dE \mu(E) e^{-E/(k_B T)}$ normalizes the distribution, and $\mu(E)$ denotes the density of states. Now, suppose that the system is quantum and evolves under a Hamiltonian H . The system thermalizes as its state (density operator) approaches $e^{-H/(k_B T)}/Z_q$, wherein $Z_q := \text{Tr}(e^{-H/(k_B T)})$. This canonical state is an example of a thermal state. Different thermal states arise if the system exchanges quantities Q_α other than heat with its environment; examples include particles. The thermal state becomes $\propto e^{-(H - \sum_\alpha \mu_\alpha Q_\alpha)/(k_B T)}$; the μ_α s denote effective chemical potentials.

To review the second law, we recall a classical monatomic gas in a box. Suppose that the gas particles are bunched together in a corner. The particles will spread across the box: the gas’s entropy, calculable with the Sackur-Tetrode equation, will end up greater than it was originally. The gas will equilibrate internally. Furthermore, suppose that the particles interact. They will thermalize; a particle’s phase-space distribution will approach the Maxwell–Boltzmann distribution.

Given the second law’s ubiquity, one should expect generic quantum many-body systems, too, to equilibrate and thermalize internally. Quantum many-body systems undergo more stages of equilibration and thermalization than classical systems do. We will synopsise some stages, which end with complexity saturation. First, we discuss the kinds of systems expected to thermalize.

Which systems thermalize is difficult to predict and prove. Thermalization is often attributed to chaos, but many definitions of quantum chaos exist [7–9]. According to early thinking, a system is quantum-chaotic if it has a chaotic semiclassical limit. Later studies defined chaos through energy-level statistics modeled with Wigner–Dyson distributions. Recent trends define chaos through out-of-time-ordered correlators [45] and spectral form factors [7, 46–48], reviewed below. Some authors acknowledge the ambiguity by writing “chaos” with quotation marks and meaning *nonintegrability* [49]. Yet debate surrounds the definition of quantum nonintegrability, too. According to a common definition, a system is integrable if it has extensively many nontrivial conserved quantities [8].⁸ To compound the ambiguity, many equilibration results follow from empirical observations, rather than from proofs, and govern specific systems, rather than general ones. We therefore write “chaotic,” with quotation marks, to communicate expectations about behaviors common to many systems called *chaotic* or *nonintegrable*.

In reviewing stages of quantum many-body equilibration, we refer to the following setup. Consider a closed quantum system of $N \gg 1$ subsystems—for example, qubits. Let the Hamiltonian H be “chaotic”; and let the interactions be k -body, for some $k \in \{1, 2, \dots, N\}$. Suppose that the system begins in a simple, pure nonequilibrium state, such as an N -qubit product state.

We now define two quantities—the out-of-time-ordered correlator and spectral form factor—used to define stages of equilibration. Let W and V denote local, Hermitian and/or unitary operators localized far apart. Examples include Pauli operators that act on distant qubits. Define the Heisenberg-picture operator $W(t) := e^{iHt} W e^{-iHt}$, and consider an arbitrary state ρ . The (four-point) out-of-time-ordered correlator is $\text{Tr}(W^\dagger(t) V^\dagger W(t) V \rho)$; we discuss its significance below. Define the partition function $Z(\beta) := \text{Tr}(e^{-\beta H})$. If $\beta, t \in \mathbb{R}$, then the spectral form factor is $|Z(\beta + it)/Z(\beta)|^2$. It measures correlations across a Hamiltonian’s spectrum.

As time progresses, our paradigmatic system will likely pass the following mileposts:

1. **Local equilibration:** Two-point correlators decay to $\sim 1/e$ of their initial values. Time-ordered correlators relax to approximately their long-time values. Small subsystems thermalize. This equilibration occurs at the *dissipation time* t_D [5]. t_D is also called the *thermalization time*. It is called the *collision time* if a system admits of a quasiparticle description. Under certain conditions (e.g., if the interactions are highly nonlocal), t_D is constant in N . Under other conditions, $t_D \sim N$. This latter scaling characterizes a one-dimensional system with nearest-neighbor interactions, by the Lieb–Robinson bound [50].
2. **Quantum information scrambling:** Initially localized information spreads across the system through many-body entanglement. Out-of-time-ordered correlators decay from their $O(1)$ initial values [45]. This scrambling occurs around the *scrambling time*, t_* . t_* can be parametrically larger than t_D , as under all-to-all coupling [41]. A lower bound limits how quickly

⁸To understand the *nontrivial*, consider eigendecomposing an arbitrary quantum Hamiltonian: $H = \sum_j E_j |j\rangle\langle j|$. The Hamiltonian conserves every eigenprojector $|j\rangle\langle j|$. Furthermore, the number of eigenprojectors is exponentially large in the system size. Yet these facts do not render H integrable; if they did, every H would be integrable. A conserved quantity must be unlike the $|j\rangle\langle j|$ s to be nontrivial.

many-body entanglement can form: $t_* \geq \frac{\hbar}{2\pi k_B T} \log(N)$ [5]. This bound saturates only if t_D is constant. In the context of semiclassical, single-particle quantum chaos, an analogue of t_* is called the *Ehrenfest time* [51].

3. **Breakdown of quantum–classical correspondence and rise in predictiveness of random-matrix theory:** This stage can begin around the same time as scrambling. Hence we have already seen one name for the time when this stage takes place: the *Ehrenfest time* t_E , also called the *Thouless time* t_{Th} . This time scale varies logarithmically with the system size: $t_E \sim \log(N)$.

How this stage manifests depends on the system and measures studied. An example setting involves transport in, e.g., electronic systems [52, 53]. Here, an initially narrow wave packet expands to cover a classically relevant length scale around t_E . The quantum system’s behavior diverges from its classical analogue’s; hence the name *Ehrenfest time* alludes to Ehrenfest’s theorem, which highlights a parallel between quantum and classical systems. In another example, at this stage, the spectral form factor changes from dipping to ramping upward: random-matrix theory begins to accurately predict the spectral form factor, which ceases to depend on microscopic details [54, 55].

4. **The spectral form factor changes from increasing linearly with time to remaining constant:** This change happens at the *Heisenberg time* t_H , or *plateau time* [54]. Denote by Δ the average inverse gap between consecutive eigenenergies. The Heisenberg time is $t_H := h/\Delta \sim e^N$ [53].
5. **Complexity saturation:** The state’s complexity grows to $\sim e^N$. The saturation time has been conjectured to scale as e^N . This conjecture has been proven under certain conditions (Sec. 4.3).

As a caveat, different authors use the same terms differently, when referring to stages of quantum many-body equilibration. Also, the above list is intended to be illustrative, not comprehensive; compiling all the stages [3, 9, 55–57] would require another review. For example, subtleties in the spectral form factor define other stages; see Sec. 1.1 of [56], and Sec. 1.4.3 of [55], for clear synopses and for references. Operator dynamics in Krylov space require their own treatment [3]. Additionally, if N is finite, then revivals (Poincaré recurrences and complexity revivals) occur long after times $\sim e^N$. Such revivals temporarily undo the equilibration but are consistent with the second law, given the system’s finite size.

Nevertheless, the list above demonstrates two points: (i) Quantum many-body equilibration involves more stages than classical equilibration. (ii) Complexity saturation constitutes a late stage.

4.3. Growth of complexity under random circuits

Random circuits form a toy model for chaotic quantum dynamics. We can prove random-circuit versions of conjectures originally formulated about chaotic dynamics’ complexities. When forming a random circuit, we choose the gates independently from a probability distribution on the unitary group $SU(4)$. Typically, we choose gates according to the Haar measure μ_H , the unique distribution that is invariant under left- and right- multiplication by any unitary. μ_H generalizes the uniform distribution on an interval, as well as the Lebesgue measure, to (locally compact) Lie groups. μ_H can be viewed as the uniform measure on these groups.

Known barriers such as the natural proof barrier discovered by Razborov and Rudich [58–60] inhibit us from proving superpolynomial lower bounds on the circuit complexity of an explicit Boolean function. The minimal number of elementary gates (such as AND, NAND, and XOR) in a Boolean function’s implementation is called its circuit complexity. Similar obstructions might inhibit us from proving superpolynomial lower bounds on quantum states’ quantum complexities. That is, the minimal number of 2-local quantum gates in any implementation of a state. One can more easily prove lower bounds on the complexities of states prepared with random circuits as random circuits quickly assume properties of the Haar measure, counting arguments about which yield lower bounds on the circuit complexity. In 1949 Claude Shannon [61] observed that the number of Boolean functions $f : \{0, 1\}^n \rightarrow \{0, 1\}$ outgrows the number of functions implementable with a subexponential number of elementary gates. A similar counting argument applies to Haar-random unitaries [62].

Sections 4.4 and Section 4.5 review two results about the growth of quantum circuit complexity. Both arguments followed from adapting Haar-measure counting arguments to random circuits. In a sense, these arguments offer to replace statements about vaguely defined “generic” dynamics as in section 4.1 with well-defined statements about average dynamics (which would intuitively be controlled by the dynamics of most systems and so would be “generic” in a well defined sense). This is done by thinking about which exact statistics/distribution should we consider for the unitaries and the circuits where now generic takes the sense of "very likely" or "of likelihood=1". Section 4.6 reviews why we still lack satisfying lower bounds on the quantum complexity of chaotic dynamics.

4.4. Linear growth of exact circuit complexity

Here, we review a proof of the exact circuit complexity’s linear growth [63]. More precisely, we show that the exact circuit complexity grows linearly with the number of layers, up to exponentially deep random quantum circuits, with unit probability over the choice of circuits. Moreover, the complexity saturates at exponentially deep circuits, again with unit probability. Just as random circuits form a toy model for chaotic dynamics, the exact circuit complexity forms a toy model for quantum complexity: the exact circuit complexity quantifies the minimal number of gates required to prepare a state or effect a unitary *exactly*. The preparation and effecting cannot include errors. Consequently, some unitaries arbitrarily close to the identity operator have exact circuit complexities of $e^{\Omega(K)}$.⁹ Recall that K denotes the system size, or number of degrees of freedom (qubits).

We now sketch a proof of Brown and Susskind’s conjecture [44] that circuit complexity grows linearly for an exponentially long time, as applied to random circuits and the exact circuit complexity. We will compare the degrees of freedom in two sets of unitaries: the unitaries generated by the depth- D circuits and the unitaries generated by smaller, depth- D' circuits. The basic idea echoes the fact that, in \mathbb{R}^3 , a plane has no volume. In terms of a well-behaved probability measure on a manifold M , every lower-dimensional submanifold has a probability of 0. Denote by \mathcal{U}_R the set of all unitaries that can be generated by R gates each. Fortunately, \mathcal{U}_R , although not a manifold, turns out to be a semialgebraic set defined by constraints $\{f_i \geq 0, g_i > 0, h_i = 0\}$, where $f_i, g_i, h_i : \text{SU}(D) \rightarrow \mathbb{R}$ are polynomials. Every semialgebraic set has a well-defined dimension similar to a manifold’s dimensionality.

⁹Throughout the rest of this section, we use big-Omega notation: $\Omega(X)$ means, roughly, “a term that grows at least as quickly as X ”.

Using the constant-rank theorem, we can apply the dimension-comparison logic above to random circuits: let $A \subset \mathcal{U}_R$ denote a semialgebraic set with $\dim(A) < \dim(\mathcal{U}_R)$. If we draw elements of \mathcal{U}_R from random circuits, then elements of A appear with probability 0.

One can lower-bound $\dim(\mathcal{U}_R)$ in multiple ways [63]. Reference [64] contains a particularly simple proof of this fact for circuits in a brickwork architecture. The bound is $\sim R/K$, roughly the number of layers. As a consequence, we find the following lower bound for the exact circuit complexity $\mathcal{C}_0(U)$ of a random quantum circuit. The minimal number of gates in an exact circuit implementation of U is

$$\mathcal{C}_0(U) \geq \Omega(R/K). \quad (12)$$

with unit probability over the choice of random quantum circuit. Up to a factor $\sim 1/K$, this is exactly the behavior predicted by the informal counting argument in Sec. 4.1. Recall that heuristic arguments predict $\mathcal{C}_0(U) \geq nK/2$, where n denotes the number of layers. This result confirms the intuition that gates typically do not cancel in circuits. In the next subsection, we discuss how to prove that even approximate cancellations have a low probability of occurring. The proof relies on unitary designs.

4.5. Linear growth of approximate circuit complexity

The simple argument of Sec. 4.4 is fine-tuned to the exact circuit complexity. Using combinatorial methods, we can obtain similar results about more operational notions of circuit complexity such as the approximate circuit complexity: the minimal number of gates to approximate a state or unitary up to some fixed error. Below, we present such a combinatorial argument, using approximate unitary designs (defined below) [65–67]. Unitary designs were first used to lower-bound quantum complexity in [68–70].

Unitary designs are probability distributions on the unitary group $SU(D)$. One cannot distinguish a unitary t -design from the Haar measure using only expectation values of degree- t polynomials. More formally, let ν denote any probability distribution on $SU(D)$. Denote by $\mathbb{E}_{U \sim \nu} f(U)$ the expectation value of a random variable $f : SU(D) \rightarrow \mathbb{R}$, over unitaries drawn according to ν . We call ν a *unitary t -design* if

$$\mathbb{E}_{U \sim \nu} (f(U, \bar{U})) = \mathbb{E}_{U \sim \mu_H} (f(U, \bar{U})), \quad (13)$$

for all balanced polynomials f of degree $2t$. *Balanced* means that the f s are polynomials in the matrix elements of U and \bar{U} such that each monomial contains the same number of U elements and \bar{U} elements. This definition is equivalent to the operator equation

$$\mathbb{E}_{U \sim \nu} (U^{\otimes t} \otimes \bar{U}^{\otimes t}) = \mathbb{E}_{U \sim \mu_H} (U^{\otimes t} \otimes \bar{U}^{\otimes t}). \quad (14)$$

There are various definitions of *approximate* unitary designs based on how to relax Eq. (14).

To see why unitary designs imply lower bounds on the approximate circuit complexity, we review why Haar-random unitaries' circuit complexities are nearly maximal with the overwhelming probability $1 - e^{-\Omega(4^K)}$. Consider a K -qubit system and an arbitrary K -qubit pure state $|\psi\rangle$. The ε -ball $B_\varepsilon(|\psi\rangle)$ around $|\psi\rangle$ consists of the pure states $|\phi\rangle$ that differ from $|\psi\rangle$ in overlap by, at most, ε : $B_\varepsilon(|\psi\rangle) := \{|\phi\rangle \in (\mathbb{C}^2)^{\otimes K}, \langle \phi | \psi \rangle = 1, |\langle \psi | \phi \rangle|^2 \geq 1 - \varepsilon\}$. We must count the ε -balls that fit into $SU(2^K)$. The volume of a ball of radius r in \mathbb{R}^d grows as $\sim r^d$. Similarly, the probability of

drawing an element of the ε -ball $B_\varepsilon(|\psi\rangle)$ from the Haar measure on $\{|\psi\rangle \in (\mathbb{C}^2)^{\otimes K}, \langle\psi|\psi\rangle = 1\}$ is $\Pr(B_\varepsilon(|\psi\rangle)) \sim O(\varepsilon^{2^K})$. Therefore, at least 2^{c2^K} (for some constant $c > 0$ depending on ε) balls $B_\varepsilon(|\psi\rangle)$ are needed to cover most of $SU(2^K)$. On the other hand, consider the circuits of R gates chosen from a finite gate set \mathcal{G} . These circuits can implement $\leq |\mathcal{G}|^R$ unitaries. Therefore, the majority of the 2^{c2^K} ε -balls are outside the set of states that can be approximated with $o(2^K)$ gates. In other words, their approximate circuit complexity is exponential.

The rough argument above applies to every ensemble of states: almost every state from any ensemble ν has a circuit complexity $\geq \max_\psi \log(\nu(B_\varepsilon(|\psi\rangle)))$. Consider the ensemble of states generated by random circuits. We can lower-bound almost every state's approximate circuit complexity by upper-bounding $\max_{|\psi\rangle} \{\nu_K(B_\varepsilon(|\psi\rangle))\}$. The design property (14) implies lower bounds on the approximate circuit complexity, via higher moments of the Haar measure [68–70]. By the above counting argument for Haar-random states, a unitary drawn from a design on $SU(2^K)$ has, with high probability, an approximate circuit complexity lower-bounded by $\Omega(Kt)$.

We can combine this bound with random circuits' quick convergence to unitary designs. Brown and Viola provided evidence for fast convergence by analyzing the spectra of moment operators via mean-field techniques [71]. Reference [69] then rigorously showed that brickwork random circuits of depth $T \geq Ct^{9.5} [2Kt + \log_2(1/\varepsilon)]^{10}$ are ε -approximate unitary t -designs, for a constant $C > 0$ (whose form the authors calculated) and for all $t \leq O(2^{2K/5})$. An approximate design is a probability distribution that relaxes the equality in Eq. (14). In particular, the notion of approximation we get is surprisingly strong and implies relative errors (also called multiplicative errors) to Haar random unitaries for the outcome probabilities of any quantum experiment that queries the t copies of U in parallel. We refer to Refs. [69, 72] for details. This relaxation of the design property is sufficient to imply a circuit lower bound of $\mathcal{C}_\delta(U) \geq \Omega(Kt)$ with probability $1 - e^{-\Omega(Kt)}$. In particular, the probability of significant short-cuts is small, not only in the system-size, but also in the number of copies t . The exponent 10.5 of t in this bound was improved to $5 + o(1)$ [73]. Ref. [72] reduced the t dependence to an optimal, linear scaling. More precisely, random circuits are ε -approximate unitary t -designs in depth

$$T \geq CK^3 [2Kt + \log_2(1/\varepsilon)]. \quad (15)$$

We can now combine the design depth in Eq. (15) with the lower bound of $\Omega(Kt)$ on the circuit complexity for unitaries drawn from a unitary t -design. Random depth- T circuits U satisfy, with a probability $1 - e^{-\Omega(T/K^3)}$,

$$\mathcal{C}_\delta(U) \geq \Omega(Kt) = \Omega(K(T/K^4)) = \Omega(T/K^3). \quad (16)$$

$\mathcal{C}_\delta(U)$ denotes the minimal number of 2-local unitaries necessary to generate any V that is δ -close to U in operator-norm: $\|U - V\| \leq \delta$. Notice that the probability of significant short-cuts is negligible even in T . In particular, for very deep circuits, this becomes increasingly crucial as the number of random bits that are required to draw a circuit of depth T scales like $\sim KT$.

Combinatorial arguments based on unitary designs are flexible: the idea of using counting arguments via moment bounds was extended to more operational definitions of complexity, such as

¹⁰We use the parameter T to denote the number of layers in a brickwork layout. This parameter is similar to the parameter n presented in Sec. 4.1. This change in notation is to avoid confusion as n is almost exclusively used for the system-size in the context of quantum information theory.

the minimal number of gates required to distinguish a state from the maximally mixed state [68]. The proof technique relies on unitary designs, as in [68, 69, 73, 74]. It offers a second advantage over the dimension-comparison technique of [63, 64]: the bound (15) holds also if we draw the gates from a universal gate set—from a finite set $\mathcal{G} \subset \text{SU}(4)$ whose gates can approximate every K -qubit unitary. Moreover, the techniques of Ref. [72] yield similar results for other circuit layouts as well as randomly chosen layouts.

Similar techniques can be used to study the growth of quantum circuit complexity in models of time-dependent dynamics. For example, a discretized model of Brownian motion converges to approximate designs as quickly as random circuits do [75]. Reference [76] provides evidence for a similar convergence by continuous Brownian dynamics.

This and the previous subsection mostly concern the quantum circuit complexity’s growth under random circuits. Using high moments (of the order $t \sim 4^K$), one can also bound the time at which quantum complexity saturates and even show that (with high probability) a recurrence to low circuit complexity happens after a doubly exponentially long time [77]. More precisely, under random circuits, the approximate circuit complexity saturates near its maximal value after a depth 2^{5K} with high probability over the choice of circuit. The approximate circuit complexity exhibits a recurrence at a depth d_{rec} that satisfies $a_\varepsilon^{2^{2K}} \leq d_{\text{rec}} \leq b_\varepsilon^{2^{2K}}$. The constants a_ε and b_ε depend only on the approximation error $\varepsilon > 0$ in the approximate circuit complexity’s definition. To tightly bound the time at which saturation of circuit complexity occurs, one would have to extend the bound in [72] to extremely high moments ($t \sim 4^K$). Such a tight bound is possible for a classical analogue of random quantum circuits called random reversible circuits [72]. The latter generate random elements in the permutation group S_{2K} acting as permutations of n -bit string.

4.6. Barriers to proving that quantum complexity grows superpolynomially under long-time evolutions

Each of the methods discussed above exploits a counting argument. The argument concerns a placeholder quantity that roughly measures the ensemble’s randomness. Finding such a quantity dependent on the ensemble is far easier than finding a similarly growing quantity for individual circuits. In the exact-circuit-complexity proof, the placeholder is the “accessible dimension” $\dim \mathcal{U}_R$. In the approximate-circuit-complexity proof, any quantity that signifies the convergence to designs (such as frame potentials [70] or the expected overlaps $\mathbb{E}_{V_1, \dots, V_d} |\langle \psi | V_d \cdots V_1 | 0^K \rangle|^2$ for random 2-qubit gates V_1, \dots, V_d) will do). This strategy dominates all our proofs of lower bounds on circuit complexity beyond linear depth. Indeed, this limitation might be fundamental as circuit complexity is known to be notoriously difficult to bound.

But this pessimism concerns individual states. What about time evolution under randomly drawn local Hamiltonians? This scenario is closer to the setting considered by Brown and Susskind [44], who conjectured that the quantum complexity grows linearly for an exponentially long time under a typical time-independent local Hamiltonian. Still, the total number of distinct local time independent? Hamiltonians is upper bounded by $2^{\text{poly}(K)}$, so clearly the above counting argument fails to establish superpolynomial lower bounds on the approximate quantum circuit complexity.

The problem of proving lower bounds on the quantum complexity for the time-evolution of local Hamiltonians turns out to be related to the separation of computational-complexity classes: Aaronson and Susskind [42] point out that the circuit complexity of exponentially long-time evolution under local Hamiltonians is superpolynomial if and only if $\text{PSPACE} \not\subseteq \text{BQP/poly}$. PSPACE is the class of all computations performable with polynomial memory. BQP/poly is the class of all

problems solvable with (nonuniform) families of polynomially sized quantum circuits. Separations of complexity classes are notoriously difficult to prove, and few such separations are known. Proving a separation of the kind $\text{PSPACE} \not\subseteq \text{BQP/poly}$ appears to require a breakthrough in theoretical computer science. Therefore, even showing the existence of a local Hamiltonian for which the complexity does not saturate after a polynomial time requires major technical advances.

5. Paradigms for complexity I: Nielsen complexity

As mentioned in the previous section, one can define two notions of complexity for a unitary operator: exact and approximate. Each notion has a downside. For starters, exact complexity can behave counterintuitively. For example, a unitary close to the identity can have a large complexity as obtaining it exactly might require fine tuned combination of very many gates. Meanwhile, approximate complexity involves a tolerance, which may seem arbitrary. One can resolve both issues by defining complexity in terms of a continuous quantity.

Nielsen *et al.* identified the optimal implementation of a global unitary U , using *complexity geometry* [78–80]. Complexity geometry is a unitary-group manifold on whose tangent space a norm is defined. A continuous trajectory on the manifold results from evolution under a time-dependent Hamiltonian. The manifold’s origin represents the identity operator, and another point represents U . A geodesic connects the points. In terms of the geodesic’s length, Nielsen *et al.* lower- and upper-bounded discrete quantum circuits’ complexities [10]. However, one can define the geodesic’s length as a stand-alone notion of the unitary’s complexity: *Nielsen’s complexity*. Nielsen’s complexity has several appealing features:

1. In Nielsen’s framework, evolution along a continuous trajectory decomposes into a sequence of infinitesimal steps. This decomposition is *Trotterization*, a technique for simulating evolution under a time-independent Hamiltonian, using a circuit (using evolution under a time-varying Hamiltonian) [81]. Hence Nielsen’s complexity is related to an important quantum-computational concept.
2. Using Nielsen’s geometry, one can upper-bound the approximate circuit complexity, and lower-bound the exact circuit complexity, discussed in Sec. 4.
3. Nielsen’s complexity is a geometric object. Therefore, one can apply to it Riemannian-geometry (or Finsler-geometry) tools.
4. Nielsen’s complexity connects naturally to Hamiltonian control problems, extensively studied in the quantum computation literature.
5. One has substantial freedom in equipping Nielsen’s complexity geometry with a distance measure on the unitary manifold. This freedom mimics the choice of a gate set in the exact and approximate circuit complexities’ definitions. *A priori*, computing Nielsen’s complexity is difficult because complexity geometry is high-dimensional and highly curved. Yet different choices of complexity geometry form equivalence classes whose elements behave the same way at long distances. Within an equivalence class, one can often find members that are only modestly curved [14, 80, 82]. This result facilitates the calculation of Nielsen’s complexity.
6. The problem of calculating Nielsen’s complexity can become exactly or approximately solvable when considering unitary representations of certain symmetry groups. Examples include unitary representations of symplectic and orthogonal groups (relevant respectively for free bosonic and fermion quantum systems), the global conformal group, and circuits constructed from the Virasoro algebra generators (relevant for spacetime transformations in CFTs).
7. Nielsen’s complexity, being continuous, resonates with continuous features of QFT and CFT and the cMERA tensor network [13, 83] and natural physical systems’ time evolution. The cMERA parallel motivated the earliest work on complexity in free QFT [84, 85].

We start in Sec. 5.1 with the definition of Nielsen’s complexity. Section 5.2 discusses possible choices for a metric on the complexity geometry, and their basic properties. In Sec. 5.3, we discuss

the required properties a complexity geometry should have in order to reproduce the linear time dependence and switchback effect for system evolution with a chaotic Hamiltonian. In Sec. 5.4, we discuss a choice of norm on the unitary manifold relevant for distributed computing, which highlights a connection between complexity and the entanglement entropy. We then turn to the studies of Nielsen complexity in QFT in Sec. 5.5.

5.1. Definition of Nielsen complexity

One can define Nielsen's complexity on a manifold formed by any Lie group G . For simplicity and clarity, we now focus on the special unitary group $SU(N)$. For the K -qubit system discussed in the Sec. 4.1, $N = 2^K$. However, one can define complexity geometries of every symmetry group. Example symmetry groups include global and local conformal groups relevant to CFT problems, symplectic groups relevant to free bosons, and orthogonal groups relevant to free fermions.

We aim to identify the optimal means of generating a target unitary U , starting from the identity operator $\mathbb{1}$. One generates U via evolution in time, t , under a Hamiltonian $H(t)$ that may vary. It is important to stress that this auxiliary time t is a priori distinct from the physical time governing unitary time evolution of a system in question. Let $\{T_I\}$ denote a basis for the space of Hermitian operators that form the unitary algebra $\mathfrak{su}(N)$. One can expand the Hamiltonian in terms of the basis elements:

$$H(t) = \sum_I Y^I(t) T_I. \quad (17)$$

The $Y^I(t)$ denote *velocities*, or *control functions*. They are the components of the vector that is tangent, at the point t , to the trajectory generated by $H(t)$ through the group manifold. Different trajectories represent different ways of generating U . We have parameterized each trajectory with $t \in [0, 1]$, such that $U(t=0) = \mathbb{1}$ and $U(t=1) = U$. At each point along the path, the unitary has the form

$$U(t) = \overleftarrow{\mathcal{P}} \exp \left(-i \int_0^t dt' H(t') \right). \quad (18)$$

The path ordering $\overleftarrow{\mathcal{P}}$ constructs the trajectory by multiplying the exponential terms from right to left. Denote by $F[Y^I(t)]$ the *cost function*, a norm on the tangent space. *Nielsen's unitary complexity* is defined as the minimal distance induced by this norm:

$$\mathcal{C}_F[U] := \min_{\{Y^I(t): U(0)=\mathbb{1}, U(1)=U\}} \int_0^1 dt F[Y^I(t)]. \quad (19)$$

The path $U(t)$ obeys the aforementioned boundary conditions. The cost function encodes the difficulty of extending the trajectory in any given direction (in the tangent space at any given manifold point).

The previous definitions refer purely to the space of unitaries. Next, we define complexity in terms of the Hilbert space of whole-system quantum states. Assume that the $SU(N)$ elements act on an N -dimensional Hilbert space \mathcal{H} . We would like to define quantum state complexity that captures the difficulty of producing an arbitrary target state $|\psi_T\rangle$ from a fixed reference state $|\psi_R\rangle$. We define *Nielsen's state complexity* as the least complexity of any special unitary that evolves the

reference to the target:

$$\mathcal{C}_F^{\text{state}}[|\psi_T\rangle, |\psi_R\rangle] := \min_{\{U \in \text{SU}(N) : |\psi_T\rangle = U|\psi_R\rangle\}} \mathcal{C}_F[U]. \quad (20)$$

The state complexity is a property of two states, yet the definition invokes the unitary complexity (19). Instead, one might prefer to rewrite the above definition in terms of a metric induced on the Hilbert space, which directly gives a notion of infinitesimal distance between states. To define such a metric, recall that the space of rays is a collection of equivalence classes. Each class consists of the vectors that differ by a global phase. This concept is captured by the stabilizer of a state $|\psi\rangle$. The stabilizer of any state $|\psi\rangle$ is the maximal proper subgroup $\text{SU}(N-1) \times \text{U}(1)$ of $\text{SU}(N)$. The stabilizer is spanned by the generators that perform no physically meaningful operations on ψ : they do not affect the physical state, except by changing the global phase. Using the stabilizer, we define equivalence classes as follows. Let V denote any element in the $|\psi\rangle$ stabilizer. Consider right-multiplying any element $U \in \text{SU}(N)$ by V . The resulting unitary, $U' := UV$, lies in the same equivalence class as U :

$$V|\psi\rangle = e^{i\phi}|\psi\rangle \quad \Rightarrow \quad U' = UV \sim U. \quad (21)$$

Equation (21) defines a quotient map from the unitary group to the complex projective space $\mathbb{C}\mathbb{P}^{N-1}$:

$$\pi : \text{SU}(N) \mapsto \mathbb{C}\mathbb{P}^{N-1} := \frac{\text{SU}(N)}{\text{SU}(N-1) \times \text{U}(1)}. \quad (22)$$

The state complexity (20) induces a norm on the state space, a minimum over the trajectories consistent with the boundary conditions. One can perform such a minimization in each infinitesimal step of a trajectory, to obtain a norm on the space of states, as follows. One fixes $|\psi(t)\rangle$ and its time derivative $|\dot{\psi}(t)\rangle$, then minimizes the cost function over the degrees of freedom in the Hamiltonian $H(t)$. This process induces the norm

$$F^{\text{state}}[|\psi(t)\rangle, |\dot{\psi}(t)\rangle] := \min_{\{\text{stab}(|\psi(t)\rangle)\}} F[Y^I(t)]. \quad (23)$$

In terms of this definition, we can express the state complexity (20) as

$$\mathcal{C}_F^{\text{state}}[|\psi_T\rangle, |\psi_R\rangle] = \min_{\{|\psi(t)\rangle : |\psi(0)\rangle = |\psi_R\rangle, |\psi(1)\rangle = |\psi_T\rangle\}} \int_0^1 dt F^{\text{state}}[|\psi(t)\rangle, |\dot{\psi}(t)\rangle]. \quad (24)$$

Using this formula, we can study geodesics in the state space without referring to unitaries.

5.2. Geometric features of Nielsen complexity

The cost function $F[Y^I]$ encodes the geometric properties of Nielsen's complexity, through the definition (19). Important cost functions have the form

$$F_{p,\vec{q}}[Y^I] = \left(\sum_I q_I |Y^I|^p \right)^{\frac{1}{p}}. \quad (25)$$

We discuss the parameter p in the next paragraph. The *penalty factors* $q_I \geq 0$ participate in a one-to-one correspondence with the generators T_I of the $\mathfrak{su}(N)$ algebra. The penalty factors quantify

the difficulties of moving along certain directions of the tangent space. One incorporates features of discrete circuits into the complexity geometry: one chooses penalty factors that reflect the difficulties of performing certain gates. For instance, few-qubit operators are naturally easier to implement than many-qubit operators. Therefore, it is natural to assign smaller penalty factors to the generators (called *easy*) that implement few-qubit operations and larger penalties to the generators (called *hard*) that act on several qubits. The terms *easy* and *hard* refer to the magnitude of the penalty factor associated with each generator. A trajectory in the group manifold can be approximated by a circuit whose gates act for short time intervals.

Returning to the cost function (25), we analyze the parameter $p = 1$. When $p = 1$, $F_{p=1, \bar{q}}[Y^I]$ has a natural physical interpretation: it counts (with an appropriate measure) the number of gates used to build the continuous trajectory in the group manifold $SU(N)$. However, $F_{p=1, \bar{q}}[Y^I]$ has the disadvantage of not being smooth. One therefore cannot apply the calculus of variations to the geodesics. When $p = 2$, the norm (25) induces a Riemannian metric on the group manifold, simplifying the study of the geodesics. In this case, the map (22) is a Riemannian submersion [86] (defined in [87]). Heuristically, a Riemannian submersion is a smooth mapping from a higher-dimensional manifold to a lower-dimensional one. This mapping preserves distances in the directions perpendicular to the fibers.¹¹ In our setting, the fibers correspond to the maximal subgroup $SU(N - 1) \times U(1)$. The submersion maps $SU(N)$ to $\mathbb{C}\mathbb{P}^{N-1}$. These facts provide a systematic means of determining the metric, induced by the cost-function minimization (23), on the state space. The Nielsen-complexity literature has mainly focused on $p = 1, 2$ [14, 30, 32, 34, 37, 44, 82, 84–86, 88–99].

One may wonder whether Nielsen’s complexity is related to the discrete gate complexity. The answer is yes: Nielsen’s complexity provides both upper and lower bounds on the gate complexity, provided the cost function satisfies certain conditions [78, 79]. The authors of [78, 79] further show that, by penalizing enough the generators acting on several qubits, one can build a trajectory that reaches a unitary in the complexity geometry with arbitrary precision. This trajectory can be built by only using generators acting on one or two qubits. The penalties required for this construction typically make the manifold highly curved. However, as we will subsequently review, Nielsen’s complexity is universal at long distances within a certain equivalence class of metrics, and this equivalence class can be shown to also contain moderately-curved metrics. A priori, this fact makes the computation of Nielsen’s complexity easier by using tools from differential geometry. When the motion in the unitary manifold is restricted to a small subgroup, exact or semi-analytic results can be obtained, which we discuss in later subsections.

Equivalence classes of metrics and the universality of penalty schedules. There is a substantial freedom in choosing a cost function. Are there any common properties shared by different cost functions? A large universality class of cost functions exists: many metrics on the group manifold share the features described below [14, 82]. This class’s constituents may differ significantly at short distances. However, they differ at large distances only polynomially in the path length and in the physical system’s size. To simplify the rest of this subsection, we denote the penalty factors by q_k and assume that they depend only on the corresponding gate’s weight, k .¹² Consider increasing any

¹¹The fibers are points, in the higher-dimensional space, that are mapped to the same point in the lower-dimensional manifold.

¹²A generator has weight k if it acts nontrivially on exactly k qubits. q_k should not be confused with the q_I introduced in Eq. (25). The notation q_k alludes to how all the generators T_I that have the same weight k share the

penalty factor while keeping the others constant. Above a critical value \bar{q}_k , the complexity ceases to depend on the penalty factor. This happens because one can implement a given unitary operator with weight k via circuits formed from other, cheaper gates. (The reason is as follows. Consider any fixed $m \geq 2$. Using the m -local gates, one can reconstruct all the m' -local gates for every m' .) Consequently, one can identify a *critical schedule*, a set $\{\bar{q}_k\}$ of the penalty factors' critical values. The universality class is the set of all the schedules such that $q_2 = \bar{q}_2$ and, for all $m > 2$, $q_m \geq \bar{q}_m$. In the universality class, the metrics may differ greatly at short separations but approximately equal each other at long separations. That is, short and long distance scales decouple. At the same time, the critical schedule is conjectured to be the only universality-class member that behaves uniformly across all the distance scales [82]. In other words, the conjugate points are pushed to infinity, and geodesics are straight lines for an exponential time in the number of qubits. Brown argued that the same universality class consists of metrics whose associated Nielsen complexity (measured by the geodesic length from the origin) is polynomially equivalent to the gate complexity. At the same time, one can always pick a metric inside each universality class such that the unitary manifold, equipped with such metric, has modest curvature [14]. Therefore, one can (in principle) more easily compute the Nielsen complexity using tools from differential geometry.

5.3. Constraints on the cost function from expected time dynamics

In Sec. 4.1, we discretized time to show that quantum complexity exhibits two behaviors: linear growth for an exponential long time and the switchback effect. These derivations relied on simple counting arguments. Afterward, we quantitatively showed that complexity exhibits linear growth, using random unitary circuits, algebraic geometry, and unitary designs (Sections 4.3–4.6). We aim to reproduce the above key features of complexity, using complexity geometry. In other words, we ask the question: what are necessary conditions for a complexity geometry to reproduce linear growth and the switchback effect when applied to the unitary unitary time evolution generated by a chaotic Hamiltonian? To do so, we select an appropriate metric on the unitary manifold $SU(N)$ (assuming $N \gg 1$). The associated cost function should satisfy the following requirements [39, 44, 80]:

1. The metric should be right-invariant, because the unitary manifold is homogeneous.
2. The group manifold has a negative average-sectional-curvature [39, 80], such that nearby geodesics diverge. This property is necessary (but insufficient) for reproducing chaotic and ergodic behaviors of the Hamiltonians that generate motion on the unitary manifold.
3. The Nielsen complexity displays the switchback effect, which requires the geometry's sectional curvatures to scale as $1/K$ (K denotes the number of qubits).

Let us comment on the implications of these requirements. First, consider the minimization, in Eq. (23), over the stabilizer group of $|\psi(t)\rangle$, yielding a metric on the space of states rather than on unitaries. Do the above properties reflect in this geometry on the space of states? The minimization breaks the geometry's homogeneity, complicating one's study of the geodesics and curvature in the space of states. [Granted, the minimization projects the metric onto a manifold of lower dimensionality than $SU(N)$'s.] Nonetheless, as mentioned earlier, for the case of Riemannian cost functions, the map (22) is a Riemannian submersion [86] (defined in [87]). Riemannian submersions interrelates the sectional curvatures in the space of unitaries and the sectional curvatures in

same penalty factor.

the space of states, via the O’Neill formula [100]. The O’Neill formula implies that the sectional curvature along a plane in the space of states is lower-bounded by the sectional curvature along an appropriate plane in the unitary manifold.

Second, the group manifold equipped with the Cartan-Killing metric—the standard metric on $SU(N)$ —does not satisfy the above requirements because it has only constant positive sectional curvatures. How can one construct a geometry that has negative sectional curvatures? One can assign the penalty factors such that the $\mathfrak{su}(N)$ algebra’s nonvanishing commutators have the structure $[easy, easy] = hard$. The *easy* and *hard* refer to generators associated with small and large penalty factors in the cost function [37]. When the penalty factors are associated to each generator such that the commutators take the above-mentioned form, then sectional curvatures’ negativity follows from the Pythagorean theorem for curved space. The latter statement was proven in the contexts of a qubit’s unitary manifold and a qutrit’s [37, 86].¹³ Manifolds equipped with right-invariant metrics must have positive sectional curvatures in some regions; otherwise, they are flat [101]. The geodesic’s length computed in flat space does not present the features expected from a measure of complexity, therefore it is not interesting for our purposes.

References [96, 98] studied time-dependent trajectories generated by the SYK Hamiltonian on the unitary manifold. The authors showed that the unitary’s geodesic distance from the origin is lower-bounded by a geodesic whose length grows linearly with time. This linear growth is truncated at conjugate points. At a conjugate point, the geodesic does not result from extending an earlier-time geodesic; a shorter path connects the origin to the unitary. Conjugate points in the critical complexity geometry described at the end of Sec. 5.2 are pushed to infinity [82]. Therefore, the linear growth of Nielsen’s complexity in that geometry persists for a time exponential in the number of qubits. In the context of spin chains, Brown showed that many complexity geometries’ diameters are exponentially large in the number of qubits [14]. This exponential relation is necessary for the complexity to saturate at an exponentially large value (Fig. 3).

We have argued that Nielsen’s complexity exhibits one behavior characteristic of quantum complexity: linear growth. Nielsen’s complexity reproduces the other behavior—the switchback effect—in toy models [44]. Qualitative features similar to the switchback effect are also displayed by single-qubit and two-qubit systems [102]. However, the comprehensive picture of the emergence of the switchback effect from the complexity geometry is still lacking and is one of the important open questions that future research in this area should address.

5.4. Relation between Nielsen complexity and entanglement: binding complexity

The penalty factors in the definition of Nielsen’s complexity can be attributed to the relative difficulty of applying certain generators. A particularly interesting choice, where analytic results can be obtained, is the case in which our system is split into subsystems, and the penalty factors associated with generators acting within a given subsystem are much smaller than those of generators acting between multiple subsystems. This setting serves as a model to describe distributed quantum computing, where a large computer is divided into small quantum computers (called *nodes*). The operations between nodes, which are possibly located far away from each other, require significantly more resources than operations within each subsystem.

The limiting case, where only operations acting between subsystems have non-vanishing cost,

¹³A qudit is a d -level quantum system, represented by a Hilbert space \mathbb{C}^d . A qubit has $d = 2$; and a qutrit, $d = 3$.

was referred to as *binding complexity* in [95]. There, the authors suggested that this notion quantifies the difficulty of distributing entanglement among multiple parties. The authors of Ref. [95] further suggested that the notion of binding complexity could serve as a measure for the robustness of entanglement. Here, one typically has in mind the n -party (with $n \geq 2$) generalizations of the W and GHZ states. The GHZ state is separable upon tracing out any subset of the parties, but the W state is not. In this sense, W states possess more robust entanglement. It was argued in [95] that the binding complexity should scale as $O(n)$ for GHZ states, and as $O(n^2)$ for W states. The paper also presented results for the binding complexity of Gaussian states of free QFT. As we review next, one can get exact results for the binding complexity of spin chains in Nielsen’s framework when the cost of generators acting within each subsystem is small enough [99]. As a bi-product, it was discovered that cost functions satisfying this property relate Nielsen’s complexity to the Rényi min-entropy in a precise way. Moreover, the above cost functions are bounded by the maximal rate of change of a state’s entanglement entropy.

To illustrate these results, let us begin with a formal definition of the binding complexity. Consider splitting a quantum system (for instance, a spin chain) into m subsystems $A_{k=1,2,\dots,m}$. The *binding complexity* is the minimal number of gates, each acting on a limited number of subsystems, needed to implement a target unitary [95]. Below, we focus on 2-local gates (which act on, at most, two subsystems each). Within Nielsen’s framework, binding complexity has a close analogue, obtained by choosing a particular cost function on the unitary space. To this aim, we consider a bipartite system whose Hamiltonian (17) decomposes as¹⁴

$$H(t) = Y_{A_1}^a(t)T_a^{A_1} \otimes \mathbf{1}^{A_2} + Y_{A_2}^i(t)\mathbf{1}^{A_1} \otimes T_i^{A_2} + Y^{ai}(t)T_a^{A_1} \otimes T_i^{A_2}. \quad (26)$$

Each of the generators $T_a^{A_1}$ and $T_i^{A_2}$ acts on only one side of the system. In contrast, $T_a^{A_1} \otimes T_i^{A_2}$ can entangle the sides. The velocities split into subsets $Y^I := \{Y_{A_1}^a, Y_{A_2}^i, Y^{ai}\}$. This division implies a decomposition of the penalty factors (25) into subsets $q_I := \{q_a^{A_1}, q_i^{A_2}, q_{ai}\}$.

Having specified the setup, we define the *Nielsen binding complexity* \mathcal{BC} . It is the unitary complexity (19) evaluated with the penalty factors

$$q_a^A = q_i^B = 0 \quad \text{and} \quad q_{ai} \geq 1. \quad (27)$$

These penalties impose greater costs on entangling (or *non-local*) gates than on single-subsystem (or *local*) operations. Let us substitute the penalties (27) into the cost function (25) and perform the minimization (20) to obtain a complexity norm on the space of quantum states. Two simplifications follow: first, the space of states contains null directions, defined as the loci of states interconnected via local unitaries along which the cost function vanishes. Second, one can integrate out non-dynamical degrees of freedom in the geodesic minimization. One obtains a norm $\mathcal{BF}[\lambda_k, \dot{\lambda}_k]$ on the space of states. \mathcal{BF} depends only on a state’s Schmidt coefficients λ_k and their derivatives $\dot{\lambda}_k$.

We can analytically compute the binding state complexity under certain choices of the penalty factors q_{ai} in Eq. (27), and of the parameter p in Eq. (25). A Riemannian cost function provides our first example. Let us write out the binding state complexity associated with the cost function

¹⁴We denote the generators of the special unitary group in subsystem A_1 with index $a \in \{1, \dots, N_{A_1}^2 - 1\}$ from the beginning of the alphabet, and the generators in A_2 with index $i \in \{1, \dots, N_{A_2}^2 - 1\}$ from the middle part of the alphabet. We also denote with a sub(super)script A_1, A_2 the subsystem where the local generators act.

(25), $p = 2$, and the penalty factors (27) with $q_{ai} = 1$ [99]:

$$\mathcal{BC}_{2,\text{hom}}^{\text{state}} = \sqrt{\frac{2}{\mathcal{N}_{A_1}\mathcal{N}_{A_2}}} \arccos\left(e^{-\frac{1}{2}S_\infty(|\psi_T\rangle)}\right). \quad (28)$$

The *hom* stands for the nonlocal generators' homogeneous penalties. The \mathcal{N}_{A_k} are normalization factors defined such that $\text{tr}(T_a^{A_k}T_b^{A_k}) = \mathcal{N}_{A_k}\delta_{ab}$. The S_∞ denotes the Rényi min-entropy of the reduced state of subsystem A_1 in the target state $|\psi_T\rangle$.

In our second example of an analytically computable binding complexity, we set $p = 1$ in the cost function (25). This binding complexity does not depend on the penalty factors for nonlocal generators (up to an overall normalization), under certain assumptions about the generators acting along the optimal trajectory. Consequently, changing the penalty factors cannot yield arbitrary functions of the Schmidt coefficients. Rather, for certain choices of the generators acting along the trajectory, the binding state complexity is a fixed function of the Schmidt coefficients, independent of the penalty factors. This independence implies that, within a certain class of cost functions, there is a universal relation between the entanglement of a state in a subsystem and its binding complexity.

The relationship between binding complexity and Schmidt coefficients leads to not only exact results, but also bounds imposed by other quantum-information quantities. For instance, one can lower-bound the binding state complexity, using the maximal entanglement rate [103–105]. Denote by S_{A_1} the entanglement entropy of subregion A_1 , by d the dimensionality of the smaller subsystem's Hilbert space, and by c a constant. The $p=1$ binding state complexity upper bounds S_{A_1} as follows:

$$\frac{S_{A_1}}{c \log d} \leq \mathcal{BC}_1^{\text{state}}[|\psi_R\rangle, |\psi_T\rangle]. \quad (29)$$

Binding complexity also provides lower bounds for other notions of complexity, such as the geometrically local complexity [106]. Further details on this quantity will be discussed around Eq. (142).

Finally, we anticipate a connection between binding complexity and a holographic dual in a black-hole background. The binding complexity has been conjectured to quantify multiboundary wormholes' interior volumes [95].

5.5. Complexity in quantum field theories

As we will review later, Nielsen's complexity experienced a revival following conjectured relationship with gravitational quantities. This connection is rooted in the holographic correspondence, which will be reviewed in Sec. 7. The holographic correspondence deals with QFTs – many-body quantum systems which do not conserve the particle number. To allow for a quantitative comparison with holographic conjectures, it was therefore essential to develop a concrete method for calculating complexity in QFTs. Naturally, the first examples studied were those of free QFTs, first bosonic [84, 85] and then fermionic [88, 89], which we review in subsection 5.5.1. While these calculations are too simple for an exact comparison with chaotic theories in general – and with holography in particular – this approach played a fundamental role in advancing the complexity community and bridging the gap between heuristic arguments and more rigorous calculations. This framework later inspired studies of complexity in more complicated field theories, including weakly interacting theories [91, 107], and conformal field theories, as described in subsections 5.5.2 and

5.5.3 below.

5.5.1. Free quantum field theories

The calculation of complexity in free field theories is based on Nielsen’s approach (see Sec. 5.1). In this framework, the evolution of quantum states along the circuit is treated continuously, with a cost assigned to each possible evolution. To simplify the problem, one often restricts the circuit evolution to unitary representations of finite-dimensional spaces. For free QFTs, this is typically achieved by restricting the circuits to transitions between Gaussian states. The groups underlying these circuits are the symplectic group for bosonic Gaussian states and the orthogonal group for fermionic Gaussian states.

Like many other quantities in QFT, complexity is expected to diverge. Intuitively, these divergences arise because quantum correlations must be built at arbitrarily short distance scales. Therefore, a regulator must be introduced to handle short distances, or equivalently, large momenta. The exact result depends on the choice of reference state, and in QFT, it is not immediately obvious which reference state to choose. Inspired by quantum computation, the reference state is often chosen to be completely unentangled, meaning it lies outside the Hilbert space of the non-regulated theory, leading to the observed divergences.

The study of complexity in scalar bosonic QFT began with [84, 85]. In these papers, the authors considered the following Hamiltonian for a scalar QFT in d -dimensional spacetime:

$$H = \frac{1}{2} \int d^{d-1}x \left[\pi(\vec{x})^2 + (\vec{\nabla}\phi(\vec{x}))^2 + m^2\phi(\vec{x})^2 \right]. \quad (30)$$

The relevant symplectic transformations were constructed using the (typically discretized set of) phase space degrees of freedom $\hat{\xi}^a = (\phi(\vec{x}), \pi(\vec{x}))$.¹⁵ Symplectic transformations of the form

$$\hat{U}(t) = \exp\left(-\frac{i}{2}\hat{\xi}^a k_{(ab)}(t)\hat{\xi}^b\right), \quad (31)$$

where $k_{(ab)}(t)$ is a symmetric matrix, move us between Gaussian states. A natural description of Gaussian states is in terms of their *covariance matrices* $G^{(ab)}$ and *displacement vector* ω^a defined as the first and second moments of the phase space variables

$$\text{Tr}\left(\hat{\rho}\hat{\xi}^a\hat{\xi}^b\right) = \frac{1}{2}\left(G^{(ab)} + i\Omega^{[ab]}\right), \quad \text{Tr}\left(\hat{\rho}\hat{\xi}^a\right) = \omega^a, \quad (32)$$

where $\hat{\rho}$ is the Gaussian density matrix, and $\Omega^{[ab]}$ encodes the anti-symmetric commutation relations of the phase space variables. The covariance matrices were not the original formulation used to study complexity in bosonic QFT. There, the authors only focused on squeezing operations, and therefore expressing everything in terms of the wavefunction was sufficient. Nevertheless the use of covariance matrices permits for more general transformations between Gaussian states which was employed in later studies, see e.g., [89, 90]. We will therefore stick with this approach in our presentation.

The quantum circuits generated by the unitary (31) can be rephrased in terms of the covariance

¹⁵These can alternatively be spanned using momentum-grid phase space variables $\hat{\xi}^a = (\phi(\vec{k}), \pi(\vec{k}))$

matrix and displacement vector as follows

$$\mathbf{G} = S\mathbf{G}S^T, \quad \boldsymbol{\omega} = S\boldsymbol{\omega}, \quad \text{where } S := e^{\Omega\mathbf{k}}, \quad (33)$$

Where \mathbf{G} , $\boldsymbol{\omega}$ and \mathbf{k} denote the covariance matrix, displacement vector and symmetric matrix in the circuit (31) and the explicit indices have been suppressed to shorten the notation. The control functions Y^I in equation (17) can be read as follows

$$Y^I = \frac{1}{2} \text{tr} (\partial_\sigma S S^{-1} K_I), \quad (34)$$

with K_I is an orthonormal basis for the symplectic group. This then serves as the input for the complexity calculation with the cost assigned according to equation (25).

When evaluating complexity in QFTs, there are several key choices to be made. The initial studies [84, 85] focused on the simplest possible choices. The cost functions were selected according to equation (25), with $q_I = 1$ and $p = 1, 2$. Only squeezing operations were considered in these early works. The target state was taken to be the regularized ground state of the bosonic field theory (30). Regularization was implemented via either a lattice discretization or a sharp momentum cutoff. The reference state was chosen as the ground state of the Hamiltonian

$$H = \frac{1}{2} \int d^{d-1}x [\pi(\vec{x})^2 + \mu^2 \phi(\vec{x})^2], \quad (35)$$

where μ is a characteristic energy scale. This Hamiltonian describes a set of independent, or unentangled, oscillators with a characteristic frequency μ . When constructing correlations at all scales, it is natural to begin with a state whose frequency is on the order of the inverse lattice spacing, so we define $\tilde{\mu} := \mu\delta$, where δ is the lattice spacing.

The original papers [84, 85] focused primarily on the structure of divergences and found some degree of agreement with holographic results. In particular, they calculated the complexity of the vacuum state of a free bosonic theory, which reads:

$$\begin{aligned} \mathcal{C}_{p=1}^{\text{upper bound}} &= \frac{1}{2} \int d^d k |\log(\omega_k/\mu)| \simeq \frac{\mathcal{V}}{2\delta^{d-1}} |\log(\tilde{\mu})| + \dots, \\ \mathcal{C}_{p=2} &= \frac{1}{2} \sqrt{\int_k [\log(\omega_k/\mu)]^2} \simeq \frac{1}{2} \left(\frac{\mathcal{V}}{\delta^{d-1}} \right)^{\frac{1}{2}} |\log(\tilde{\mu})| + \dots, \end{aligned} \quad (36)$$

where for $p = 1$ only an upper bound was found. In the previous equation \mathcal{V} stands for the spatial volume of the system, δ is an ultraviolet cutoff (for example a lattice spacing) and the dots stand for less divergent terms. The full details of these calculations can be found in the original references and in the pedagogical review [2]. These results should be contrasted with those obtained from holography (114). We will later see that the $\mathcal{C}_{p=1}$ expression matches well with the volume-law divergence found in holographic calculations, see Eq. (114). Additionally, the choice of reference scale in the field theory parallels the choice of the counterterm scale L_{ct} in holography, as we will see in, e.g., Equation (117a).

Subsequent studies explored a variety of alternative choices in the complexity calculations. These included different cost functions, free theories with other fields such as charged bosons, fermions,

and gauge fields, weakly interacting theories and other target states, including the thermofield-double state, and mixed states [88–95, 107–112]. These studies concluded that, in general, the structure of divergences observed in QFT complexity calculations qualitatively matches the results from holography. This is not particularly surprising, since at very short distances (or equivalently, near the cutoff scale), the precise details of the theory tend to become irrelevant. On the other hand, the time dynamics of the theory shows significant deviations from holographic results, which is to be expected, as free and chaotic theories typically exhibit very different dynamical behavior. In particular, a natural expectation is that in free systems in finite volume upon penalization of Gaussian gates coupling distant parts complexity growth associated with Hamiltonian time evolution will terminate at times of the order of the volume (and even sooner without the aforementioned penalization [90]). In chaotic systems, one expects the complexity growth to occur over significantly longer timescales, exponential in the volume.

While many basic insights were obtained from the above approach, as mentioned earlier, it fails to reproduce many important properties of holographic complexity including those related to its temporal dynamics. This motivated a shift of focus to the study of complexity in field theories more closely related to holography. This includes attempts to study complexity in conformal field theories focusing on universal conformal symmetry, which will be described in the following subsections.

5.5.2. Two dimensions - complexity of Virasoro circuits

Nielsen’s geometric approach is certainly very appealing from a mathematical (geometric) point of view, and it is tailor-made to mimic discrete quantum circuits built with gates available in our laboratories. However, defining gates in a generic QFT is not obvious and might generally involve considering all local operators, as an operator product can be represented as a sum over local operators within the operator product expansion. On top of that comes a question of choosing a meaningful cost function giving rise to an optimization problem that is not completely out of control.

These challenges forced the community to approach the problem of Nielsen’s complexity in QFT in a creative way. The progress made can be ultimately traced to originate from [30], which proposed to study Nielsen’s complexity of conformal transformations in 2-dimensional CFTs, i.e. coordinate transformations that preserve the form of the metric up to an overall scalar factor.

The immediate advantage of this approach was that it focused on universal properties shared by all CFTs, regardless of the value of the interaction strength. As a result, it brought a promise of finding precise gravitational realizations of complexity within holography. This goal was at least partially reached, as we will review in Sec. 7. Of course, this universality poses also a significant restriction, as resulting complexity measures will be insensitive to the microscopic dynamics with the results not allowing to distinguish between chaotic and integrable QFTs.

The connection with gates being local operators in a QFT occurs due to conformal transformations being generated by the most universal local operator present in any QFT, the energy momentum-tensor, smeared over a time-slice. For example, a familiar case of the conformal transformation is time translation generated by the Hamiltonian, which in turn is an integral over energy density - the time-time component of the energy-momentum tensor.

In more details, the setup of [30] and subsequent studies focused on in two-dimensional CFTs living on a Lorentzian cylinder. The spatial circle of unit radius will be parametrized by σ and the physical time as t , see Fig. 6. In two dimensions the energy-momentum tensor of a CFT has

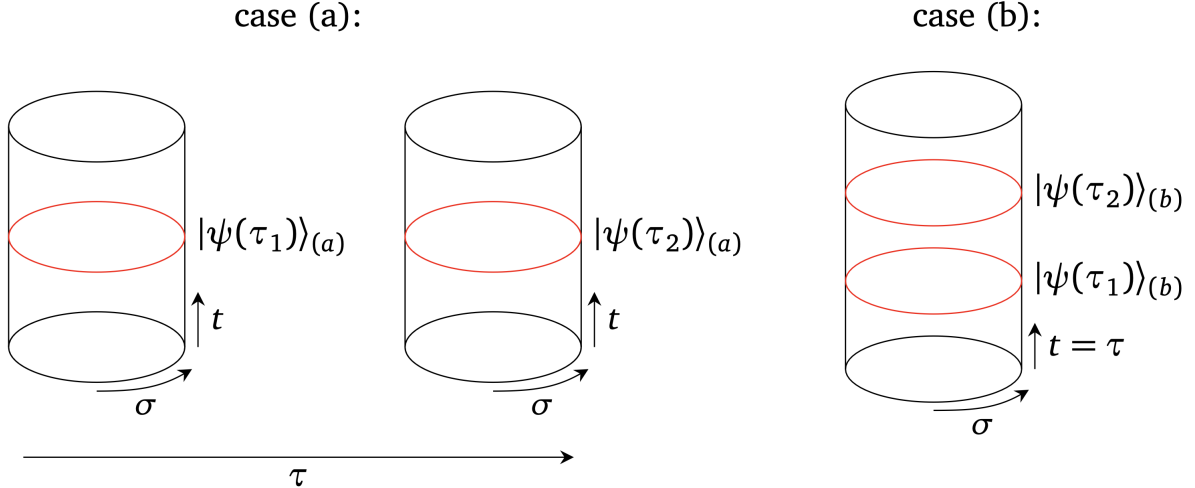


Figure 6: Two kinds of circuits one can consider in the context of conformal transformation in particular and QFT circuits more generally. In the latter situation one should think of σ as a set of coordinates on spatial slices. Case a): The circuit parameter τ is an auxiliary parameter whose increase takes one CFT state to another CFT state. The transformation does not lead to a shift in the physical time t . This is the setting addressed in [30]. Case b): The circuit parameter τ is identified with the physical time t , as considered for the first time in [113]. Figure adapted from [113].

two independent components that happen to commute with each other. In the following we will predominantly focus on one of them only, taken to be $T(\sigma) \equiv \frac{1}{2}T_{tt} + \frac{1}{2}T_{t\sigma}$. The algebraic structure underlying this construction is that of the Virasoro algebra

$$[L_n, L_m] = (n - m)L_{n+m} + \frac{c}{12}n(n^2 - 1)\delta_{n+m,0}. \quad (37)$$

whose generators L_j are related to Fourier modes of $T(\sigma)$

$$T(\sigma) = \sum_{n \in \mathbb{Z}} \left(L_n - \frac{c}{24}\delta_{n,0} \right) e^{-in\sigma}. \quad (38)$$

In the above expressions c is the central charge of the CFT, which can be thought of as measuring the number of degrees of freedom in the following sense: for N free boson CFTs $c = N$, which is the number of bosonic degrees of freedom (whereas for N free fermion CFTs, $c = \frac{N}{2}$). In holography, where the boundary CFTs are strongly coupled, $c \rightarrow \infty$. Since the algebra is the same for CFTs with the same value of c , one explicitly sees here the point we introduced earlier: the properties of Virasoro algebra-based complexity will not differ between $N \rightarrow \infty$ free bosons and strongly coupled holographic theories.

The setup of interest for [30] as well as subsequent works including [114, 115, 115, 116] are continuous unitary circuits

$$U(\tau) = \overleftarrow{\mathcal{P}} \exp \left[\int_0^\tau Q(\tau') d\tau' \right]. \quad (39)$$

acting on a CFT Hamiltonian eigenstate $|h\rangle$ with the label h corresponding to a primary operator with conformal dimension h ($h = 0$ gives the vacuum state). The circuit generator in (39) is a

smearred component of the energy-momentum tensor operator over the full time slice

$$Q(\tau) := \int_0^{2\pi} \frac{d\sigma}{2\pi} \epsilon(\tau, \sigma) T(\sigma) = \sum_{n \in \mathbb{Z}} \epsilon_n(\tau) \left(L_{-n} - \frac{c}{24} \delta_{n,0} \right), \quad (40)$$

where

$$\epsilon(\tau, \sigma) \equiv \sum_{n \in \mathbb{Z}} \epsilon_n(\tau) e^{-in\sigma}. \quad (41)$$

In comparison with Eq. (17) discussed in the context of qubit systems, the integral over σ is the analogue of the summation over the I -index, the $\epsilon(\tau)$ factor is the tangent space velocity $Y^I(t)$ and the generators can be thought of as $T(\sigma)$. Alternatively, one can use the Virasoro generators as defining circuit generators in which case summation over them is the analogue of I in Eq. (17) and the tangent space velocity is related to $\epsilon_n(\tau)$.

In considering the complexity there is an important choice to be made regarding the interpretation of the τ parameter [113]. The first choice is to regard it as an auxiliary parameter with respect to the physical time t , see case (a) in Fig. 6. For this choice, relevant for [30], the function $\epsilon(\tau)$ associated with the diffeomorphism $\sigma \rightarrow f(\tau, \sigma)$ is given by

$$\epsilon(\tau, \sigma) = \frac{\partial_\tau f(\tau, \sigma)}{\partial_\sigma f(\tau, \sigma)}. \quad (42)$$

The hardness minimization problem at hand concerns now finding a function of two parameters $f(\tau, \sigma)$ subject to the condition $f(\tau = 0, \sigma) = \sigma$ and $f(\tau = 1, \sigma) = f(\sigma)$, where $f(\sigma)$ is a desired diffeomorphisms that transforms the state $|h\rangle$ according to the CFT rules.

The papers [30, 114, 115, 117] uncovered and developed a very beautiful relation between optimizing cost functions

$$F[\epsilon] = \sqrt{\int_0^{2\pi} d\sigma \int_0^{2\pi} d\kappa \Pi(\sigma - \kappa) \epsilon(\tau, \sigma) \epsilon(\tau, \kappa)}, \quad (43)$$

and Euler-Arnold-type partial differential equations (PDEs) of significant relevance for mathematical physics. In particular, for the penalty schedules of the form

$$\Pi(\sigma - \kappa) = a \delta(\sigma - \kappa) + b \delta''(\sigma - \kappa) \quad (44)$$

with a and b being constants and $\delta(\sigma - \kappa)$ being the Dirac delta function, the solutions of the optimization problem are the solutions of the following paradigmatic PDEs [115]

- Korteweg-de Vries equation predicting solitons: $a = 1, b = 0$,
- Hunter-Saxton equation relevant for liquid crystal physics: $a = 0, b = 1$,
- Camassa-Holm equation modelling wave breaking: $a = 1, b = 1$.

Furthermore, Refs. [115, 117] considered the Fubini-Study cost which corresponds to Eq. (43) with

$$\Pi(\sigma - \kappa) = \frac{c}{32 \sin^4((\sigma - \kappa)/2)} - \frac{h}{2 \sin^2((\sigma - \kappa)/2)}, \quad (45)$$

and solved the associated optimization in a perturbative manner for sample conformal transformation close to identity. This result was subsequently used for comparisons with holography, building on [118], see Sec. 7.

There are further generalizations of the approach described above. In [114] an additional global symmetry was incorporated connecting with the rich literature of the Kac-Moody groups. Furthermore, in [119] a scalar primary operator as an additional generator on top of the energy-momentum tensor operator was incorporated in a perturbative manner. The main limitation of the works prior to [119] is that the previously described unitary circuits remain bounded inside a conformal family (the so-called *Verma module*) of the Virasoro algebra, which is unrealistic. Results in [119] concern trajectories that move between different Verma modules in a given CFT and lessons on the dependence of the Fubini-Study cost of such circuits on the source function of the primary generator. This constitutes an important first step towards the general picture of Nielsen's complexity with local operators viewed as generators advocated above.

Finally, another line of works devoted to complexity in CFT was concerned with circuits in which the physical time t is the circuit parameter τ [34, 113, 116], see Fig. 6 case (b). In the context of the examples considered, this approach requires slightly different choice of the circuit velocity $\epsilon(t, \sigma)$. The main advantage of this approach is making the direct contact with the spacetime (path integral) formulation of QFTs. Since holography is naturally formulated in the language of path integrals, this led to the embedding of quantum circuits similar to the ones discussed in the present section on the boundary of the AdS spacetime and allow to find explicit gravitational duals to quantum circuits and the Fubini-Study cost function [34].

5.5.3. Circuits in the conformal group in $d \geq 2$

As we have just shown in Sec. 5.5.2, the computation of Nielsen's complexity is a challenging task for infinite-dimensional quantum systems as the number of generators to consider is infinite. However, a simplification occurs if a system in question realizes a finite dimensional symmetry group G . This leads to soluble instances of the Nielsen's complexity, as envisioned originally in [120]. In this context, the global conformal group $\text{SO}(d, 2)$ associated with symmetries of the vacuum of CFTs in d spacetime dimensions plays a key role in connection to holography, since it coincides with the local isometries of AdS spacetime. Within the setup discussed in Sec. 5.5.2 this corresponds to the subgroup¹⁶ of the Virasoro algebra associated with the generators L_{-1} , L_0 and L_1 .

This framework is similar to the qubit setup discussed in Sec. 5.1, with the exception that we now consider a unitary representation of a (possibly non-compact) Lie group G .¹⁷ For concreteness, a generic trajectory on the conformal group can be constructed out of the generators P_μ , D , $L_{\mu\nu}$

¹⁶The global conformal group for CFTs living in two spacetime dimensions, $\text{SO}(d, 2)$, factorizes into a product of two $\text{SO}(1, 2)$. The Virasoro generators considered in Sec. 5.5.2 correspond to one of these $\text{SO}(1, 2)$. The other $\text{SO}(1, 2)$ originates from the remaining independent component of the energy-momentum tensor operator being $\frac{1}{2}T_{tt} - \frac{1}{2}T_{t\sigma}$.

¹⁷One can always build a unitary and finite-dimensional representation of a Lie group by using Euclidean generators.

and K_μ (translations, dilatations, rotations and special conformal transformations) as follows,

$$U(\sigma) = e^{i\alpha(\sigma)\cdot P} e^{i\gamma_D(\sigma)D} \left(\prod_{\mu<\nu} e^{i\lambda_{\mu\nu}(\sigma)L_{\mu\nu}} \right) e^{i\beta(\sigma)\cdot K}, \quad (46)$$

where α_μ , γ_D , $\lambda_{\mu\nu}$ and β_μ are complex variables, and $\sigma \in [0, 1]$ is a path parameter along the circuit. The reference state is chosen to be a primary state $|\Delta\rangle$, such that $D|\Delta\rangle = \Delta|\Delta\rangle$ and $K_\mu|\Delta\rangle = L_{\mu\nu}|\Delta\rangle = 0$. The states reached by the unitaries (46) live within the same conformal family; the extension to a larger family of CFT states is still an open question.

From now until the end of the Section, we will discuss the Nielsen's state complexity associates with a target state $|\psi_R\rangle$, reached by acting on a primary state $|\Delta\rangle$ with a unitary operator of the form (46). The projection of a Riemannian right-invariant cost function from a Lie group G to the coset space G/H (where H is the maximal proper subgroup of a state) is unique, and it is defined by a pseudo-Riemannian submersion. This statement provides a systematic procedure to induce a metric from the conformal group $\text{SO}(d, 2)$ to the coset space $\mathcal{B} = \frac{\text{SO}(d, 2)}{\text{SO}(2) \times \text{SO}(d)}$. Moreover, the projection procedure is equivalent to two other ways of generating a metric over the quotient: the minimization in Eq. (23), and the use of a geometric action associated with the geometry of coadjoint orbits [121].

A coadjoint orbit is the space of all equivalent configurations that can be reached by acting with the symmetry group on a point in the dual space of the corresponding Lie algebra. Physically, it represents a phase space corresponding to a fixed value of a conserved charge, where the symmetry group of the system allows movement within this space. Two cost function candidates were considered in the literature in this context [30, 32]

$$ds_{\text{FS}} = F_{\text{FS}} d\sigma \equiv \left(\langle \psi_R | dU^\dagger dU | \psi_R \rangle - |\langle \psi_R | U^\dagger dU | \psi_R \rangle|^2 \right)^{1/2}, \quad (47a)$$

$$F_{p=1, \vec{q}=1} d\sigma = |\langle \psi_R | U^\dagger dU | \psi_R \rangle|. \quad (47b)$$

The Fubini-Study (FS) line element ds_{FS} given by Eq. (47a) has two advantages as a cost function. The first one is general and stems from ds_{FS} utilizing the fundamental notion of a scalar product, which makes it realizable in exactly the same in any quantum system. The second advantage is specific to the present setup and concerns the Fubini-Study metric being the natural metric on the coset space \mathcal{B} of the conformal group, whose geodesics are known. There are also two features of the Fubini-Study cost that one may view as its limitations. The first one is related to the fact that the Fubini-Study metric is a variance of the circuit Hamiltonian in an instantaneous state. As a result, it is different from the standard Nielsen's complexity costs, such as (25), which assign the same hardness to a given circuit Hamiltonian no matter where it appears in the circuit. The second limitation of the Fubini-Study metric is the impossibility of introducing penalty schedule while retaining this and other of its virtues.

On the other hand, while the candidate cost $F_{p=1, \vec{q}=1}$ given by Eq. (47b) is naturally connected to the geometric action associated with coadjoint orbits, it assigns nonzero cost also to gates that change a state only by a phase. As a result, it is not a good cost function to consider [115, 117].

It is still an open problem to generalize the results of [32] to account for non-trivial penalty factors; this is the subject of ongoing research [121].

6. Paradigms for complexity II: Krylov and spread complexities

In the previous sections, we explained notions of complexity that arise from thinking about physical time evolution as a computation. From this perspective, the complexity of a physical process is quantified by asking how many elementary or cheap operations are needed to effect it, given some fixed repertoire of operations or a function quantifying their cost. Alternatively, consider that in classical physics, if we start with systems populating some small compact region of phase space, we might call the dynamics “simple” if these initial conditions are transported to some other small region of phase space at a later time. We might call the dynamics “complex” if the initial systems are spread out throughout the phase space by the dynamics. A notion of quantum complexity quantifying this sort of spread would seem to have a natural relation to physical phenomena like thermalization and chaos in quantum many-body systems and QFT.

One approach in quantum mechanics is to quantify the growth of different operators over time via the notion of *Krylov complexity* developed in [16]. Alternatively, we could ask how different initial states dynamically explore the Hilbert space during unitary evolution via the notion of *spread complexity* developed in [17]. These approaches are related, but each of them is convenient for answering different questions. In both approaches, the key insight is to recognize that, while physicists often analyze quantum systems by diagonalizing the Hamiltonian to extract the density of states, it is much more convenient to *tri-diagonalize* the Hamiltonian if we want to study dynamics. The diagonal and immediately off-diagonal components of the triadiagonalized Hamiltonian are called the Lanczos coefficients, and *any* quantum dynamics can be written as a one-dimensional hopping chain in terms of the Lanczos coefficients and the associated Krylov basis for the Hilbert space. Among other things, this representation of a quantum system makes it possible to explicitly quantify and compute how a quantum wavefunction or an operator spreads under Hamiltonian dynamics across the Hilbert space or operator space.

Below, we describe the conceptual basis of Krylov and spread complexity, and how to compute these quantities. We will present numerical methods, analytical results in systems with a lot of symmetry, and a general analytical formula relating the density of states of a system to its Lanczos coefficients. We will also present a formula for the correlations in the Lanczos coefficients of Random Matrix Theories. Along the way, we will relate these ideas to Nielsen complexity, and describe applications to the study of chaos and integrability. In the next Section, devoted to holography, we will describe a precise relationship between the length of wormholes in the two-dimensional JT gravity, and the spread complexity of the Thermofield Double state of the dual SYK model, see Sec. 7.5.1. Readers may also wish to consult the excellent recent review [3].

6.1. Spread complexity of evolving states

Consider unitary time evolution of some initial quantum state $|\Psi_0\rangle$

$$|\Psi(t)\rangle = e^{-iHt}|\Psi_0\rangle = \sum_{k=0}^{\infty} \frac{(-it)^k}{k!} H^k |\Psi_0\rangle, \quad (48)$$

where H is a time-independent Hamiltonian. Since the evolution is unitary, the state at any given time is just a fixed vector in the Hilbert space. Standard methods, including the Out-Of-Time-Order-Correlation (OTOC, see definitions in Sec. 2), quantify how time evolution spreads a collection of nearby states through the Hilbert space. At least at early times, this process can be

characterized by computing quantities akin to the Lyapunov exponent. Instead, we will quantify how widely the trajectory of a *single* state explores the Hilbert space over time. One way of doing this is to measure the spread of the support of a time-evolving state in some fixed basis. Which basis should we pick? The early work of Kolmogorov, defining the complexity of sequences as the size of the smallest Turing machine that produces them, suggested a paradigm: the complexity of a system should be measured in terms of the size of its minimal representation. Taking this perspective, we could define the complexity of an evolving state by minimizing the spread of the wavefunction over all possible bases. The authors of [17] proved that there is a unique orthonormal minimizing basis throughout a finite time interval for continuous evolution, and at all times in the case of discrete evolution. This is the Krylov basis which can be constructed by a variety of methods described below.

For discrete time evolution, a simple argument explains how the Krylov basis minimizes the spread of the wavefunction. Consider an initial state $|\psi_0\rangle$, and a basis supporting the state on a single basis element $|K_0\rangle = |\psi_0\rangle$. Time evolution produces the state at time 1 as $|\psi_1\rangle = U_1|\psi_0\rangle$, where U_1 is a unitary operator. By picking the second basis element $|K_1\rangle$ to be proportional to the part of $|\psi_1\rangle$ orthogonal to $|\psi_0\rangle$, we can support $|\psi_1\rangle$ on two basis elements, $\{|K_0\rangle, |K_1\rangle\}$. Continuing in this way by recursively orthogonalizing the time-evolving state, we produce a basis that obviously minimizes the support of the state at any time. The analogous proof for continuous time evolution is more subtle and is described in [17].

6.1.1. Recursion method and tridiagonalization

To represent the time evolving state (48) in the minimizing Krylov basis for continuous time evolution, we write

$$|\Psi(t)\rangle = \sum_{k=0}^{\infty} \frac{(-it)^k}{k!} H^k |\Psi_0\rangle = \sum_{n=0}^{\mathcal{K}-1} \psi_n(t) |K_n\rangle, \quad (49)$$

where \mathcal{K} is the dimension of the span of the time-evolving state, $|K_0\rangle = |\psi_0\rangle$, and the remaining $|K_n\rangle$ are constructed by the iterative Lanczos algorithm [122]:

$$|A_{n+1}\rangle = (H - a_n)|K_n\rangle - b_n|K_{n-1}\rangle, \quad |K_n\rangle = b_n^{-1}|A_n\rangle. \quad (50)$$

The Lanczos coefficients a_n and b_n are defined as

$$a_n = \langle K_n | H | K_n \rangle, \quad b_n = \langle A_n | A_n \rangle^{1/2}, \quad (51)$$

with $b_0 = 0$. This procedure is just a systematic way of applying Gram-Schmidt orthonormalization to the Krylov subspace $\{H^k|\Psi_0\rangle\}$, and will terminate at some $n = \mathcal{K}$ for which $b_{\mathcal{K}} = 0$. Thus \mathcal{K} , the dimension of the Krylov basis, measures the dimension of the subspace of the Hilbert space explored by time evolution of the initial state.

Tridiagonalization. The construction (50) implies that the Hamiltonian acts tridiagonally in the Krylov basis

$$H|K_n\rangle = a_n|K_n\rangle + b_n|K_{n-1}\rangle + b_{n+1}|K_{n+1}\rangle. \quad (52)$$

In other other words, the Hamiltonian in this basis can be written as a matrix with entries a_n along the diagonal, and entries b_n just above and below it. For finite dimensional systems, this is called the Hessenberg form of the Hamiltonian. Numerically stable algorithms for computing the

Hessenberg form of a matrix are implemented by standard libraries in Python and Mathematica (see [17]). These methods improve upon the numerically unstable Lanczos procedure, but generally require a change of basis to represent the desired initial state in a canonical form required by the implemented algorithm. We can use the Hessenberg form to extract the Lanczos coefficients without explicitly constructing the Krylov basis.

Finally, differentiating Eq. (49) with respect to t and using Eq. (52), we find the Schrödinger equation

$$i\partial_t\psi_n(t) = a_n\psi_n(t) + b_n\psi_{n-1}(t) + b_{n+1}\psi_{n+1}(t), \quad (53)$$

that we should solve with the initial condition $\psi_n(0) = \delta_{n,0}$. This equation describes the dynamics of an effective “particle” hopping on a one-dimensional chain with sites labeled by the Krylov index $n \in \{0, 1, 2, \dots\}$. The Lanczos coefficients a_n determine the probability for staying at site n , whereas b_n determine the probability of hopping to the left or right. Thus, the procedure we have described reduces *any* quantum dynamics to an effective one-dimensional hopping chain – i.e., a quantum Markov process – where the states defining the chain and transition coefficients are determined from the initial state $|\psi_0\rangle$ and the Hamiltonian.

6.1.2. Moment method and the survival amplitude

The Lanczos coefficients can be efficiently extracted from the moments of the Hamiltonian in the initial state

$$\mu_n = \langle K_0 | (-iH)^n | K_0 \rangle. \quad (54)$$

To see why, suppose that a quantum system is localized, at $t = 0$, in the initial state $|K_0\rangle$. The Markov-like structure of Eq. (52) means that the probability amplitude for remaining in $|K_0\rangle$ after one application of the Hamiltonian is $-ia_0$, while the amplitude for transitioning to $|K_1\rangle$ is $-ib_1$. Next, let us apply the Hamiltonian a second time. The amplitude to wind up in $|K_0\rangle$ again is $i^2(a_0^2 + b_1^2)$. But we already know a_0 from the first step. So if we also know the second moment of the Hamiltonian $\langle K_0 | H^2 | K_0 \rangle$ through some means, then we can extract b_0 by subtracting a_0^2 and taking a square root. Proceeding recursively in this way, we can show that each successive moment allows the extraction of an additional Lanczos coefficient – the a_n are computed from the odd moments by dividing out products of already computed b_n s, and the b_n s are likewise computed from the even moments. Applied numerically, this procedure is potentially sensitive to rounding errors from repeated divisions, but there are methods for circumventing this potential obstacle [17]. We can use the moment method to compute the Lanczos coefficients without constructing the Krylov basis.

6.1.3. Survival amplitude

The moments of the Hamiltonian are all encoded in the so-called *survival* or *return* amplitude for the state to remain unchanged over time:

$$S(t) \equiv \langle \psi(t) | \psi_0 \rangle = \langle \psi_0 | e^{-iHt} | \psi_0 \rangle \implies \mu_n = \langle K_0 | (-iH)^n | K_0 \rangle = \left. \frac{d^n}{dt^n} S(t) \right|_{t=0}. \quad (55)$$

So if we have access to the survival amplitude through some other means, we can use it as a moment generating function for the Hamiltonian, and then proceed as described above to extract the Lanczos coefficients without explicitly constructing the Krylov basis. For example, consider a thermofield

double state¹⁸

$$|\psi_\beta\rangle = \frac{1}{\sqrt{Z_\beta}} \sum_n e^{-\beta E_n} |n, n\rangle, \quad (56)$$

an entangled state in two copies of the same system. Tracing over either copy yields the thermal density matrix with partition function Z_β in one copy. Suppose the two copies have Hamiltonians H_L and H_R . Time evolution by $H = (H_L + H_R)/2$ or separately by $H = H_{L,R}$ produces the state

$$|\psi_\beta(t)\rangle = e^{-iHt} |\psi_\beta\rangle = |\psi_{\beta+2it}\rangle, \quad (57)$$

and the associated analytically continued partition sum $Z_{\beta-it} = \sum_n e^{-(\beta-it)E_n}$. A short calculation shows that the survival amplitude can be written as

$$S(t) = \langle \psi_{\beta+2it} | \psi_\beta \rangle = \frac{Z(\beta - it)}{Z(\beta)}. \quad (58)$$

Thus, given an analytic form for the partition sum of a system, we can analytically continue to compute the survival amplitude for the thermofield double, and hence its Lanczos coefficients following the procedure discussed above. It is also interesting to note that the square of this survival amplitude is precisely the spectral form factor

$$\text{SFF}_{\beta-it} = \frac{|Z_{\beta-it}|^2}{|Z_\beta|^2}, \quad (59)$$

which has been used to study late time quantum chaos [123, 124] in random matrix theory and quantum gravity, quantum speed limits [125], and other phenomena that depend on energy spectrum statistics.

6.1.4. Coarse-grained Lanczos spectrum and the density of states

Suppose we tridiagonalize the Hamiltonian by the recursion method or the moment method, as described above. The resulting Hamiltonian, written entirely in terms of the Lanczos coefficients, should still have the same spectrum as the original one. So we may wonder whether we can directly relate the energy spectrum, or equivalently the density of states, to the tridiagonal Lanczos spectrum (i.e., the distribution of Lanczos coefficients). Indeed, as we will discuss below, we can find such a relation in the limit of large system size, given some smoothness assumptions and after coarse-graining the Lanczos spectrum [126].

Consider a quantum system with an N dimensional Hilbert space. Let n be the Lanczos index and define $x = n/N$. In the large N limit, x is a real number between 0 and 1 and it is convenient to write the Lanczos coefficients as functions $a(x)$ and $b(x)$ instead of as a_{xN} and b_{xN} . Let us consider Hamiltonians and initial states for which $a(x)$ and $b(x)$ have a continuous large N limit. As we will explain, if the large N limit is continuous in this way, there is an analytical formula relating the density states of the theory to the Lanczos spectrum, coarse-grained in a way that we describe below.

Recall from Sec. 6.1.1 that the Lanczos coefficients a_n and b_n describe hopping dynamics on a

¹⁸The notation in Eq. (56) is analogous to Eq. (5) in the key notions. Here we stress the dependence of the state on the inverse temperature β .

one dimensional chain defined by the Krylov basis. Cut this chain into segments of length L such that $L/N \rightarrow 0$ at large N . For example, we can take $L \sim \sqrt{N}$. We are assuming that $a(x)$ and $b(x)$ with $x = n/N$ have a continuous large N limit. This requires that a_n and b_n vary slowly within the blocks of length L . Coarse-graining over these blocks, which represent infinitesimal intervals of x , we can approximate the Hamiltonian as consisting of N/L blocks within each of which the Lanczos coefficients are constant, i.e., it is Toeplitz. A standard formula from linear algebra then tells us that the energy eigenvalues associated to the block of size L are $E_k = 2b \cos(k\pi/(L+1)) + a$ for $k = 1, \dots, L$, where a and b are the constant values of the Lanczos coefficients in the block. Thus, keeping in mind from the Lanczos algorithm that we can take a real and b positive, the density of states within each segment is

$$\rho_{(a,b)}(E) = \frac{1/L}{|dE_k/dk|} = \frac{H(4b^2 - (E - a)^2)}{\pi \sqrt{4b^2 - (E - a)^2}}. \quad (60)$$

The union of the block eigenvalues must reproduce the complete energy spectrum. In the large N limit both $L \sim \sqrt{N}$ and N/L are large, so we can write the full density of states as an integral over the blocks indexed by x :

$$\rho(E) = \int_0^1 dx \frac{H(4b(x)^2 - (E - a(x))^2)}{\pi \sqrt{4b(x)^2 - (E - a(x))^2}}. \quad (61)$$

This analytical formula universally relates the density of states and the coarse-grained Lanczos coefficients for large systems. For the systems like the SYK model and Random Matrix Theories that are defined by ensembles of Hamiltonians, this formula will also relate to the ensemble average of Lanczos coefficients for random initial states. The authors of [126] give a more formal analysis for why this formula is true, and explain how to invert it to calculate $a(x)$ and $b(x)$ from the density of states. The formula is valid for initial states for which the large N limit of $a(x)$ and $b(x)$ is continuous, and so long as x is not too close to the edge, i.e., $x \sim O(1/N)$. At the edge we have to use the recursion or moment methods described above to find the Lanczos coefficients step by step.

6.1.5. Defining spread complexity

Suppose we have derived the Lanczos spectrum using one of the methods described above. We can use it to solve the Schrödinger equation (53) for the wavefunction in Krylov basis (49). Squaring the $\psi_n(t)$ yields a probability distribution that quantifies the spread of the wavefunction over the Krylov basis

$$p_n(t) := |\psi_n(t)|^2, \quad \sum_{n=0}^{\mathcal{K}-1} p_n(t) = 1. \quad (62)$$

From the 1d chain perspective, the wavefunction starts out localized on $|K_0\rangle$. As time passes the peak of the wavefunction moves to the right (higher Krylov index n) and spreads out. The wavefunction has a sharp, tsunami-like edge as it moves outward [17]. This recalls the sharp edge seen in the spread of entanglement after a quench [127–131] at least in two dimensional conformal systems and in theories with a holographic dual. In chaotic systems like Random Matrix Models (RMTs), the spreading wavefunction retains this coherence until it “bounces off” the end of the Krylov chain ($n = \mathcal{K}$) and settles down to equilibrium with broad support on all the basis elements. As we will discuss below, this bounce arises distinctively from the spectral correlations in

chaotic theories. This was illustrated in [17] by comparing chaotic RMTs in the Gaussian Unitary, Orthogonal, and Symplectic Ensembles (GUE, GOE, GSE) with systems having the same density of states but Poisson, i.e., uncorrelated, spectral statistics.

Complete information about the spread of the wavefunction is contained in the distribution (62). We could quantify the width of this distribution in various ways. For example, we could consider moments of the distribution $\langle n^s \rangle = \sum_n n^s p_n(t)$. The first moment, or average position in the Krylov chain, was called the *spread complexity* in [17]

$$\mathcal{C}_K(t) = \langle n \rangle = \sum_n n p_n(t), \quad (63)$$

and the analogous quantity for the spread of operators (which we will discuss below) is often referred to as the Krylov complexity (its study was initiated in [16]). These quantities have proved useful in characterizing many aspects of quantum dynamics and, as we will discuss in Sec. 7, turn out to be geometrized in the duality between the SYK model and Jackiw-Teitelboim gravity as the wormhole's length.

While the spread complexity in (63) has turned out to have many applications, alternative measures of the spread of the wavefunction surely also have uses. First of all there are the higher moments we mentioned above – see, e.g., [132]. Another natural measure of spread would be the entropy of the distribution (62) or its exponential

$$H(t) = - \sum_{n=1}^{\kappa-1} p_n(t) \ln p_n(t) \quad ; \quad C_H(t) \equiv e^{H(t)}, \quad (64)$$

This quantity was studied in the operator and state contexts in [133–136], but has not yet been widely applied.

Of course, we could have defined a distribution like (62) in any basis. The proofs in [17] demonstrated that the Krylov basis minimizes both spread complexity $\mathcal{C}_K(t)$ and the entropic measure $C_H(t)$ at least in some finite time interval starting at $t = 0$. The Krylov basis is also, in a sense, the most classical representation of the spreading wavefunction. This is because, as shown in [137], the Wigner function associated to the one dimensional Krylov chain has the lowest possible negativity as compared to any other basis. The Wigner function is the closest thing in quantum mechanics to a classical description of the state. Indeed, a quantum system with a Wigner function that is everywhere positive for all times can be efficiently simulated on a classical computer through standard methods for describing statistical systems. But if the Wigner distribution has negative regions, quantum phenomena play an essential role, indicating a likely advantage for quantum computers in simulating these systems.

Below we will apply these methods to many physical systems including particles moving on group manifolds, spin systems, the SYK model, random matrix theories (RMTs), and Jackiw-Teitelboim gravity. For lack of space we will not discuss applications to quantum billiards [138–140], which are especially fascinating because such systems can have vanishing Lyapunov exponents, but can nevertheless manifest chaos. In some of these systems such as the SYK model and RMTs, there are efficient techniques to calculate the average of the survival amplitude $\overline{S(t)}$ over an ensemble of theories. Note that in these cases $\overline{S(t) S(t')}$ need not equal $\overline{S(t) S(t')}$. This similarly implies that correlations between Lanczos coefficients that affect the structure of the dynamics must be directly

computed and will not be accessed by just computing the average of these coefficients over the pertinent ensemble. Above we focused entirely on systems with time-independent Hamiltonians. It would be interesting to extend the methods to systems with time-varying Hamiltonians. We also only discussed closed systems and pure quantum states, but many of the techniques can be extended to open systems and mixed states [141, 142], as reviewed in [3]. Since the density matrix describing mixed states can be considered an operator on the Hilbert space, it is natural to think about this in terms of the spread of operators, to which we turn now.

6.2. Krylov complexity of evolving operators

In Sec. 6.1, we followed [17] to quantify how quantum states spread dynamically over the Hilbert space. In this section we will discuss a similar approach to the spread of operators [16], which was introduced earlier than Ref. [17]. We started with a description of the spread of states because it is technically simpler to some extent, and the proofs of minimality of the Krylov basis were developed in that context. But the relation between the operator-based methods of this subsection and the state-based methods of the previous section is analogous to the relation between the Heisenberg and Schrödinger approaches to quantum mechanics – either approach may be more convenient depending on the question we are studying.

The idea of defining operator size through an expansion in a natural basis was, to our knowledge, first explored in holographic systems such as the SYK model [143–146]. This concept was later quantified in [16], whose authors studied operator spread in the Krylov basis, and proposed to quantify operator size in terms of Krylov complexity (the operator analog of (63)). In this framework, we consider the Heisenberg evolution of an initial, "simple" operator $\mathcal{O}(0)$

$$\partial_t \mathcal{O}(t) = i[H, \mathcal{O}(t)]. \quad (65)$$

This equation can be formally solved as

$$\mathcal{O}(t) = e^{iHt} \mathcal{O}(0) e^{-iHt} := e^{i\mathcal{L}t} \mathcal{O}(0), \quad (66)$$

where in the second step we introduced the Liouvillian super-operator $\mathcal{L} = [H, \cdot]$. As before, we can expand the operator $\mathcal{O}(t)$ as a power series in t that involves nested commutators of the Hamiltonian with $\mathcal{O}(0)$ or equivalently various powers of the Liouvillian acting on $\mathcal{O}(0)$. As in Sec. 6.1 this series builds the Krylov subspace to which we want to apply the Lanczos procedure. If the Hilbert space is N -dimensional, the associated operator space in which we carry out this procedure is N^2 -dimensional because operators have matrix elements O_{ab} , with $a, b = 1, \dots, N$.

The procedure for extracting the Krylov basis for operators and the associated Lanczos coefficients is the same as described in Sec. 6.1 for states, after vectorizing operators by mapping them into an auxiliary Hilbert space by the GNS (Gelfand-Naimark-Segal) construction (see, e.g., the discussion in [147]). In quantum information theory such a vectorization also appears as the Choi-Jamiolkowski isomorphism, also known as channel-state duality [148, 149]. After vectorizing operators in this way, $\mathcal{O} \rightarrow |\mathcal{O}\rangle$, we also have to choose an inner product on the auxiliary Hilbert space. The authors of [147] showed that the Krylov complexity defined with respect to the alternative choices behaves differently as a function of time. However, the approach described in Sec. 6.1 suggests that we should pick the inner product that produces a Krylov basis that minimizes the spread of operators. As discussed in [17] the results of [147] imply this minimization is achieved

by the Wightman product. Indeed, this was the choice advocated in [16], albeit for other reasons. Thus, we set

$$(A|B) = \langle e^{\frac{\beta}{2}H} A^\dagger e^{-\frac{\beta}{2}H} B \rangle_\beta, \quad \langle X \rangle_\beta := \frac{1}{Z(\beta)} \text{Tr} (e^{-\beta H} X), \quad (67)$$

where $Z(\beta)$ is the thermal partition function at inverse temperature $\beta = 1/T$. For finite dimensional Hilbert spaces, we often use the $\beta \rightarrow 0$ version of this formula which is the Hilbert-Schmidt inner product.

Finally, we map the operator evolution into a time-dependent state

$$|\mathcal{O}(t)\rangle = e^{i\mathcal{L}t} |\mathcal{O}(0)\rangle = \sum_{n=0}^{\mathcal{K}-1} i^n \varphi_n(t) |K_n\rangle. \quad (68)$$

For Hermitian operators the a_n 's vanish and we derive the Schrödinger equation

$$\partial_t \varphi_n(t) = b_n \varphi_{n-1}(t) - b_{n+1} \varphi_{n+1}(t). \quad (69)$$

Solving it yields the probability $p_n(t) = |\varphi_n(t)|^2$ and the Krylov complexity that generalizes the notion of the operator size is computed by (63). Interestingly, [150] showed that the dimension \mathcal{K} of the Krylov space for operators is bounded by

$$1 \leq \mathcal{K} \leq N^2 - N + 1, \quad (70)$$

where N is again the dimension of the Hilbert space.

As in Sec. 6.1, the Lanczos coefficients can be computed by either the recursion method or the moment method. As explained above, the moments of the Hamiltonian can be extracted from the survival amplitude,¹⁹ written in terms of the Wightman inner product as

$$S(t) = \langle e^{\frac{\beta}{2}H} \mathcal{O}(t) e^{-\frac{\beta}{2}H} \mathcal{O}(0) \rangle_\beta = \frac{1}{Z(\beta)} \sum_{n,m} |\langle n | \mathcal{O} | m \rangle|^2 e^{-(\frac{\beta}{2}-it)E_n} e^{-(\frac{\beta}{2}+it)E_m}. \quad (71)$$

In the second equality, we introduced the resolutions of the identity in the energy basis and represented the answer in terms of the matrix elements of the operator.

The spread of states and operators can be used as a probe for understanding the dynamics of quantum systems. Below we will show how to use this tool in a number of different systems. General results can also be obtained. For example, the authors of the pioneering paper [16] performed numerical and analytical studies of Krylov complexity in integrable and chaotic systems, including the SYK model, and found that the growth of Lanczos coefficients b_n is at most linear in n

$$b_n \leq \alpha n + \kappa. \quad (72)$$

They conjectured that theories in which operator growth saturates this bound are chaotic, in the same sense as probed by the OTOC correlators (see Sec. 2 for a definition of these correlators). In particular, they related the coefficient α to the characteristic exponent λ_K in an exponential

¹⁹Sometimes the survival amplitude is referred to as the auto-correlation function in this context.

growth of the Krylov complexity for chaotic theories, i.e., $\lambda_K = 2\alpha$. In the case of the SYK model, this exponent coincided with the Lyapunov exponent read from the OTOC, which we label with λ_{OTOC} . In other words, they observed that for the SYK model $\lambda_K = \lambda_{\text{OTOC}}$. This match will be further discussed in section 6.3.3. However, in many theories, including 2D CFTs, operator return amplitudes are universal and do not readily distinguish between integrable and chaotic models. Therefore the hypothesis of [16] requires refinement; indeed, as we will discuss below in Sec. 6.3.4, the difference between chaos and integrability may be more apparent in the cross-correlations between the Lanczos coefficients and the effects of these correlations on the dynamics.

6.3. Applications

6.3.1. Particles on group manifolds

Explicit solutions of the Lanczos algorithm can be obtained when there are dynamical symmetries governing time evolution on the 1D Krylov chain [16, 134, 151, 152]. Since the Krylov space representation depends on both the Hamiltonian and the initial state, this emergent symmetry need not arise from the fundamental symmetries of the model. As we have seen, Lanczos coefficients can be constructed from the survival amplitude. Within the same model, some scenarios may exhibit dynamical symmetries, while others may not. Below, we present examples in which a dynamical symmetry arises from the motion of a particle on a group manifold [17, 134].

Consider a family of Hamiltonians based on the $\text{SL}(2, \mathbb{R})$ group,

$$H = \alpha(L_{-1} + L_1) + \gamma L_0 + \delta 1 \quad ; \quad [L_0, L_{\pm 1}] = \mp L_{\pm 1} \quad ; \quad [L_1, L_{-1}] = 2L_0. \quad (73)$$

Here γ , α , δ and h are constants that depend on the details of the physical set-up such as the operator dimension, temperature or the initial state as well as the physical, evolving Hamiltonian. Recall, that in the discrete series representation with scaling dimension h , $L_0|h, n\rangle = (h+n)|h, n\rangle$, $L_{-1}|h, n\rangle = \sqrt{(n+1)(2h+n)}|h, n+1\rangle$, and $L_{+1}|h, n\rangle = \sqrt{n(2h+n-1)}|h, n-1\rangle$. Now suppose we start at $t=0$ with a highest weight state. Then, applying the recursion method or the moment method, the Krylov basis elements are $|K_n\rangle = |h, n\rangle$ by construction. Using this we also find that

$$a_n = \gamma(n+h) + \delta, \quad b_n = \alpha\sqrt{n(n+2h-1)}, \quad (74)$$

are the Lanczos coefficients. For coefficients of this form, one can solve the Schrödinger equation (53) analytically and a general form of the spread/Krylov complexity in this scenario is given by

$$\mathcal{C}_K(t) = \frac{2h}{1 - \frac{\gamma^2}{4\alpha^2}} \sinh^2 \left(\alpha t \sqrt{1 - \frac{4\gamma^2}{\alpha^2}} \right). \quad (75)$$

This form also appears in other contexts such as the SYK model at large q . Indeed, for the growth of operator with dimension $h \sim 1/q$ we have $\gamma = 0$ and $\alpha = \pi/\beta$. Quantum speed limits have also been used to show that this form leads to the fastest possible universal growth of operators [153]. More generally, (75) can be divided into three different classes depending on the relative magnitude of parameters. The class with $\gamma < 2\alpha$ where complexity grows exponentially, the class with $\gamma > 2\alpha$ where complexity is periodic and the intermediate class with exactly $\gamma = 2\alpha$ where the spread complexity grows quadratically.

For compact semi-simple Lie groups, we generically end up with finite dimensional Krylov spaces.

For example, we can consider the $SU(2)$ symmetry and discrete series representations labeled by the spin j . There are $2j + 1$ Lanczos coefficients that read

$$a_n = \gamma(n - j) + \delta, \quad b_n = \alpha\sqrt{n(2j + 1 - n)}. \quad (76)$$

Again, the constants depend on details of the physical setup. After solving (53) analytically, we find the corresponding complexity is periodic in time

$$\mathcal{C}_K(t) = \frac{2j}{1 + \frac{\gamma^2}{4\alpha^2}} \sin^2 \left(\alpha t \sqrt{1 + \frac{\gamma^2}{4\alpha^2}} \right). \quad (77)$$

Finally, we can work out a similar class of solutions controlled by the Heisenberg-Weyl symmetry for which the Lanczos coefficients are

$$a_n = \gamma n + \delta, \quad b_n = \alpha\sqrt{n}, \quad (78)$$

and the complexity becomes

$$\mathcal{C}_K(t) = \frac{4\alpha^2}{\gamma^2} \sin^2 \left(\frac{\gamma t}{2} \right). \quad (79)$$

As a consequence, for $\delta = \gamma = 0$ the evolving state can be recast into the form

$$|\psi(t)\rangle = e^{\alpha(a^\dagger + a)t}|0\rangle, \quad (80)$$

and its Krylov complexity grows quadratically in time

$$\mathcal{C}_K(t) = \alpha^2 t^2. \quad (81)$$

In [151] some of these solutions were found by mapping the Schrödinger equation into the Toda system that was then solved analytically. In [152], the symmetry approach was explained by recognizing that the Schrödinger equation can be effectively written as a three-term recursion relation for orthogonal polynomials in the Liouvillian (or the Hamiltonian). Consequently, when the Lanczos coefficients have a particular dependence on n , which makes this equation coincide with the defining relation of known polynomial families, analytical solutions for the wave functions and complexity can be obtained. For example the $SL(2, \mathbb{R})$ family with b_n given by (76) corresponds to Meixner orthogonal polynomials.

For the symmetry classes discussed above, Krylov complexity admits a geometrical interpretation. Namely, the dynamics on the Krylov chain can be mapped onto motion in the phase space spanned by coherent states. Using the Fubini-Study (FS) metric on the corresponding phase spaces, operator growth in the $SL(2, \mathbb{R})$, $SU(2)$, and Heisenberg-Weyl cases corresponds to particle (geodesic) motion on the hyperbolic disk, the sphere, and the complex plane, respectively. Moreover, Krylov complexity is proportional (with a factor of π) to the volume enclosed from the origin to the radius determined by the particle's position at time t . An example of this for the $SL(2, \mathbb{R})$ symmetry is illustrated in Fig. 7 (from [134]). This result may seem counterintuitive given the conventional intuition from Nielsen's definition of complexity, which associates complexity with geodesic length. Nevertheless, Krylov complexities in all of the symmetry examples above exhibit this feature. Interestingly, at late times, it is the Krylov entropy (64), that scales in a manner similar to the geodesic

length in the Fubini-Study geometry [134].

6.3.2. Operator growth in spin chains

Extensive numerical studies of operator growth and Krylov complexity have been conducted in [16, 133, 150, 154, 155]. In generic finite-dimensional, non-integrable systems, the growth of the Lanczos coefficients b_n with n exhibits three distinct regimes, which determine the scaling behavior of Krylov complexity. Denoting the number of degrees of freedom by K , the first regime is characterized by a linear growth of b_n 's, leading to the exponential growth of Krylov complexity. For infinite-dimensional systems, this exponential growth persists indefinitely. For finite dimensional systems, after times of order $t \geq \log(K)$ or Krylov index $n \sim K$, the Lanczos coefficients saturate at a constant value $b_n \sim \Lambda K$, where Λ is a parameter related to the system's spectral bandwidth. In this regime, Krylov complexity grows linearly with time. Finally, at exponentially large times $t \sim e^K$, the Lanczos coefficients gradually decrease toward zero, leading to the saturation of Krylov complexity.

Moreover, the authors of [155] examined how operator growth differs between integrable and chaotic spin-chain models. The authors studied the XXZ spin chain with integrability-breaking deformations, allowing them to interpolate between the two regimes. Noting that the behavior of the Krylov complexity depends both on the Hamiltonian and the choice of initial operator, they focused on examples like the sum of the pair of spin operators located at some fixed distance from the ends of the chain. In these examples they found that the late-time plateau value is suppressed in the integrable phase, whereas in the chaotic phase, it is larger and eventually matches the prediction of random matrix theory for a system of the same dimension. The authors argued that this suppression arose from a sort of Anderson localization in the one dimensional Krylov chain arising from disorder in the Lanczos coefficients. More details can be found in the review [3].

However, at least for generic initial operators/states, the plateau value cannot serve as signature of chaos vs. integrability, for the reasons described below. Recall, from Sec. 6.1.4 that there is an analytical formula relating the density of states and the coarse-grained Lanczos spectrum. This results applied to Hamiltonians and initial states for which the Lanczos coefficients have a continuous large system limit, such as those arising for generic initial states with continuous support in the energy basis. The authors of [156] showed that for such states, the late time plateau of the spread



Figure 7: Operator growth and Krylov complexity for $SL(2, \mathbb{R})$ on the Fubini-Study geometry. Operator evolution becomes a geodesic (in orange) on the hyperbolic disc. Volume (in yellow) of the region enclosed by the particle's position is proportional to the Krylov complexity.

complexity can be determined analytically in terms of the coarse-grained Lanczos spectrum. Since the relation between this spectrum and the density of states is universal, i.e., it applies to both integrable and chaotic theories which can have the same density of states, the plateau value cannot generally separate integrability and chaos, although it may do so for specially prepared initial conditions. That said, as will see in Sec. 6.3.4, the central phenomenon driving the results of [155], i.e., order vs disorder in the Lanczos coefficients, can be distilled into a sharp conjecture regarding the covariances of the Lanczos coefficients for chaotic theories [126, 156]. These covariances affect the approach of the spread complexity to the late time plateau even in cases where the plateau value is the same between integrable and chaotic theories. We will describe this conjecture and compare explicitly with integrable and chaotic spin chains in Sec. 6.3.4

6.3.3. SYK model

The authors of [16] originally suggested Krylov complexity as a diagnostic of chaos. They proposed that this quantity would grow exponentially in chaotic systems because of the rapid spreading of operators expected there. In particular, according to [16], if the Lanczos coefficients grow linearly at large n

$$b_n \sim \alpha n \quad (82)$$

the Krylov complexity will grow exponentially at early times

$$\mathcal{C}_K(t) \sim e^{\lambda_K t}, \quad \lambda_K := 2\alpha. \quad (83)$$

For chaotic systems where (82) holds, [16] also proposed that the Krylov exponent upper bounds the Lyapunov exponent

$$\lambda_{\text{OTOC}} \leq \lambda_K \leq \frac{2\pi}{\beta}. \quad (84)$$

The first inequality was proven at infinite temperature in [16] and under the assumption of certain analytic and smoothness properties of the Lanczos coefficients, the right inequality was proven at finite temperature in [157, 158]. The inequality $\lambda_{\text{OTOC}} \leq \frac{2\pi}{\beta}$ where β is the inverse temperature $\beta = 1/T$ is the bound on chaos in quantum mechanical systems from [5] (the definition of λ_{OTOC} is reviewed in Sec. 2).

These conjectures have been studied extensively in the SYK model, which has had important applications in the description of strange metals, the study of quantum chaos and as a model for quantum gravity, see, e.g., [124, 145, 159–164]. The SYK Hamiltonian is constructed from N Majorana fermions satisfying anti-commutation relations $\{\psi_i, \psi_j\} = \delta_{ij}$ with $i, j = 1, \dots, N$:

$$H_q = (i)^{q/2} \sum_{1 \leq i_1 < i_2 < \dots < i_q \leq N} J_{i_1 i_2 \dots i_q} \psi_{i_1} \psi_{i_2} \dots \psi_{i_q}. \quad (85)$$

The couplings J are real, and are drawn identically and independently from a Gaussian distribution with zero mean and fixed variance

$$\langle J_{i_1 i_2 \dots i_q} \rangle = 0, \quad \langle J_{i_1 i_2 \dots i_q}^2 \rangle = \frac{2^{q-1} \mathcal{J}^2 (q-1)!}{q N^{q-1}}. \quad (86)$$

The SYK model approaches a nearly conformal fixed point at low temperatures, where the fermions

acquire a conformal dimension of $1/q$ and the model becomes (nearly) maximally chaotic in the sense of the chaos bound [5]. The case $q = 2$ is special – it is integrable rather than chaotic.

The SYK model admits some simplifications in the limit of infinite N , and even more when we take q to also be large.²⁰ In this case, the survival amplitude averaged over the SYK ensemble is known analytically and one can use it to extract an averaged Lanczos sequence. At large N , some quantities are self averaging including the thermal two-point function [164] and many texts including the pioneering [16] work under the assumption that the Krylov complexity is similarly self-averaging. These works extract the Lanczos sequence from the ensemble averaged survival amplitude using the moment method described in Sec. 6.1.2. As we will see in below in the discussion of Random Matrix Theory in Sec. 6.3.4, ensemble averages of this kind match the coarse-grained Lanczos coefficients described in Sec. 6.1.4, but do not capture higher moments such as covariances of the Lanczos spectrum. Applying the moment method to the ensemble averaged survival amplitude the leading contribution to the Lanczos coefficients at large q reads

$$b_{n,\beta}^{\text{SYK}} = \begin{cases} 2\nu\beta^{-1}\sqrt{2/q} + O(1/q) & \text{if } n = 1, \\ 2\nu\beta^{-1}\sqrt{n(n-1)} + O(1/q) & \text{if } n > 1. \end{cases} \quad (87)$$

where ν is implicitly defined via the relation $\beta\mathcal{J} = 2\nu/\cos(\nu)$.

In this limit, the leading large q contribution to the Krylov exponent is exactly equal to the Lyapunov exponent [16]:²¹

$$\lambda_K = \lambda_{\text{OTOC}} = 4\nu/\beta. \quad (88)$$

This surprising equality suggested that the Krylov exponent, which is simpler to compute than the OTOC, would provide a shortcut for computing the Lyapunov exponent of the latter. However, at large but finite q , the equality fails at order $1/q$, that is [165]

$$\frac{\beta}{2\pi}(\lambda_K - \lambda_{\text{OTOC}}) = \frac{4\pi^2}{3q\beta J}. \quad (89)$$

Larger deviations can also occur. For example, consider deforming the SYK Hamiltonian by another SYK Hamiltonian with $\tilde{q} < q$

$$H_{\text{def}} = H_q + sH_{\tilde{q}} \quad (90)$$

The perturbation is an infrared deformation of the original SYK since it has effective dimension $\tilde{q}/q < 1$ around the fixed point of the original Hamiltonian. This means that as we keep flowing to the infrared a new fixed point will appear that is dominated by the deformation. This type of deformation has been studied in, e.g., [166–175]. In the context of chaos, we expect the infrared deformation to induce a transition between two chaotic regimes, or if $\tilde{q} = 2$, between chaos and integrability along the RG flow controlled by the temperature parameter. We can try to diagnose these chaos-chaos or chaos-integrability transitions using the OTOC and Krylov exponents [165]. Fig. 8 show that while the Lyapunov exponent exhibits features indicative of such transitions, the

²⁰Here we mean that we first take the limit $N \rightarrow \infty$ and then we take $q \rightarrow \infty$. In the language of double scaled SYK (DSSYK), where N is taken to infinity keeping the ratio $\lambda_{\text{SYK}} = 2q^2/N$ fixed, our limit has $\lambda_{\text{SYK}} = 0$.

²¹A particularly interesting case is the limit of low temperatures (large β). In this case both exponents approach the chaos bound $2\pi/\beta$.

Krylov exponent does not.

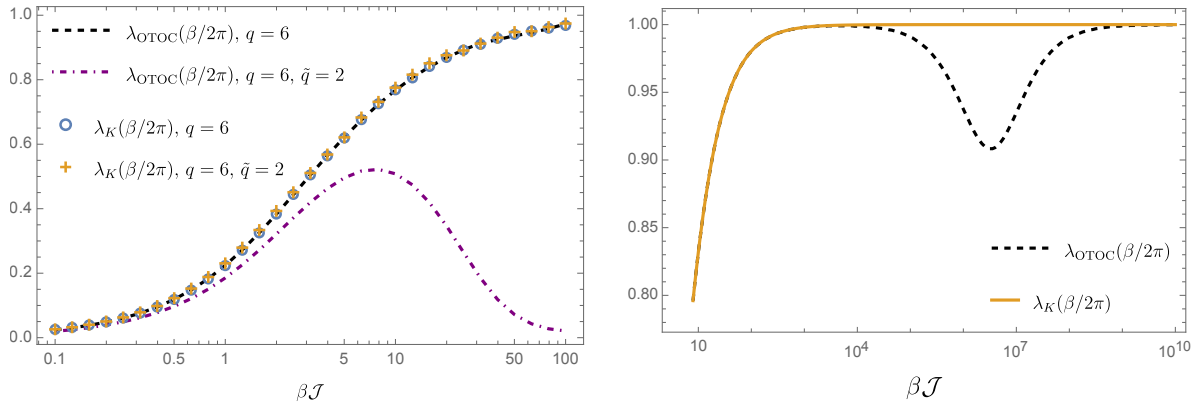


Figure 8: Lyapunov and Krylov exponents for flow SYK theories (90). Left: a flow from $q = 6$ to $q = 2$ at large N with $s = 0.2$. The Lyapunov exponent indicates that chaos develops at intermediate temperature (in the intermediate IR) but integrable behavior is approached at much lower temperatures (in the deep infrared). Right: flow between two chaotic regimes at large N and large q where $\tilde{q}/q = 2$ is kept fixed when taking the limit and $s = 10^{-3}$. We observe two regimes of near maximal chaos with a clear transition indicated by the OTOC exponent’s minima but not by the Krylov exponent. Plots adapted from [165].

Perhaps this should not come as a surprise, as the starting point for extracting the Lanczos sequence in the above discussion was the ensemble averaged two point function and Lanczos coefficients. As the next section suggests, to diagnose chaos we may need the ensemble fluctuations and correlations of the Lanczos sequence rather than their average. Additionally, the studies described above are investigating early time chaos. As we will discuss below, the spread complexity of chaotic systems grows to a peak at late times that are exponential in the entropy, and then slopes back down to a plateau. The presence of this peak and slope depend on characteristic spectral correlations that are absent in integrable theories with Poisson spectra [17]. We will discuss this below in the context of Random Matrix Theory, but all the characteristic behavior of spread complexity that we will describe applies equally to chaotic SYK models.

6.3.4. Random Matrix Theory

A standard paradigm for quantum chaotic behavior is time evolution under a random matrix Hamiltonian drawn from the measure

$$\frac{1}{Z_{\beta,N}} e^{-\frac{\beta N}{4} \text{Tr}[V(H)]}, \quad (91)$$

where H is the Hamiltonian, $V(H) = \sum_{n=0}^{\infty} v_n \text{Tr}(H^n)$ is a potential, and the partition sum $Z_{\beta,N}$ normalizes the measure. The Dyson index is $\beta = 1, 2, 4$ depending on whether we choose H to be Hermitian, real and symmetric, or quaternionic, corresponding to unitary, orthogonal, or symplectic ensembles. If V is quadratic, we say that the Random Matrix Theory (RMT) is described by the Gaussian Unitary, Orthogonal or Symplectic Ensembles (GUE, GOE, GSE). We are going to study time evolution and spread complexity of a generic state in the basis in which the Hamiltonian is drawn. Since the matrix is being drawn randomly we can pick this to be the state $(1, 0, 0, \dots)$ if we like.

Suppose we diagonalize the Hamiltonian in the exponent of (91) by a unitary transformation. Famously, the change of variables introduces the Vandermode determinant $\Delta = \prod_i < j |\lambda_i - \lambda_j|^\beta$ in the measure, leading to a distribution over eigenvalues of the form

$$p(\lambda_1, \dots, \lambda_N) = Z_{\beta, N} e^{-\frac{\beta N}{4} \text{Tr}[V(\Lambda)]} \prod_{i < j} |\lambda_i - \lambda_j|^\beta = Z_{\beta, N} e^{-\frac{\beta N}{4} \sum_n v_n \sum_k \lambda_k^n} \prod_{i < j} |\lambda_i - \lambda_j|^\beta, \quad (92)$$

where $V(\Lambda)$ is the potential evaluated on the diagonal matrix of eigenvalues. There is also an important relation between the potential V and the ensemble averaged density of states:

$$V'(\omega) = \text{p.v.} \int dE \frac{\rho(E)}{\omega - E}, \quad (93)$$

where V' is the derivative of the potential, $\rho(E)$ is the density of states, and p.v. indicates the principal value of the integral. We will use these relations to work out expressions for the Lanczos spectrum.

As explained in [126], we can use (93) to calculate the density of states from the potential of the RMT, and then we can use (61) from Sec. 6.1.4 to determine the coarse-grained Lanczos spectrum and the spread complexity. This construction is averaged over the ensemble, but as shown in [126], at large N this gives the same result as coarse-graining over nearby Lanczos indices in a single draw from the ensemble, i.e., using the coarse-graining procedure outlined in Sec. 6.1.4. But we can do better than this and determine the distribution of Lanczos coefficients. For Gaussian RMTs, this distribution was worked out in [176]. The Jacobian arising from the basis transformation to get a tridiagonal Hamiltonian will be the same for any potential. The authors of [126] used this to show that for an RMT with an arbitrary potential like (91) the distribution of Lanczos coefficients is

$$p(a_0, \dots, a_{N-1}; b_0, \dots, b_{N-1}) \propto \left(\prod_{n=1}^{N-1} b_n^{(N-n)\beta-1} \right) e^{-\frac{\beta N}{4} \text{Tr}[V(H)]}, \quad (94)$$

where within the trace H is understood as tridiagonalized to the Lanczos form.

At large N the distribution (94) is sharply peaked. So we can use the method of saddle points to extract the ensemble average (the saddle point) and the covariances (from the quadratic expansion around the saddle point). The ensemble average precisely reproduces (61) which we already derived through other means, and which applies to any theory for which we know the density of states. A formula for the covariances of the a_n and b_n is derived in [126, 156]. We will not repeat the derivation here for lack of space, but the result is

$$\text{cov}(a_i, a_{i+\delta}) = 4\text{cov}(b_i, b_{i+\delta}) = \frac{1}{2\pi\beta N} \int_0^{2\pi} dk \frac{2^{ik\delta}}{\lambda(k, a_i, b_1)}, \quad (95)$$

with

$$\lambda(k, a_i, b_i) = \int dE \frac{V'(E) - V'(a_i)}{b_i(E - a_i)} \eta((E - a_i)/b_i, e^{ik}), \quad \eta(x, t) = \frac{x}{\pi\sqrt{4 - x^2}} \frac{1}{t + 1/t - x}. \quad (96)$$

Among other things, these results show that the variance in $a(x)$ around the ensemble mean should

be four times the variance in $b(x)$ for any RMT, where we are taking $x = n/N$ and coarse-graining as described in Sec. 6.1.4. The authors of [126] showed that these analytical formulae reproduce numerical results for RMTs with various potentials.

Following [17] the spread complexity of the time-evolved thermofield-double state for a GUE Hamiltonian is plotted in Fig. 9 for various matrix sizes N and inverse temperatures β . The dynamics exhibit four characteristic regimes: a linear ramp up to a peak that is exponential in the entropy, followed by a slope down to a plateau. The authors of [17] showed that the peak and slope arise from eigenvalue correlations known as spectral rigidity in chaotic theories. These correlations can be removed by drawing eigenvalues at random from the Wigner semicircle distribution and the evolution with such a spectrum (Fig. 9 in light hues) shows only the ramp and plateau. Thus, the peak and slope are characteristic of late time chaos. The same patterns appear in the late time spread complexity of the chaotic SYK model [17].

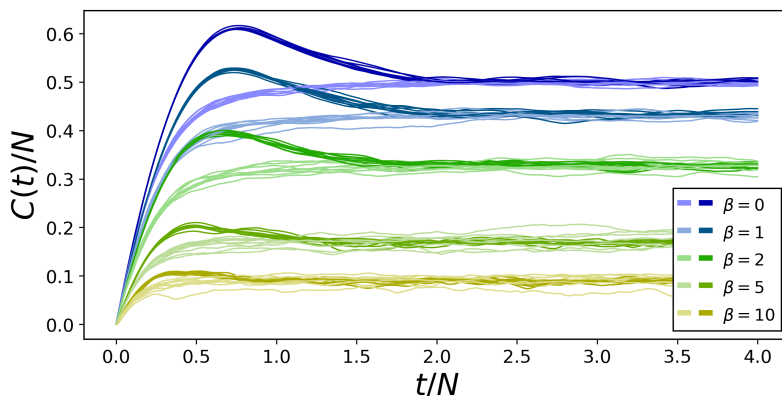


Figure 9: Quantum state complexity of the time-evolved thermofield-double state over an exponentially large period of time for different values of N and β , as described in the main text. **Dark Hues:** GUE ensemble. Going from highest (blue) to lowest (yellow) curves we have $\beta = \{0, 1, 2, 5, 10\}$. In each case we have plotted ensembles with $N = \{1024, 1280, 1536, 1792, 2048, 2560, 3072, 3584, 4096\}$. Complexity grows linearly to a peak, followed by a downward slope to a plateau. **Light Hues:** Ensemble with the same density of states as GUE, but without correlations between eigenvalues. In this case, the curves plateau without reaching a peak followed by a downward slope.

Quantum chaotic systems are conjectured to have spectra that are well-described by RMT statistics [46, 177]. In view of the results above, [156] conjectured that: *Quantum chaotic systems display a Lanczos spectrum that is well described by RMT.* As we discussed, the coarse-grained Lanczos spectrum can be determined from just the density of states. So the content of this conjecture lies in the correlations – it is saying that the covariances of the Lanczos coefficients are described by the RMT formulae stated above. To test this conjecture, we can numerically compute the Lanczos spectrum of integrable and chaotic spin chains such as

$$\begin{aligned}
 H_{\text{int1}} &= A_{\text{int1}} \left(\sum_{i=1}^{K-1} X_i X_{i+1} + \sum_{i=1}^K C_1 Z_i \right), \\
 H_{\text{cha1}} &= A_{\text{cha1}} \left(\sum_{i=1}^{K-1} X_i X_{i+1} + \sum_{i=1}^K C_2 Z_i + C_3 X_i + H_{\text{site}} \right) + B_{\text{cha1}}, \quad (97)
 \end{aligned}$$

where X_i, Y_i, Z_i are Pauli spin operators on site i ; A_k, B_k and C_k are numerical parameters, and $H_{\text{site}} = 0.5Z_3 + 0.3X_3$ is a one-site disorder operator that helps breaks parity and symmetry under the action of $\sum_i Z_i$. The model defined by H_{int1} is integrable, while H_{cha1} is chaotic as suggested by their level statistics, and have been explored in the literature [155, 178]. Indeed, as shown in [156], the analytical formulae developed above give an excellent description of the Lanczos coefficients in all cases, but the variances and covariances deviate significantly from the RMT formula for integrable spin chains, and in particular are much larger.

We can also write down an explicit formula for the height of the late time plateau in the spread complexity. First, let $\hat{n} = \sum_n n|K_n\rangle\langle K_n|$ be the position operator along the Krylov chain associated to an initial state $|\phi\rangle$. Then, define the complexity of an energy eigenstate $|E\rangle$ relative to $|\phi\rangle$ as $\mathcal{C}_E = \langle E|\hat{n}|E\rangle$. A short calculation [156] shows that the height of the late time plateau in the spread complexity will be

$$\mathcal{C}_{\text{plateau}} = \sum_E p(E) \mathcal{C}_E, \quad (98)$$

where $p(E) = |\langle E|\phi\rangle|^2$ is the initial probability of eigenstate $|E\rangle$. If $p(E)$ is continuous we can replace \mathcal{C}_E by the local mean to get

$$\mathcal{C}_{\text{plateau}} = \int dE \rho(E) P(E) \overline{\mathcal{C}_E}. \quad (99)$$

This means that for large systems and initial states with continuous support in the energy basis, the plateau of the spread complexity will not discriminate between chaotic and integrable theories with the same average density of states. However, if $P(E)$ is “noisy” rather than smooth, and the noise is negatively correlated with the noise in \mathcal{C}_E , the plateau can be significantly lower than the averaged value in (99). This lowering can be larger for integrable theories because, as we discussed above, the variance in the Lanczos is higher, leading to a form of Anderson localization of energy eigenstates along the Krylov chain (see also [155]). So if an eigenstate is “centered” further from the beginning of the chain it tends to have less overlap with the initial state for an integrable theory. It would be interesting to investigate further how tuning the initial state leads to differences in the late time behavior for integrable versus chaotic theories because of variances and covariances in the Lanczos spectrum

These analyses have been extended to a broad class of integrable and chaotic models, including the SYK model and spin chains. Key aspects such as the presence or absence of the peak and slope [179], the peak height [180], and the system’s approach to the plateau [181] have been advocated as indicators of chaos. However, it seems that Krylov complexity [182] and spread complexity [183] are not sensitive to saddle-dominated scrambling (exponential growth due to unstable saddle points in phase space), at least for the initial states/operators studied in these papers, a phenomenon that OTOCs also fail to distinguish from genuine quantum chaos [184].

6.4. Open problems and directions

We will conclude this section on the complexity of the spread of states and operators with a discussion of some open questions and progress towards answering them.

Krylov complexity in QFT. As we discussed, Krylov complexity can be evaluated from the survival amplitude. If we adopt the Wightman inner product for the reasons discussed in Sec. 6.2, we can

compute the survival amplitude from the thermal two-point functions

$$S(t) = \langle \mathcal{O}(t - i\beta/2)\mathcal{O}(0) \rangle_\beta. \quad (100)$$

These quantities are known exactly in some QFTs. For example, in 2D CFTs, thermal two-point correlators are universally determined by Ward identities and are the same for both integrable and chaotic CFTs. In this case, there is an infinite sequence of b_n Lanczos coefficients that grow linearly for large n [185]. At least at first sight, this serves as a counterexample to the universal operator growth hypothesis. This issue was explored in [186, 187], where the authors argued that to meaningfully characterize operator growth in QFTs, one must first introduce appropriate cut-offs. They analyzed the effects of both UV and IR cut-offs, and concluded that the chaotic or scrambling properties of QFTs may be captured by b_n 's larger than the UV cut-off Λ . Meanwhile, the IR cut-off (e.g. modeled by introducing a mass) induced a separation (staggering) between even and odd Lanczos coefficients that grew linearly with different intercepts [187].

Thus, distinguishing characteristic features of chaotic and integrable operator growth in continuum QFTs remains an open problem. A promising approach could be to employ von Neumann algebras and algebraic QFTs. Some progress in this direction has been made in [188, 189], but a direct connection with Krylov-basis methods has not been established. Alternatively, we could compute the covariances of the Lanczos coefficients in QFT, in view of the conjecture in [126, 156] that their structure separates chaos from integrability. In theories with a discrete spectrum, it may also help to project onto a microcanonical band of energies (see also [190]) thereby rendering the accessible Hilbert space finite dimensional, thus enabling us to directly adopt the ideas and methods that have been developed for such systems.

Connecting Nielsen and Krylov complexities. The relation between Krylov and Nielsen's approaches has been debated in several works. In [191], the authors argued that Krylov complexity can be interpreted geometrically as a distance in a certain projection of the Fubini-Study geometry that is natural in quantum optics, making it amenable to a circuit interpretation. However, as we already saw from the symmetry based examples, Krylov complexity, as a function of time, is proportional to the volume in the Fubini-Study geometry. As a volume, rather than a length, it does not respect some properties of geodesics, such as the triangle inequality. Such properties were suggested in [192] as an obstruction to Krylov complexity serving as a distance measure. However, it is not clear that the Fubini-Study setting is the one in which we should seek a relation with Nielsen complexity. Indeed, [193] argued that, in certain setups, there can be a relation between the time average of spread complexity of state evolution and an upper bound on Nielsen complexity with specific fine-tuned penalty factors. Recalling that the Nielsen approach has ambiguities in the choice of gate set and cost function, it remains possible that some judicious choice could establish a direct relation between the Nielsen and Krylov/spread approaches to complexity, at least for some specific choices of states. Perhaps useful progress could be achieved by formulating Krylov/spread complexity approach to general, time-dependent Hamiltonians (see progress in [194]). This would be closer in spirit to the starting point in Nielsen's definitions and could allow us to use bounds on circuit complexity to constrain Krylov complexity. Indeed, if we treat the evolution parameter as a circuit time, we can mathematically think about the complexity of formation of states in the language of spread complexity [195]. Thus it remains an interesting problem to relate the complexity of state/operator spreading to circuit complexity.

Other systems. It would be interesting to extend the spread/Krylov complexity approaches to new systems. First, the generalization to time dependent Hamiltonians is important to achieve for the reasons described above, and because we would like to understand systems that are driven by external sources. Second, if we contemplate external sources, we should also consider open quantum systems, whose dynamics are controlled by Lindbladian evolution of the density matrix. There is a substantial literature on the Lindbladian formalism which is partly reviewed in [3]. The interaction with an external bath with an open system certainly affects the structure of entanglement spreading (see, e.g., [196]), and has generally been a subject of significant recent interest in condensed matter physics through the study of measurement driven phase transitions (see, e.g., [197]). Another interesting avenue is to study the spread complexity of Carrollian theories of relevance for flat space holography. Likewise it would be interesting to study the kind of chiral theories that appear in the AdS/CFT dual to highly rotating extremal black holes [198–200] and the matrix models that appear as the dual to the 11-dimensional M-theory [201–203].

7. Quantum complexity and space-time: a more concerted approach

In 2009, several connections between geometry and entanglement were established, including a schematic relation of entanglement in AdS spacetime to tensor networks [4]. Hartman and Maldacena computed the entanglement entropy’s dynamics in excited states of a CFT on an infinite space, using black-hole interiors [204, 205]. Specifically, they showed how the interior’s growth with time, as quantified by the area of the Hubeny-Rangamani-Takayanagi (HRT) surface, predicts a linear increase of the entanglement entropy, followed by a saturation, once the black hole reaches effective equilibrium [204]. The interior keeps growing long after the entanglement saturates. Therefore, Susskind suggested that the growth of the black hole’s interior should be encoded via the AdS/CFT correspondence by a dual quantum mechanical quantity that increases for a time exponential in the system’s size. The candidate dual quantity was quantum complexity [206].

To make the relation more precise, it was important to identify geometrical quantities that captured the interior’s linear growth and switchback effect exhibited by complexity in quantum circuits (see Sec. 4). The first proposal²² was the wormhole’s volume, suggested by the ER=EPR principle [205]. This idea was later refined, leading to several alternative conjectures that we present in Sec. 7.1. All these holographic proposals reproduce linear growth and the switchback effect [19–24], as we show in Sec. 7.2. There, we also discuss a two-dimensional case where holographic complexity exhibits an expected saturation at exponential time in the black hole entropy. This saturation of complexity was discussed in the context of circuit dynamics in Sec. 4.1. In addition to the time-dependent properties of quantum complexity, we are also interested in the structure of UV divergences of the geometrical quantities. The time-independent properties of the holographic complexity conjectures are analyzed in Sec. 7.3. By now, holographic complexity has been investigated in a plethora of cases, including subregions, geometries with defects, black holes in de Sitter space, and more. We summarize the main results obtained from these investigations in Sec. 7.4.

Before proceeding, let us stress that the gravitational quantities associated with the holographic complexity proposals are all well-defined geometrical measures. However, this line of research suffered for a while from a major issue: there was no precise quantitative matching between a gravitational proposal and a dual field-theory version of complexity. Most computations involved a qualitative comparison with quantum circuit counting arguments, tensor-networks and free-field-theory results. Section 7.5 collects quantitative matches between the boundary complexity and the bulk observables. These include: the relation between the size of an ERB in two-dimensional JT gravity and a double-scaled SYK model’s spread complexity (see Sec. 2 for its definition) [26, 27], a relation between Krylov complexity and the momentum of a particle in AdS spacetime, and results regarding Nielsen’s complexity in CFT. Nonetheless, matching geometrical observables in the gravitational setting with quantum complexity in field theory is difficult. This difficulty led to questions about the foundations of quantum computation in the context of the AdS/CFT correspondence. Pseudorandomness, addressed in Sec. 7.6, can be used to argue that entries in the holographic dictionary can be hard to compute, or alternatively, that quantum gravity solves problems efficiently that take a quantum computer exponentially long times. This unexpected line of research was revealed through the study of quantum complexity.

²²The term holographic conjectures appears interchangeably with holographic proposals in many texts on the subject, to emphasize that the duality between holographic complexity and complexity of quantum systems is in general conjectural (except in special cases, see below).

7.1. Holographic complexity proposals

We begin by defining the holographic complexity proposals, depicted in Fig. 10. We describe their time evolutions, including linear growth and the switchback effect, in Sec. 7.2.

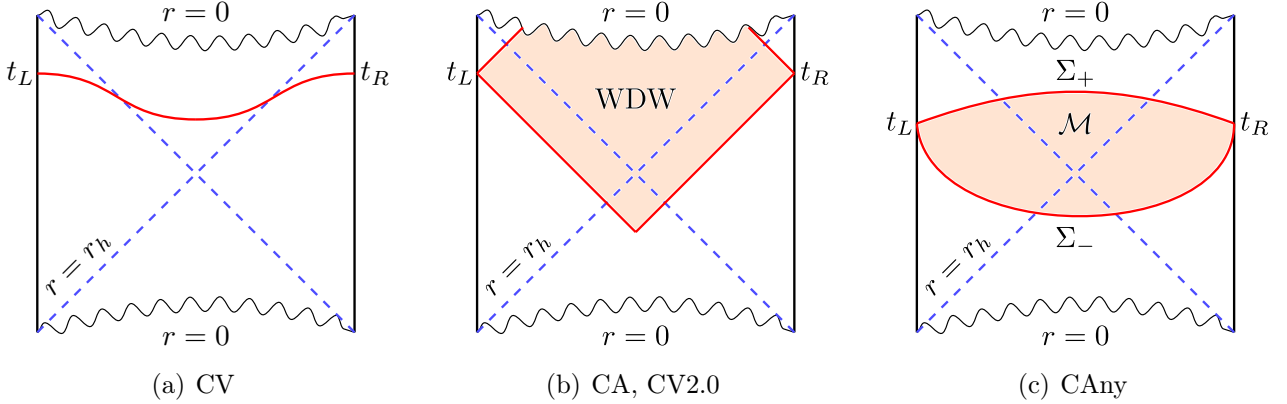


Figure 10: Geometric objects defining holographic complexity proposals drawn inside the Penrose diagrams of the Schwarzschild-AdS black hole. Pictures adapted from [21, 24]. (a) Maximal-volume codimension-one surface used in the CV proposal [Eq. (101)]. (b) WDW patch used to compute CA and CV2.0 in Eqs. (102) and (103). (c) Bulk region \mathcal{M} with codimension-one boundaries Σ_{\pm} defined by extremizing Eq. (104) in the CAny proposals.

The *complexity equals volume* (CV) proposal [18, 19] declares that holographic complexity is proportional to the maximal volume \mathcal{V} of a codimension-one spacelike surface \mathcal{B} anchored at the $(d-1)$ -dimensional boundary slice Σ_{CFT} where a CFT state is defined (see fig. 10(a)), i.e.,

$$\mathcal{C}_V(\Sigma_{\text{CFT}}) = \max_{\partial\mathcal{B}=\Sigma_{\text{CFT}}} \left[\frac{\mathcal{V}(\mathcal{B})}{G_N \ell_{\text{bulk}}} \right], \quad (101)$$

where ℓ_{bulk} is a length scale introduced to maintain dimensional consistency. In the case of AdS spacetime, ℓ_{bulk} is often identified with the AdS radius L . The maximal surface anchored on both boundaries of an eternal black hole penetrates the black hole interior, but avoids the singularity and regions with high curvature. This makes the maximal volume's value reliable in the semiclassical approximation, without the need to make further assumptions.

Other holographic proposals involve gravitational observables evaluated on the Wheeler-De Witt (WDW) patch, i.e., the bulk domain of dependence of a spacelike surface anchored at the boundary slice Σ_{CFT} (see fig. 10(b)). The first conjecture, *complexity equals action* (CA), associates complexity with the on-shell gravitational action I_{WDW} [20, 21]

$$\mathcal{C}_A(\Sigma_{\text{CFT}}) = \frac{I_{\text{WDW}}}{\pi \hbar}. \quad (102)$$

The gravitational action receives contributions from the null boundaries of the WDW patch, as required to make the variational principle in general relativity well-defined (see [207] or appendix A of [208]). The second proposal, *complexity=volume 2.0* (CV2.0), identifies complexity as the spacetime volume of the WDW patch [22]

$$\mathcal{C}_{2.0V}(\Sigma_{\text{CFT}}) = \frac{\mathcal{V}_{\text{WDW}}}{G_N \ell_{\text{bulk}}^2}. \quad (103)$$

Each of the previous proposals presents ambiguities. CV and CV2.0 require a length scale ℓ_{bulk} in the holographic dictionary. The CA proposal contains contributions from the null boundaries of the WDW patch, whose normal vectors depend on an arbitrary normalization constant. The last dependence can be removed by including certain counterterms in the gravitational action, but those in turn come equipped with their own (arbitrary) length scale, which we denote L_{ct} [207]. When studying black holes, the CA and CV2.0 proposals probe regions near the black hole singularity. A delicate cancellation between the diverging blackening factor and the vanishing volume of the sphere in the angular directions near the singularity leads to a result which does not diverge. Nevertheless, its validity in the semiclassical approximation is uncertain since the region near the singularity is not well understood in this limit.

The above ambiguities were taken as features of the holographic complexity proposal, rather than bugs, since computational complexity is also affected by several ambiguities: for instance, the choice of allowed gates in a circuit, the tolerance to reach a target state, the cost of gates *etc.*, see Sec. 4. This perspective was taken a step further with the recent proposal that *complexity equals anything* (CAny), i.e., complexity may be dual to any one out of an infinite class of geometric observables. CAny requires a codimension-zero bulk region \mathcal{M} with future (past) boundary Σ_+ (Σ_-) anchored at the CFT slice $\partial\Sigma_{\pm} = \Sigma_{\text{CFT}}$. One defines the following functional (see fig. 10(c)) [23, 24, 35]

$$W_{G_2, F_{2,\pm}}(\mathcal{M}) = \frac{1}{\ell_{\text{bulk}}} \int_{\mathcal{M}} d^{d+1}x \sqrt{-g} G_2(g_{\mu\nu}) + \int_{\Sigma_+} d^d x \sqrt{h} F_{2,+}(g_{\mu\nu}, X_+^\mu) + \int_{\Sigma_-} d^d x \sqrt{h} F_{2,-}(g_{\mu\nu}, X_-^\mu), \quad (104)$$

where $G_2, F_{2,\pm}$ are scalar functions, $g_{\mu\nu}$ is the bulk metric and X_{\pm}^μ are embedding coordinates for the inclusion of the codimension-one boundary surfaces Σ_{\pm} inside the background geometry. The functional (104) selects a specific bulk region by imposing the extremization condition

$$\delta_{X_{\pm}} [W_{G_2, F_{2,\pm}}(\mathcal{M})] = 0, \quad (105)$$

where the shape of the boundaries Σ_{\pm} is varied. When more than one solution exist, the one with maximal $W_{G_2, F_{2,\pm}}$ is chosen. Once the unique codimension-zero region $(\bar{\mathcal{M}}, \bar{\Sigma}_{\pm})$ solving Eq. (105) is identified, holographic complexity is computed by the observable

$$\begin{aligned} \mathcal{C}_{\text{Any}}[G, F_{1,\pm}, \bar{\mathcal{M}}](\Sigma_{\text{CFT}}) &= \frac{1}{G_N \ell_{\text{bulk}}^2} \int_{\bar{\mathcal{M}}} d^{d+1}x \sqrt{-g} G_1(g_{\mu\nu}) \\ &+ \frac{1}{G_N \ell_{\text{bulk}}} \int_{\bar{\Sigma}_+} d^d x \sqrt{h} F_{1,+}(g_{\mu\nu}, X_+^\mu) + \frac{1}{G_N \ell_{\text{bulk}}} \int_{\bar{\Sigma}_-} d^d x \sqrt{h} F_{1,-}(g_{\mu\nu}, X_-^\mu), \end{aligned} \quad (106)$$

where $G_1, F_{1,\pm}$ are scalar functions. In summary, the CAny conjecture consists of two steps: an extremization governed by the function (104) to select the relevant bulk region in the geometry, followed by the computation of the gravitational observable in Eq. (106). CAny is a large class of physical observables, compatible with qualitative features of complexity (such as a linear growth and the switchback effect), that can be built out of the building blocks available in the gravitational system.

One can recover CV, CA and CV2.0 from CAny. To recover CV and CV2.0, let us take the functionals (104) and (106) to be the same (i.e., $G_1 = G_2$ and $F_{1,\pm} = F_{2,\pm}$), together with constant

scalar functions:

$$\mathcal{C}_{\text{gen}} = \frac{1}{G_N \ell_{\text{bulk}}} \left[\frac{\alpha_B}{\ell_{\text{bulk}}} \int_{\mathcal{M}} d^{d+1}x \sqrt{-g} + \alpha_+ \int_{\Sigma_+} d^d x \sqrt{h} + \alpha_- \int_{\Sigma_-} d^d x \sqrt{h} \right]. \quad (107)$$

CV and CV2.0 are recovered by making different terms in Eq. (107) dominant. The CV prescription is recovered by keeping α_-, α_B constant while performing the limit $\mathcal{C}_V = \lim_{\alpha_+ \rightarrow \infty} (\alpha_+^{-1} \mathcal{C}_{\text{gen}})$. In other words, only the future codimension-one surface Σ_+ survives, the extremization problem imposes that the slice has maximal volume, and the physical observable is the volume itself. To recover CV2.0, one fixes the bulk coefficient α_B and computes $\mathcal{C}_{2.0V} = \lim_{\alpha_{\pm} \rightarrow 0} (\alpha_B^{-1} \mathcal{C}_{\text{gen}})$. In this limit, the boundary surfaces Σ_{\pm} are pushed towards the null surfaces originating from the CFT slice Σ_{CFT} , thus composing the WDW patch. One can also recover CA from CAny, but now the functionals (104) and (106) should differ from each other. Specifically, one needs to extremize \mathcal{C}_{gen} in Eq. (107) in the limit $\alpha_{\pm} \rightarrow 0$ to identify the WDW patch, but use the gravitational action (102) as the observable which computes complexity.

7.2. Time-dependent properties of the holographic proposals

In this subsection, we show that all the holographic complexity proposals defined in Sec. 7.1 exhibit the advocated universal behaviour, i.e., linear growth at late times and the switchback effect in a black-hole background.

We display these features for the CAny proposal, since it encodes all the other proposals. Consider the planar Schwarzschild-AdS black hole solution

$$ds^2 = -f(r)dt^2 + \frac{dr^2}{f(r)} + r^2 d\vec{x}^2, \quad f(r) = \frac{r^2}{L^2} \left(1 - \frac{r_h^d}{r^d} \right), \quad (108)$$

where r_h is the horizon radius. This two-sided geometry is dual to the thermofield-double state |TFD) of two decoupled boundary CFTs (see Eq. (5)). The isometries of the background (108) allow to express the complexity observable \mathcal{C}_{Any} in Eq. (106) as follows,

$$\mathcal{C}_{\text{Any}}(t) = \frac{V_x}{G_N L} \sum_{\varepsilon=+,-} \int_{\Sigma_{\varepsilon}} d\sigma \mathcal{L}_{\varepsilon}(r, \dot{r}, \dot{v}), \quad (109)$$

where $\cdot := d/d\sigma$ (σ is an intrinsic radial parameter), $V_x = \int d^{d-1}x$ is the transverse volume, and $v = t + r^*(r)$ is an infalling null coordinate defined in terms of $dr^* = dr/f(r)$.

Since v is cyclic for $\mathcal{L}_{\varepsilon}$ in Eq. (109),²³ the conjugate momenta $P_v^{\varepsilon} = \partial \mathcal{L}_{\varepsilon} / \partial \dot{v}$ are conserved along the profiles of Σ_{ε} . The late time regime $t \rightarrow \infty$ is achieved when each of the codimension-one surfaces Σ_{\pm} hug a final slice at constant radial coordinate, such that the momenta approach constant values, up to exponentially-suppressed terms. This leads to the linear growth [23, 24]

$$\lim_{t \rightarrow \infty} P_v^{\pm} = P_{\infty}^{\pm} - \mathcal{O}(e^{-t}), \quad \Rightarrow \quad \lim_{t \rightarrow \infty} \mathcal{C}_{\text{Any}} \approx \frac{V_x}{G_N L} (P_{\infty}^+ + P_{\infty}^-) t. \quad (110)$$

One can further show that $P_{\infty}^{\pm} \propto TS$, where T is the Hawking temperature and S the entropy.

²³This means that $\mathcal{L}_{\varepsilon}$ depends on \dot{v} but not on v .

Let us consider the switchback effect, see e.g., [19, 43, 209]. We modify the thermofield-double state as follows [210, 211]

$$|\Psi(t_L, t_R)\rangle = e^{-iH_L t_L - iH_R t_R} W_L(t_n) \dots W_L(t_1) |\text{TFD}(t=0)\rangle, \quad (111)$$

where W_L are low-energy perturbations acting on the left boundary. These perturbations carry energies of the order of the black hole's temperature (thermal-scale perturbations), which is assumed to be much smaller than the black hole's mass. Let us assume that $|t_{k+1} - t_k| > t_*$, where t_* is the scrambling time, and the label $k = 0, 1, \dots, n+1$ in the inequalities includes the boundary times via the definitions $t_0 = -t_R$ and $t_{n+1} = t_L$. We also assume that, in the sequence of times t_0, \dots, t_{n+1} there are n_{sb} switchbacks (also called *time folds*): in other words, the absolute values $|t_{k+1} - t_k|$ change sign $n_{\text{sb}} \leq n$ times. To keep the bulk solutions as simple as possible, we assume that the perturbations are approximately spherically symmetric. The bulk geometry dual to the perturbed state (111) can be modeled by a black hole with $n \geq 1$ shock waves produced by null matter. In this setting, any CAny observable in the late time limit reads [24]

$$\lim_{t_L, t_R \rightarrow \infty} \mathcal{C}_{\text{Any}} \propto \frac{V_x}{G_N L} (P_\infty^+ + P_\infty^-) (|t_R + t_1| + |t_2 - t_1| + \dots + |t_L - t_n| - 2n_{\text{sb}} t_*). \quad (112)$$

The contribution $-2n_{\text{sb}} t_*$ reflects the spreading of the perturbations into the system during a time scale measured by the scrambling time $t_* = \frac{1}{2\pi T} \log(M/E) \approx \frac{1}{2\pi T} \log S$, where $E \ll M$ is the energy of the shock, and T the black hole's temperature. This characterizes the switchback effect for the CAny observables. At late boundary times (t_L, t_R) , holographic complexity will grow linearly with the sum of the boundary times $t_L + t_R$, but with a delay induced by the scrambling time of the perturbation. This phenomenon was already observed in earlier studies of the CV, CV2.0 and CA proposals [19, 21, 22]. This should not come as a surprise. As we said, those proposals can be obtained from CAny by appropriate limiting procedures.

Behavior at early and intermediate times. Let us discuss other refined properties of the holographic conjectures, associated with early and intermediate times compared to the scrambling time and the inverse temperature scale. It was originally speculated that the black hole mass M should provide an upper bound on the complexity rate $d\mathcal{C}/dt \leq 2M/\pi$, based on Lloyd's bound on the computational speed [212]. This statement was supported by the full time evolution of CV in an eternal AdS black hole background, since the volume rate showed a monotonically increasing rate approaching a constant value from below at late times (e.g., see Fig. 7 in [213]). This constant exactly saturates Lloyd's bound for large black holes. However, the rate of CA reached a maximum at finite time before approaching from above a constant final value saturating the Lloyd's bound (e.g., see Fig. 22 in [213]). Therefore, the intermediate regime in the evolution of CA violated the bound. Since then, many other counterexamples were found [214–223]. It was argued in [224] that a black hole should be modeled by simple gates (i.e., close to the identity), thus being incompatible with the hypotheses used to derive the Lloyd's bound. The adaptation of Lloyd's bound to holographic complexity is an open problem.

Next, one can study the reaction of the holographic observables to shock waves corresponding to the insertion of null matter at arbitrary boundary time [43, 209]. Earlier, we assumed that the insertion times t_k of the perturbations (which included the boundary times t_L, t_R) were separated by an interval larger than t_* , see the discussion below equation (111). Here we will not make this

assumption. For simplicity, let us fix $t_L = t_R = 0$. We consider the case of a single *time fold* at the (negative) time $-t_w$ when the shock is inserted, and study the dependence of physical quantities on this time. In these cases, CV and CA show a plateau, where complexity is nearly constant, at early times $t_w \ll t_*$. Next, the holographic conjectures approach a linear growth at late times $t_w \gg t_*$. The plateau becomes longer when the shock is inserted at earlier times or when the perturbation has smaller energy, showing signatures of scrambling characteristic to chaotic systems. This is another manifestation of the switchback effect. The scrambling time can be extracted by studying the plateau size, and reads $t_* \approx \frac{1}{2\pi T} \log(M/T)$, as expected. Applying the CV conjecture, the results are summarized in Fig. 11. Furthermore, one can study the precise early t_w dependence of holographic complexity. A careful analysis (summarized in Fig. 27 of [43]) shows that the complexity grows exponentially $\mathcal{C}(t_w) \approx \exp(2\pi/\beta(t_w - t_*))$, with a characteristic exponent which is exactly equal to the Lyapunov exponent of maximally chaotic systems (see λ_{OTOC} in the key notion 6) [5]. Remarkably, all these behaviors of holographic complexity agree with Eq. (11), obtained from the simple circuit models presented in Sec. 4.1. The matching is evident by comparing Figs. 11 and 5. Finally, let us mention reference [43] extends previous studies to cases where the shocks have energies above the thermal scale.

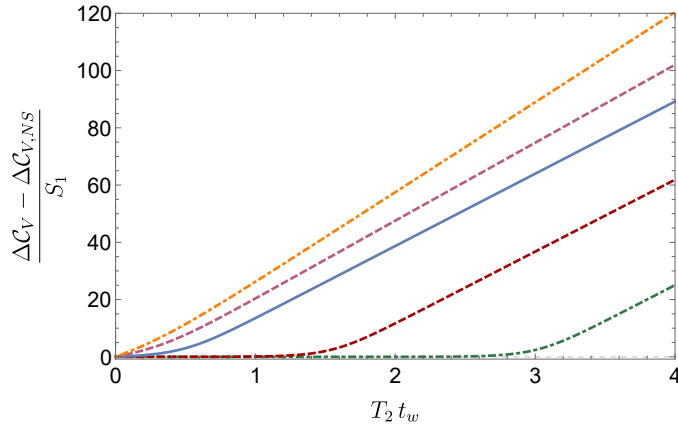


Figure 11: Volume complexity $\Delta\mathcal{C}_V$, compared to the value $\Delta\mathcal{C}_{V,NS}$ in vacuum AdS, as a function of the boundary insertion time $-t_w$ of the shock wave. S_1 is the thermal entropy of the black hole solution before the shock wave insertion; T_2 the Hawking temperature after the insertion of the shock. Picture taken from reference [43].

Beyond semiclassical gravity: late-time behavior. As we have shown earlier in this subsection, all the holographic complexity proposals by construction display a linear growth until late times. This result was derived in a semiclassical regime: we considered the black-hole geometry (108) as a solution of general relativity in asymptotically AdS spacetime, without introducing quantum gravity corrections. As a result, holographic complexity could only be explored until times exponential in the black hole’s entropy. Quantum complexity, on the other hand, is expected to saturate and reach a plateau after the linear growth, until double-exponential times in the black hole’s entropy (see the discussion around Fig. 3). This expectation from quantum circuits naturally leads to the following questions: can one compute quantum corrections to any of the geometric observables discussed so far? Does the inclusion of quantum corrections cause the holographic complexity proposals to saturate at late times?

In the case of the CV conjecture, the answer to both questions is affirmative for two-dimensional models of dilaton gravity, including JT gravity. Reference [25] proposed a nonperturbative definition of the ERB's length that includes quantum corrections from surfaces with higher topologies. We denote by γ any non self-intersecting geodesic with length ℓ_γ , $\Delta > 0$ a regulator, and $\langle \dots \rangle$ the sum over geodesics defined over surfaces of any topology within the gravitational path integral. The nonperturbative length ℓ of the ERB reads

$$\langle \ell \rangle := \lim_{\Delta \rightarrow 0} \left\langle \sum_{\gamma} \ell_{\gamma} e^{-\Delta \ell_{\gamma}} \right\rangle. \quad (113)$$

Denoting by S_0 the leading-order entropy of a black hole in JT gravity, the ERB's length grows linearly until it saturates at a time and value both of order e^{S_0} (see Fig. 1 and Fig. 5 of [25]). This behavior matches the time evolution of quantum complexity depicted in Fig. 3, but with a difference. The variance of the ERB's length is negligible at times $t \sim \mathcal{O}(e^{S_0})$, but it monotonically grows until becoming of the same order as $\langle \ell \rangle$ at times $t \sim \mathcal{O}(e^{2S_0})$.

Recently, the authors of [225] made further progress in defining a nonperturbative version of holographic complexity. Rather than focusing on the length expectation value (113), they studied the spectral decomposition of $\langle e^{-\Delta \ell} \rangle$, and identified the latter quantity as a generating function to calculate quantum complexity. The generating function shows a slope-ramp-plateau structure similar to the case of the SFF, see Figs. 6-7 of [225]. Instead, in the limit $\Delta \rightarrow 0$, the ramp disappears from the time evolution of the holographic CV (see Fig. 12 of [225]), leading to the characteristic linear growth and late time saturation of complexity. Additional definitions leading to a late time saturation are based on Krylov complexity [27], and will be discussed in Sec. 7.5.1.

7.3. Time-independent properties of the holographic proposals

To understand the time-independent predictions of the complexity conjectures, we need to deal with the UV divergences that these observables display as a consequence of approaching the AdS boundary. On the field theory side, complexity is expected to diverge due to the short distance correlations. The structure of these divergences is a robust feature, which cares very little about whether the theory is weakly or strongly coupled. It is therefore ideally suited for comparing the holographic conjectures to simple set-ups in free field theory, which we reviewed in the section 5.5.1. In holography, these divergences are regularized by introducing a short distance cutoff near the boundary of the asymptotically AdS spacetime, while in QFT they can be regularized, for instance, by placing the theory on a lattice with spacing δ .

A similar divergent behavior appears when studying the entanglement entropy. In that case, the leading divergence behaves as an area law²⁴ A/δ^{d-2} with A the area of the entangling surface, δ a short distance cutoff and d the spacetime dimension of the boundary field theory. This is true both in holographic settings and in free field theories [226, 227]. Furthermore, in the case of a smooth entangling surface, the divergences jump in powers of two, capturing different geometric features of the entangling surface. Universal contributions, depending on the anomalies of the theory, appear as coefficients of either the logarithmic or the constant parts of the expansion in the short-distance cutoff.

²⁴Note that area law here refers to the term dominant at short values of the UV cutoff, not the term dominant at high energies, as is often the case in the condensed matter literature.

The above results motivated the study of UV divergences for the complexity of a vacuum state. In [228], the authors explored the CV and CA proposals in empty AdS spacetime, see Fig. 12. It was found that the complexity always diverges with a volume law, proportional to the volume \mathcal{V} of the system as

$$\mathcal{C} \propto k_d C_T \mathcal{V} / \delta^{d-1} + \dots \quad (114)$$

with k_d a coefficient which depends on the dimension and on various ambiguities in the evaluation of complexity and the dots stand for less divergent terms. Subleading divergences in the complexity appear in jumps of two powers of the cutoff and accompany various geometric features of the boundary slice of interest. These predictions resonate well with the results for free QFTs reported in Sec. 5.5.1.

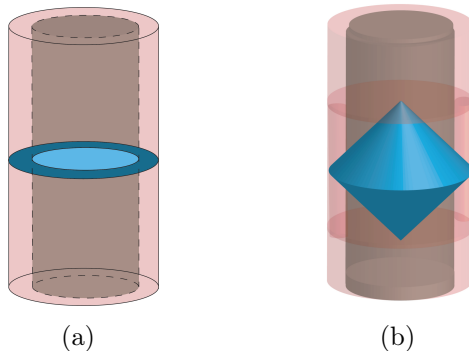


Figure 12: Illustration of the CV (left) and CA (right) proposals in empty AdS spacetime for a state living on a constant-time boundary slice. The geometric quantities are evaluated inside the brown region with ends fixed by the short distance cutoff illustrated in the figure as the pink region. Figure adapted from [229].

Next, one can consider complexity for more general states, such as the thermofield-double state dual to the two-sided eternal black hole (108). In this case, one defines the *complexity of formation* as the excess complexity required to construct this state compared to the complexity of two copies of the vacuum, i.e., $\mathcal{C}_{\text{form}} := \mathcal{C}(|\text{TFD}(t=0)\rangle) - 2\mathcal{C}(|\text{vac}\rangle)$. This quantity was evaluated in [229] using the CV and CA proposals and it was found that in the high temperature regime and in dimensions $d > 2$, it grows linearly with the entropy of the system, i.e., $\delta\mathcal{C} = k_d S$. Conversely, when $d = 2$ the complexity was found to be a fixed constant, independent of the temperature.

7.4. Generalizations of the holographic proposals

One can perform additional tests of the holographic complexity proposals. We focus on the following relevant cases: **(1)** the extension to the case of subregions, **(2)** settings with defects or boundaries, and **(3)** the applications to de Sitter spacetime.

Subregions. Consider a mixed state associated with a subregion \mathcal{A} of the boundary. The CV proposal can be extended to this case by computing the maximal volume of a codimension-one surface delimited by the subregion \mathcal{A} and its HRT surface [230]. According to the bulk reconstruction paradigm (see [231] for a review), the information carried by the reduced density matrix $\rho_{\mathcal{A}}$ of a mixed state is holographically encoded by the entanglement wedge (EW), which is the bulk domain of dependence of a region contained within \mathcal{A} and its HRT surface [232]. Therefore, in the case of

CA (CV2.0) conjecture, subregion complexity was defined as the gravitational action (spacetime volume) in the bulk region given by the intersection of the WDW patch with the EW [208].

The general structure of CV and CA proposals has been classified for a ball-shaped subregion \mathcal{B} in arbitrary dimensions, giving a leading UV divergence similar to the full system [208]. That is, $\mathcal{C}_{\text{sub}} \propto c_d \mathcal{V}(\mathcal{B})/\delta^{d-1}$, where c_d carries information on various ambiguities and the dimensionality of the system, while $\mathcal{V}(\mathcal{B})$ is the volume of the ball. In general, the subregion complexity proposals have been shown to be superadditive in a pure state;²⁵ CA is an exception, since one can tune the null-boundaries' counter term scale L_{ct} (defined below equation (103)) to either get a subadditive or superadditive behaviour [94, 233–236]. However, restricting the counter term scale L_{ct} such that the leading divergence in CA is positive, results in CA being superadditive too. Subsequent studies of holographic complexity in the presence of a subregion were carried out, e.g., in Refs. [94, 208, 230, 233, 234, 236–248].

Subregion complexity showcases an interesting behavior in the BTZ black hole geometry. Given a boundary subregion composed by q segments of total length ℓ_{tot} , the CV proposal reads [238]

$$\mathcal{C}_V = \frac{2c}{3} \left[\frac{\ell_{\text{tot}}}{\delta} + \pi(q - 2\chi) \right], \quad (116)$$

where c is the central charge, χ the Euler characteristics of the maximal surface, and δ a UV cutoff regulator. Interestingly, this formula is topological, i.e., it does not depend on the temperature. This feature is not shared by subregion CV in higher dimensions [230, 237]. The subregion CA and CV2.0 conjectures for a *single* segment of length ℓ in the BTZ background are given by [246]

$$\mathcal{C}_A = \frac{c}{6\pi^2} \log \left(\frac{L_{\text{ct}}}{L} \right) \frac{\ell}{\delta} - \log \left(\frac{2L_{\text{ct}}}{L} \right) \frac{S_{\text{EE}}}{\pi^2} + \frac{c}{24}, \quad (117a)$$

$$\mathcal{C}_{2.0V} = \frac{2c}{3} \frac{\ell}{\delta} - 4S_{\text{EE}} - \frac{\pi^2}{6}c, \quad S_{\text{EE}} = \frac{c}{3} \log \left[\frac{1}{\pi T \delta} \sinh(\pi T \ell) \right], \quad (117b)$$

where L_{ct} is a length scale introduced by a counterterm on null surfaces in the gravitational action, see the discussion below Eq. (103), and S_{EE} the entanglement entropy of the segment. These results present an appealing feature. The constant term points towards a topological structure analogous to the CV computation (116). However, an analysis of CA and CV2.0 conjectures in the case of multiple segments in the BTZ background reveals an intricate dependence on the entanglement entropy (see Eqs. (4.23)–(4.24) of [246]), which breaks the structure in Eqs. (117a)–(117b) [108, 246]. Moreover, the simple relation between complexity and entanglement entropy cannot hold in dynamical situations, since we argued at the beginning of Sec. 7 that they evolve differently.

²⁵Consider any holographic complexity conjecture $\mathcal{C}(\Sigma)$ defined on a spacetime region anchored to a boundary Cauchy slice Σ . Let us split the Cauchy slice Σ into a subregion \mathcal{A} and its complementary $\bar{\mathcal{A}}$. Denote with $\mathcal{C}(\mathcal{A})$ and $\mathcal{C}(\bar{\mathcal{A}})$ the corresponding subregion complexities, we say that holographic complexity is superadditive if

$$\mathcal{C}(\Sigma) > \mathcal{C}(\mathcal{A}) + \mathcal{C}(\bar{\mathcal{A}}), \quad (115)$$

and subadditive if the inequality is inverted.

Defects and boundaries. Defects and boundaries are extended objects that break the translational invariance of a system. They provide important probes in QFT, and are ubiquitous in condensed matter systems. Moreover, they can be engineered holographically, thus providing a playground to test the complexity conjectures. We analyze the UV divergences of CV and CA in three settings.

The first is the two-sided Randall-Sundrum (RS) model, a gravity solution where two patches of AdS spacetime are glued together at the location of a thin codimension-one brane [249]. The second is the AdS/BCFT model, where an end-of-the-world brane, corresponding to a boundary in the dual CFT, delimits vacuum AdS [250, 251]. The last is Janus AdS, a dilatonic deformation of AdS spacetime dual to an interface CFT and arising from the dimensional reduction of a solution in type IIB supergravity [252, 253].

We summarize the main features of CV and CA conjectures in these geometries in the case of a subregion of length ℓ in 2+1 dimensions, see Table 1. The results refer to the *complexity of formation* $\Delta\mathcal{C}$, defined as the complexity in the geometry with a defect (or boundary), minus the complexity evaluated in empty AdS spacetime. This quantity identifies the additional contributions due to the presence of the boundary or defect. Scanning the table, we note that the UV divergence is always logarithmic in the length regulator δ , independently of the kind of defect (or boundary) under consideration. Therefore, the CV conjecture is, to some degree, more universal than the CA proposal; the latter exhibits a different degree of UV divergences depending on the specific defect or boundary under consideration. We further observe that Janus geometry is the only case where the degree of divergence is universal across the different holographic proposals. Janus defects describe an interface CFT with a smooth holographic dual which can be obtained as a reduction of type IIB supergravity. This fact may suggest that they provide a better setup for investigating of holographic complexity (or any other holographic quantity).

	$\Delta\mathcal{C}_V$	$\Delta\mathcal{C}_A$
2-sided Randall-Sundrum	$\frac{2}{3}c\eta_{\text{RS}} \log\left(\frac{\ell}{\delta}\right) + \text{finite}$	0
AdS ₃ /BCFT ₂	$\frac{2}{3}c\eta_{\text{BCFT}} \log\left(\frac{\ell}{\delta}\right) + \text{finite}$	finite
Janus AdS ₃	$\frac{2}{3}c\eta_{\text{JAdS}} \log\left(\frac{\ell}{\delta}\right) + \text{finite}$	$\frac{2}{3}c\tilde{\eta}_{\text{JAdS}} \log\left(\frac{\ell}{\delta}\right) + \text{finite}$

Table 1: Subregion complexity of formation $\Delta\mathcal{C}$ for an interval of length ℓ in the cases of CV and CA, compared to empty AdS spacetime. The coefficients of the log divergences $\eta, \tilde{\eta}$ depend on the details of the defect or boundary, see [249–253].

Holographic complexity was studied in Janus AdS geometry under different regularization schemes [254]. In dimensions $d = 2, 4$, the authors found a scheme-independent logarithmic divergence, while in odd-dimensions a scheme-independent finite term was observed instead. This result parallels the behavior of the entanglement entropy of smooth subregions, see e.g., [227].

Holographic complexity in de Sitter space. De Sitter spacetime is a maximally symmetric solution of Einstein’s equations with a positive cosmological constant. It describes the early and late stages of evolution of our universe (e.g., see the reviews [255–257]). Since there is no timelike boundary in de Sitter spacetime, it is challenging to find a holographic interpretation of this geometry in

terms of a microscopic quantum mechanical system. Nevertheless, the physical relevance of this spacetime stimulated several attempts [173, 173, 258–302]. Recent developments suggest that the inclusion of an artificial timelike boundary in de Sitter spacetime is needed for the consistency of thermodynamics [292], microstate counting [281, 287, 299], and to take into account for role played by an observer [275, 294–296, 302]. These observations led to a revival of *static patch holography*, according to which a dual quantum theory lives on a codimension-one timelike surface (the *stretched horizon*) located just inside the cosmological horizon [261, 270, 273, 280, 286, 288–290, 297, 298, 300, 301]. The holographic complexity proposals introduced in subsection 7.1 can be applied to de Sitter spacetime by requiring that the geometric objects of interest are anchored at the stretched horizons on the two sides of the geometry [288]. The study of these generalizations, while quite speculative, may hint towards the expected properties of the quantum mechanical dual to de Sitter space.

Let us discuss the time evolution of the holographic conjectures. A main novelty, compared to the AdS case, is that CV, CV2.0 and CA conjectures include contributions from spacetime regions close to timelike infinity, therefore they diverge at a finite critical time, e.g., see Eq. (3.17) of [303].²⁶ It was argued in [288] that this behavior should be interpreted as a *hyperfast* growth of complexity corresponding to circuits where the gates involve a large number of qubits at each step in the time evolution (e.g., see [291]). The hyperfast growth also occurs in two dimensions [304] and in models of inflation where a bubble of de Sitter spacetime is inside an AdS geometry [305]. However, there are two significant exceptions to this trend. First, there exists a class of codimension-one CAny observables that exhibit linear or exponential growth persisting forever, without a divergent rate at finite time [306]. Second, CV conjecture is only defined for a short time of the order of the inverse temperature in the case of two-dimensional centaur geometries, i.e., gravitational models where de Sitter spacetime is glued to an asymptotic AdS region with a standard timelike boundary [307]. It would be interesting to understand a microscopical reason for these distinct behaviors.

Next, let us consider the switchback effect. In the case of a finite-energy shock wave perturbing a black hole solution in asymptotically de Sitter spacetime, the standard complexity conjectures (CV, CV2.0 and CA) admit a plateau around $t = 0$ when complexity is approximately constant [308, 309], similar to the AdS case.²⁷ Notably, the duration of this regime increases when the shock crosses the stretched horizon at earlier times (see figs. 23, 25 in [308]), and corresponds to special geometrical configurations that arise because the Penrose diagram of de Sitter spacetime grows taller when a null pulse carrying positive energy is inserted in the bulk [310]. The critical time at which hyperfast growth occurs in CV, CV2.0 and CA conjectures is always delayed by the presence of a shock wave moving along the cosmological horizon [311]. Reference [312] showed that the codimension-one CAny observables displaying linear growth at late times present a delay in this evolution satisfying the same structure obtained in Eq. (112) in the AdS case. All the previous behaviors support the existence of a switchback effect for the holographic conjectures applied to de Sitter spacetime. It would be desirable to match the above behaviors with those of relevant circuit

²⁶One can regularize both holographic complexity and its rate by introducing a cutoff surface at future infinity of dS spacetime. After introducing the cutoff, holographic complexity grows linearly, e.g., see Eq. (3.30) of [303].

²⁷The de Sitter shock waves considered in [308, 309] correspond to the (spherically symmetric) ejection of mass into the cosmological horizon. As a consequence, the cosmological horizon is pushed further away from an observer sitting at some fixed radius. While this setting may seem somewhat peculiar, such geometries are consistent with the null energy condition and provide a simple setup in which complexity can be studied.

models, similarly to the arguments of section 4.1.

7.5. Quantitative matches between the boundary complexity and the bulk observables

In this section, we will review proposals for quantitative matches between notions of complexity in the boundary theory and geometric observables in the dual bulk. The basic challenge is to frame the definition of complexity in terms of the holographic dictionary [313, 314] in order to get a corresponding quantity in the bulk gravity. A notable recent success is the matching between the length of wormholes in Jackiw-Teitelboim gravity and spread complexity in a dual Double Scaled SYK model.

7.5.1. Spread complexity in double-scaled SYK model equals wormhole length

The SYK model was defined above in Sec. 6.3.3 and we repeat the formulae here for convenience in a slightly different notation that will be useful for our purposes. The model contains N Majorana fermions ψ_i , $i = 1, \dots, N$,²⁸ interacting via the Hamiltonian (85). The couplings J are real, independently distributed, Gaussian random variables with first and second moments

$$\langle J_{i_1 i_2 \dots i_p} \rangle = 0, \quad \langle J_{i_1 i_2 \dots i_p}^2 \rangle = (1 - e^{-\lambda}) \binom{N}{p}^{-1} \mathcal{J}^2, \quad (118)$$

where $\lambda = \frac{2p^2}{N}$. The scaling of the couplings is tuned so that the density of states is bounded between $-2\mathcal{J}$ and $2\mathcal{J}$ in the large- N limit with p fixed (see [162] for a review). Here we focus on the so-called Double Scaled SYK (DSSYK) model in which $N, p \rightarrow \infty$ with $\lambda = 2p^2/N$ fixed (see the review [315]). Below, we will also refer to a triple scaling limit that is defined by $\lambda \ll 1$ and energies $E/\mathcal{J} \ll 1$. In this limit the theory is governed by the Schwarzian action [161, 316].

To compute the spread complexity of the DSSYK model we need the Lanczos coefficients. As we discussed above these can be computed either by tridiagonalizing the Hamiltonian by the moment method, or through an integral formula applied to the density of states. To apply the moment method we have to calculate the expectation values of powers of the Hamiltonian in the initial state which we take to be the thermo-field double. So we have to calculate

$$M_{2k} = \langle \text{Tr}(H^{2k}) \rangle = i^{kp} \sum_{I_1 \dots I_{2k}} \langle J_{I_1} \dots J_{I_{2k}} \rangle \text{Tr}(\psi_{I_1} \dots \psi_{I_n}), \quad (119)$$

where we introduced the multi-index $I_k = (i_{i_1} \dots i_{p_k})$. We have only written the even moments because the odd moments vanish. To finish the computation we have to Wick contract the multi-indexed fermion terms in pairs. As discussed in [317, 318] the Feynman diagrams describing these contractions are called *chord diagrams* and can be visualized by placing $2k$ points on the circumference of a circle and then contracting the dots in pairs. Carrying out these contractions we arrive at the moments

$$M_{2k} = (1 - q)^k \mathcal{J}^{2k} \sum_{\text{diag. with } k \text{ chords}} q^{\text{number of intersections}} = \langle 0|T^{2k}|0 \rangle. \quad (120)$$

²⁸We normalize them as $\{\psi_i, \psi_j\} = \psi_i \psi_j + \psi_j \psi_i = 2\delta_{ij}$.

The second equality expresses the moments in terms of a triangular transfer matrix T acting on $|0\rangle$, an auxiliary state with zero chords, that represents the thermofield double state at infinite temperature [318]. Essentially by construction T is the tridiagonalized Hamiltonian, the apparently auxiliary chord basis is precisely the Krylov basis. Now, following the moment method, one can automatically read-off Lanczos coefficients. They are

$$b_n = J \sqrt{\frac{1 - q^n}{\lambda(1 - q)}}. \quad (121)$$

We can then solve the Schrodinger equation, and compute spread complexity. In the double scaling limit, $N \rightarrow \infty$ and hence the Hilbert space is infinite dimensional. Using the Lanczos coefficients in (121) we find a spread complexity that grows linearly forever. Meanwhile we can apply an additional low-energy scaling limit [318]. This so-called triple scaling limit is effectively a continuum limit for the chord basis in which the T , the tridiagonalized Hamiltonian, reduces to a boundary description of a bulk Jackiw-Teitelboim (JT) gravity. In this limit, [26, 316] showed that the quantity calculating the length of the wormhole in the TFD state of JT gravity is precisely the spread complexity being computed above. This construction establishes a precise correspondence between wormhole length in gravity and spread complexity in this limit of JT gravity and the dual DSSYK model.

However, this construction leads to a puzzle. At any finite N , the Hilbert space should be finite dimensional and hence the spread complexity should saturate at late times, and along with it the quantum analog of wormhole length. How can we see this? Fortunately, the results of [317] demonstrate that these moments of the SYK Hamiltonian described above arise from the distribution

$$\rho(E|q) = \frac{2}{\pi \sqrt{4\mathcal{J}^2 - E^2}} \prod_{k=0}^{\infty} \left[\frac{1 - q^{2k+2}}{1 - q^{2k+1}} \left(1 - \frac{q^k E^2}{\mathcal{J}^2(1 + q^k)^2} \right) \right]. \quad (122)$$

In other words this is the density of states at the given q . Following the discussion in Sec. 6.1.4 we can directly compute the Lanczos spectrum from this density of states via an integral formula. This procedure was carried out in [27], where the authors demonstrated that the Lanczos coefficients for the SYK model match the computations of [318] described above in an initial range of Krylov indices, but then decline systematically to zero. The decline occurs over the whole range of the Hilbert space, with a slope of $1/N$, where N is the dimension of the Hilbert space. This descent to zero for the Lanczos coefficients causes the spread complexity to saturate at late times. If we maintain the identification between wormhole length and spread complexity that applies at early times, we would say that the wormhole length is saturating at late times. From the bulk JT gravity point of view this decline thus corresponds to a non-perturbative quantum effect in gravity that corrects the steady increase in the Lanczos coefficients and wormhole size expected from the early time classical description of the system. Of course at late times we could imagine alternate non-perturbative definitions of the wormhole length in JT gravity that also agree with the early time identification with spread complexity. Interesting developments along this line are presented in [225, 319].

In a related vein, [320] utilized new developments identifying the gravity dual to DSSYK [321] to show that the relation between the spread complexity and the bulk volume extends past the limits used in the studies of [26] to the full DSSYK regime at arbitrary temperatures. The key finding of [320] was that the match with the volume on the gravity side requires computing spread com-

plexity for the finite temperature state preparation using the Euclidean path integral, as opposed to including the Euclidean state preparation in the reference state and assigning complexity only to purely Lorentzian evolution. Furthermore, as the calculations in [320] extended also to the quantum regime, they were able to extract the form of the leading correction to the volume=complexity proposal originating from the contributions of quantum fields in two dimensional bulk. This correction was crucially needed for the quantitative match with the boundary spread complexity. Interestingly, the correction exhibits behavior compatible with it being the spread complexity of the bulk quantum fields, but a precise relation remains unknown.

These findings suggest that Krylov-basis definitions of complexity are natural from a bulk perspective and could provide a non-perturbative definition of bulk volumes. A crucial next step would be to extend these studies to higher dimensions, beginning with AdS₃. While the powerful exact results available in DSSYK may not extend directly, recent progress with Virasoro TQFTs [322] could offer insights into the bulk Hilbert space and its relation to the Krylov basis.

7.5.2. Rate of spread-complexity growth and proper momentum

The above comparisons between the Krylov basis definitions of complexity and holography were made in the context of low-dimensional toy models. This progress was possible due to the explicit definition of the thermofield-double state in the double-scaled SYK model using the transfer matrix (and its q -deformed algebra). However, extending this approach to higher-dimensional, genuinely holographic setups may be significantly more challenging. Nevertheless, several universal insights about operator growth and spread complexity can already be tested in higher dimensions. One of the most concrete examples is the relation between the growth rate of operator complexity (or size) and the radial momentum of its dual massive particle in AdS. Intuitively, we expect that the time derivative of complexity (the rate of complexity) of the Heisenberg operator $\mathcal{O}(t)$ should be proportional to the radial momentum of the particle

$$\partial_t \mathcal{C}(t) \sim P_{radial}. \quad (123)$$

This relation has been argued in various ways in [38, 120, 323–325], including qualitative models of operator growth within epidemic models [326]. Furthermore, Refs. [327–329] essentially proved this relation under the assumption of the CV proposal. However, at that time, a precise definition of complexity satisfying Eq. (123) was missing.

By now, there are several setups where this formula can be precisely evaluated on both sides of the holographic correspondence. Firstly, in the SYK model at large q , one can directly compute the expectation value of the size operator [145, 330], which is defined in terms of two copies of fermions (left and right in the thermofield-double construction, denoted with subscripts l and r respectively) as

$$\hat{S} = i \sum_j \psi_l^j \psi_r^j + \frac{N}{2}, \quad (124)$$

and match its rate with the radial momentum of a particle in AdS₂ [330] (see also [331]).

More recently, this correspondence was also confirmed between the spread complexity in 2D CFTs and the proper radial momentum of particles in AdS₃ spacetime. Reference [332] studied a local operator quench where a CFT state is locally excited by a primary operator with conformal dimension Δ , and evolved unitarily with the Hamiltonian. Holographically, this setting corresponds to a particle with mass $m = \Delta$ propagating from the boundary towards the bulk, with the particle's

initial position corresponding to the operator's energy regulator ϵ . Interestingly, the rate of spread complexity for this dynamical state is related to the particle's momentum via

$$\partial_t \mathcal{C}_K(t) = -\frac{1}{\epsilon} P_\rho(t). \quad (125)$$

However, the key observation is that the momentum must be computed in the proper radial distance coordinate ρ (for example, this relation would not hold in Poincaré coordinates). The relation between Krylov complexity and momentum has also been analyzed from a slightly different perspective in [333, 334]. The connection between the position on the Krylov chain n and (proper) radial distance in the bulk was also substantiated in [335].

Finally, the evolution of spread complexity following local quench protocols in 2D CFTs was studied in [136]. These more geometric setups also follow the pattern of the $SL(2, \mathbb{R})$ analytical solutions discussed in Sec. 6.3.1. They studied the case of joining quenches where, at $t = 0$, two uncoupled CFTs (on half-spaces) at finite temperature were joined at $x = 0$ and then evolve unitarily. In this context, the spread complexity was proportional to the central charge of the CFT as follows

$$\mathcal{C}_K(t) = \frac{c \beta^2}{32\pi^2 \epsilon^2} \sinh^2 \left(\frac{\pi t}{\beta} \right). \quad (126)$$

This local quench setup is described holographically using the AdS/BCFT correspondence [336], where the end-of-the-world (EOW) brane is time-dependent. Interestingly, the tip of the EOW brane, which probes the deepest part of the AdS bulk, follows a geodesic of a massive particle (with heavy mass $m = c/16$). The radial momentum of this particle, computed in the proper distance coordinate, satisfies

$$\partial_t \mathcal{C}_K(t) = -\frac{1}{2\epsilon} P_\rho(t). \quad (127)$$

These explicit checks suggest that, depending on the initial state, it may be possible to engineer precise holographic setups where the spread complexity rate can be directly compared to a quantity in gravity (and integrated). Particularly encouraging is the overall dependence on the central charge in (126), which was also crucial in comparing the RT formula [337] with entanglement entropy in 2D CFTs. To finish, let us point that an intriguing perspective on the Krylov basis was also presented in [137], where, using Wigner functions, the authors argued that the Krylov basis is "the most classical" basis in QFT, potentially making it a natural candidate for describing the evolution of semi-classical states in the bulk code subspace.

7.5.3. Nielsen's complexity and geometry

There are also attempts to understand holographic complexity by exploiting equivalence between bulk and boundary symplectic forms [24, 36, 338], inspired by behavior under conformal transformations in Bañados geometries [118, 339].

The relation to symplectic forms also motivated the connection between quantum complexity in CFTs and gravity for the FS cost function obtained in section 5.5.3. To understand this relation, we observe that one can map trajectories built from the unitary operators (46) of a CFT_d to the geodesics of a massive particle of mass m in AdS_{d+1} spacetime. The FS metric (47a) receives a natural geometric interpretation in terms of the minimal δX_{\min} and maximal δX_{\max} perpendicular

distances between infinitesimally nearby geodesics (as illustrated in Fig. 1 of reference [32])

$$ds_{\text{FS}}^2 = \frac{m^2}{2} (\delta X_{\text{min}}^2 + \delta X_{\text{max}}^2) . \quad (128)$$

It would be very interesting to generalize the relation (128) to complexity associated with states that are related by a finite transformation. Furthermore, the connection to other than Fubini-Study cost functions is a subject of an ongoing investigation [121].

We should stress that the considerations in Sec. 5.5.3 and the relation (128) belong to the case (a) in Fig. 6. Also, the bulk quantity defined by Eq. (128) is special to this setup in which different states are parametrized by geodesic trajectories in the empty AdS. In this special situation it makes sense to put two such trajectories together in the same AdS geometry. For general excited states in holography one deals with two distinct bulk geometries whose direct comparison occurs via covariant notions (for example, through one of the holographic complexity proposals) associated with each of the corresponding asymptotic boundaries.

As a result, a natural question in this context is about the generality of the relation (128). In the case (a) in Fig. 6 it is unknown. However, the case (b) in Fig. 6 is different and allows in fact to make a general statement, as originally proposed in [34]. The key idea is the following. For circuits in which the circuit parameter is the physical time in QFT, one layer of the circuit is simply given by the instantaneous QFT Hamiltonian. This Hamiltonian is defined in terms of the energy-momentum tensor components smeared along a time slice, e.g. $H = \int d^{d-1}x T_{tt}(\vec{x})$. The infinitesimal increment of the Fubini-Study distance (47a) is proportional to the variance of the Hamiltonian in an instantaneous state. However, given that the Hamiltonian is a sum of local operators, its variance is given by a sum of two-point functions of local operators. In AdS/CFT, the holographic dictionary [313, 314, 340, 341] provides a systematic geometric way of computing correlations functions of the boundary QFTs. As a result, the Fubini-Study cost (47a) associated with one layer of time evolution on the boundary is always geometric by the virtue that all its ingredients are geometric. This statement therefore expresses an exact mapping between two geometries: the auxiliary complexity geometry of the Fubini-Study cost on one hand and the gravitational geometry of the bulk.

It is important to stress that while the above statement is geometric, the originating bulk manifestation of the Fubini-Study cost is rather complicated and implicit. However, in the context of holographic two-dimensional CFT and states represented holographically as solutions of the Einstein's equations with negative cosmological constant in three bulk dimensions one can relate two-point functions of the energy-momentum tensor to geodesic lengths in the bulk [34]. This leads to a much more explicit expression for the Fubini-Study cost and a direct connection to the kinematic space program [342–344].

At the moment of writing this review there are two major open holographic questions relevant for the Nielsen's complexity. The first one has to do with a holographic interpretation of other than the Fubini-Study cost functions. This question is a question of infinitesimal transformations. For finite transformations, the major open question is about even a single explicit holographic manifestation of Nielsen's complexity. The goal when considering these problems should be to find a way of thinking about holography and Nielsen's complexity that would allow for a general proof of what the gravitational manifestation of the latter is. However, it is also possible that such a relation does not exist in a simple form. Indeed, the results described in previous subsections indicate that

perhaps one should seek for the microscopic explanation of some members of holographic complexity proposals in terms of the Krylov (spread) complexity.

7.6. Computational pseudorandomness and the holographic dictionary

In all the above discussions, the protagonist was the wormhole’s volume. It was observed by Susskind [206] that the steady growth of a wormhole’s volume poses a challenge in the context of the AdS/CFT correspondence: The dual quantity to the wormhole’s volume cannot be a local observable as those are expected to equilibrate and hence saturate quickly in a quantum theory. Instead, it was proposed that the dual of the wormhole’s volume is a global property of the dual state such as quantum complexity. However, from a complexity-theoretic point of view, there appears to be a mismatch between these two quantities. The volume of a wormhole is a comparably simple quantity that can be estimated from a wormholes description. In comparison, quantum complexity is notoriously difficult to compute or even bound. Making this mismatch concrete, Ref. [345] argues that either quantum gravity cannot be simulated efficiently on a quantum computer, or the holographic dictionary requires exponentially long computations. The former would violate the extended Church-Turing thesis– the widely held belief that all physical processes can be efficiently simulated on a quantum computer. More precisely, Ref. [345] models the dual CFT as a quantum system initialized in a thermofield-double state $|\text{TFD}\rangle$ dual to a zero-volume wormhole. This state is undergoing time evolution under a fixed Hamiltonian H_{CFT} such that $|\text{TFD}\rangle$ is a low-energy state for H_{CFT} . However, in this time evolution, the system undergoes a number of random ‘shocks’ acting locally on single qubits:

$$e^{-it_1 H_{\text{CFT}}} S_1 e^{-it_2 H_{\text{CFT}}} S_2 \dots e^{-it_l H_{\text{CFT}}} S_l e^{-it_{l+1} H_{\text{CFT}}} |\text{TFD}\rangle. \quad (129)$$

In Ref. [345], the authors conjecture that the time-evolution with shocks in Eq. (129), while efficiently simulable on a quantum computer, is computationally indistinguishable from a Haar random state. Such an asymmetry between the easiness of preparing a state and the hardness of distinguishing it from a random state is called quantum pseudorandomness [346, 347]. More precisely, an ensemble of states, parameterized by a random key k is called pseudorandom if 1) it can be efficiently prepared by polynomial-sized quantum circuits and 2) any quantum computer requires superpolynomial time to distinguish the ensemble from Haar random states. This implies that even if the CFT evolution under shocks is computationally simple, its output states may appear indistinguishable from truly random states, making certain bulk properties computationally inaccessible from the CFT side. In particular, quantum circuit complexity cannot be computable using only polynomial-time quantum computations and measurements as such a distinguisher would break pseudorandomness. The existence of pseudorandom states was proven in Ref. [346] under mild cryptographic assumptions.

We can now consider two time evolutions as in Eq. (129) for vastly different times, both undergoing shocks. Pseudorandomness implies that the two resulting states cannot be efficiently distinguished from Haar randomness and, therefore, from each other. However, the two states will correspond to wormholes of different volumes in any holographic dictionary, and the volume is efficiently computable from the AdS state using only coarse-grained properties of the metric. This contradiction, it is argued in Ref. [345], can only be resolved if 1) quantum gravity is not efficiently simulable on a quantum computer or 2) the holographic dictionary cannot be computed in polynomial time. Notice that this argument actually does not require the Volume=Complexity

conjecture. In fact, the existence of pseudorandomness implies that any quantity that distinguishes between deep time-evolutions under shocks and short time evolutions under shocks needs to be computationally hard to estimate.

A central concept in the AdS/CFT correspondence is the duality of entanglement and geometry as explained by the Ryu-Takayanagi formula [337]. It was shown in Ref. [348] that “geometric reconstruction” is hard even for states whose entanglement entropy satisfies inequalities referred to as the holographic entropy cone [349]. These inequalities define a cone in the space spanned by the entanglement entropies of subregions. In particular, satisfying the holographic entropy cone is a necessary requirement for the Ryu-Takayanagi formula. Geometric reconstruction refers to the task of estimating basic properties of the underlying bulk geometry from a CFT state (see, e.g., [350–354]). Similar to the argument made in Ref. [345] this hardness result uses pseudorandomness and, more precisely, the concept of pseudoentanglement. Pseudoentanglement [355, 356] refers to the phenomenon that even exponentially large gaps in entanglement can be computationally hard to detect [355], which indicates that entanglement is an “unfeeling” quantity, similar to quantum circuit complexity. In particular, Ref. [348] uses recently constructed low-entangling pseudorandom unitaries [357] to show that two states with arbitrary bulk geometries can correspond to indistinguishable states in the CFT. As the construction in Ref. [348] does not require event horizons, the result suggests that reconstruction of the bulk geometry might even be hard outside the event horizon. Previously, the presence of an event horizon was identified by Susskind [358] as a way to reconcile the Church-Turing thesis with the duality of volume and complexity: An observer that needs to cross the event horizon to estimate the volume will then be unable to communicate the findings to an outside observer. The latter, it was argued, would be in agreement with an exponentially hard-to-estimate dual quantity, such as complexity. The construction in [348] does not take the CFT Hamiltonian into account and produces high-energy states. Consequently, more work is required to draw conclusions about realistic holographic scenarios.

These results raise questions about the broader landscape of computational complexity in holography, particularly in relation to the Python’s Lunch conjecture [359]. This conjecture posits that if a geometry contains a local minimal surface that is not globally minimal, then finding the CFT operator corresponding to a local bulk operator inserted in the region surrounded by the local minimal surface is exponentially hard. The conjecture suggests that if the bulk contains locally minimal but not globally minimal surfaces, then efficient application of operators in the CFT is exponentially complex. The *strong Python’s lunch conjecture* then further posits that locally minimal surfaces are the only obstruction to efficient “operator reconstruction” [348]. A follow-up [360] shows that the strong Python’s lunch conjecture is compatible with the findings of Ref. [345] on the reconstruction of a wormhole’s volume. The results of Ref. [348] then suggest that the complexity of operator reconstruction in the CFT does not always align with the complexity of bulk geometry reconstruction. These questions about the complexity of the holographic dictionary, inspired by the volume=complexity, require and deserve future investigations.

8. Paradigms for complexity III: tensor-network-inspired definitions of complexity

Path-integral complexity [28, 29] was the first proposal for complexity in QFTs motivated by holography. In the early days of holographic complexity, the concept of complexity was often discussed in the context of tensor networks, which provide variational ansätze for many-body quantum wavefunctions. In particular, optimized tensor networks such as, e.g., MERA [12, 361] or its continuous counterpart cMERA [13, 83], give rise to a geometric structure that reflects the entanglement patterns of a quantum state.

This picture strongly resonated with the earlier idea of holography emerging from tensor networks [4]. This proposal started a new line of research, termed AdS/TN (Anti-de Sitter/Tensor Network). In fact, it was within the AdS/TN framework that Susskind [18] argued that the growth of the Einstein-Rosen bridge should be related to complexity, estimated by the number of tensors (the effective volume of the network) in the tensor-network representation of the time-evolved thermofield-double state of Hartman and Maldacena [204]. In Sec. 8.1, we review a definition of a notion of complexity in CFT, inspired by the above-mentioned parallelism with tensor networks, called *path-integral complexity*. We discuss the holographic interpretation of this quantity in a bulk AdS spacetime in Sec. 8.2.

8.1. Complexity from path-integral optimization

Motivated by these developments, Ref. [28] aimed to extend the tensor-network intuitions to general, strongly-interacting QFTs and define a natural measure of complexity using path integrals. A brief review of their construction proceeds as follows.

In QFTs, wave functions are prepared using path integrals over physical space and Euclidean time. They are computed by integrating over all field configurations, subject to specified boundary conditions on the fields. As an example, consider two-dimensional CFTs on a flat, Euclidean plane \mathbb{R}^2 with coordinates (τ, x) , and collectively denote all fields in the CFT by $\Phi(\tau, x)$. The ground state wave function $\Psi_{\text{CFT}}[\Phi(x)]$, which in QFTs becomes a functional of the boundary conditions imposed at the time slice $\tau = 0$: $\Phi(x) := \Phi(x, \tau = 0)$, is defined as

$$\Psi_{\text{CFT}}[\Phi(x)] = \int \prod_{-\infty < \tau \leq 0, x} [D\tilde{\Phi}(\tau, x)] e^{-S_{\text{CFT}}[\tilde{\Phi}]} \delta(\tilde{\Phi}(0, x) - \Phi(x)), \quad (130)$$

where S_{CFT} is the Euclidean action of the 2D CFT and $D\tilde{\Phi}$ is the path integrals measure.²⁹

The main new idea in [28] was to introduce a non-trivial background metric on the space where the path integral (130) is performed (keeping the boundary conditions for the fields fixed), and interpret this metric as an (unoptimized) density of gates of a *continuous tensor network*. For our 2D CFT example, all the metrics can be put into the Weyl-flat form parametrized by a scalar function $\phi(\tau, x)$ as follows:

$$ds^2 = e^{2\phi(\tau, x)}(d\tau^2 + dx^2), \quad e^{2\phi(0, x)} = \frac{1}{\epsilon^2} := e^{2\phi_0}. \quad (131)$$

²⁹Formally one may need to deform the theory by putting it in a finite volume or introducing a small mass in order to have a gapped spectrum so that the path integral (130) acts as a proper vacuum projector.

The second equation is the boundary condition for the Weyl-factor to reduce to the original flat space metric (with lattice spacing ϵ) as $\tau \rightarrow 0$.

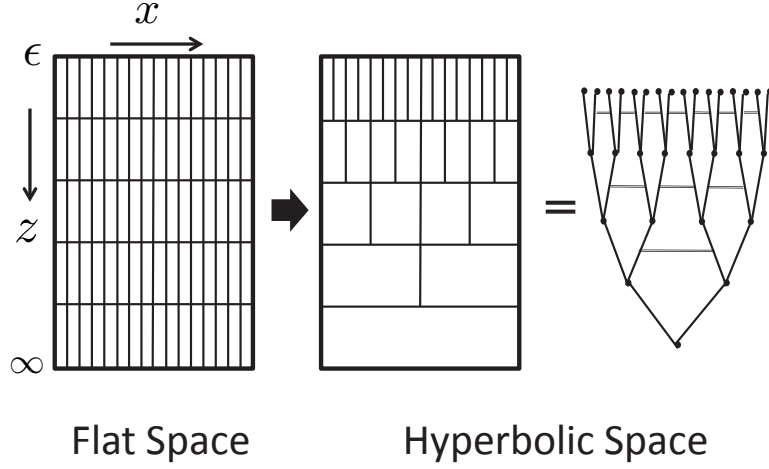


Figure 13: A cartoon explaining path-integral optimization as an analog of tensor-network optimization in CFTs. Figure from [28] with Euclidean time denoted as $z = -\tau$.

Next, one can introduce the actual optimization procedure. Namely, if we now compare the wave functions computed with a background flat metric (denoted with $\Psi_{\text{CFT}}^{\phi_0}[\Phi(x)]$) and with a curved metric (denoted with $\Psi_{\text{CFT}}^{\phi}[\Phi(x)]$), they are proportional to each other

$$\Psi_{\text{CFT}}^{\phi}[\Phi(x)] = e^{S_{\mathcal{L}}[\phi] - S_{\mathcal{L}}[\phi_0]} \Psi_{\text{CFT}}^{\phi_0}[\Phi(x)]. \quad (132)$$

The proportionality factor between the two wave functions is given by an exponent of the Liouville action

$$S_{\mathcal{L}}[\phi] = \frac{c}{24\pi} \int_{-\infty}^{\infty} dx \int_{-\infty}^0 d\tau [(\partial_x \phi)^2 + (\partial_\tau \phi)^2 + \mu e^{2\phi}], \quad (133)$$

where c is the central charge of the 2D CFT.³⁰ Intuitively, the proportionality factor in Eq. (132) can be interpreted as a measure of how many repetitions of path-integration per site we perform to construct the state. Hence, the *optimal path integral* is selected by minimizing the Liouville action with respect to ϕ , i.e., picking the metric that solves the Liouville equation

$$4\partial\bar{\partial}\phi(w, \bar{w}) = \mu e^{2\phi(w, \bar{w})}, \quad w := \tau + ix, \quad (134)$$

with the boundary condition (131). Recall that the metric encoded the density of gates in the tensor network. This procedure is therefore called the *path-integral optimization*.

For example, for the CFT vacuum that is obtained by performing a Euclidean path integral on the half-plane, the optimal geometry is given by the hyperbolic plane. Similar results can be obtained for path integrals on the circle, that prepares the vacuum state of a CFT on the

³⁰The coefficient μ of the potential term can be set to 1 by shifting ϕ .

circle; as well as path integrals on the strip of size β used to prepare the thermofield-double state with inverse temperature β . In the former case, the background obtained via the path-integral optimization procedure is the hyperbolic geometry of the Poincaré disc. In the latter case, the background geometry is the hyperbolic strip, also called the Euclidean trumpet geometry. We can think about these geometries as the counterparts of effective tensor-network geometry that emerges after the optimization procedure. In fact, in the spirit of AdS/TN discussions in holographic CFTs, it is tempting to interpret all these solutions as geometries on time slices of higher-dimensional AdS spacetime. We will return to this point in Sec. 8.2.

Another central idea of references [28, 29] was to interpret the Liouville action as a novel measure of complexity for the wave functions prepared using Euclidean path integrals, dubbed *path-integral complexity*. The main reason to advocate this interpretation was that the proportionality of the on-shell Liouville action to the volume of the space on which the path integral was computed. Indeed, after fixing the normalization such that the integral of the Weyl factor over a square region of the size ϵ has value 1, we can interpret the volume of the Euclidean space as the number of tensors in the optimal network. The on-shell action associated with the CFT vacuum state reads

$$\mathcal{C}_{\Psi_0} = \text{Min}[S_{\mathcal{L}}[\phi]] = \frac{cL}{12\pi\epsilon}, \quad L = \int dx. \quad (135)$$

This result is also consistent with qualitative expectations from holography, that we discuss in the next subsection.

Later on, researchers extended the path-integral optimization method to other settings. References [28, 29] proposed a higher-dimensional generalization of the action (135). The optimization of 2D CFTs deformed by relevant operators was studied in [362], where a modified Liouville action was minimized over both metrics and local deformation couplings. The authors of [363] investigated path integrals for inhomogeneous CFTs, interpreted as CFTs coupled to non-trivial background metrics. Soon after [28], reference [364] argued that a variation of path integral complexity in holographic 2D CFTs leads to Einstein's equations in the bulk of AdS₃. Moreover, the Liouville action (or its covariant version, called the Polyakov action) motivated the treatment of Nielsen's complexity by introducing trajectories on the unitary manifold generated by sequences of 2D conformal transformations [30] (see Sec. 5.5.2).

Liouville action also inspired a series of developments in the tensor-network community. They used the path integral approach to cMERA to define tensor networks in terms of the background geometry on which the state is prepared [365, 366]. In particular, they showed how the background metric's parameters translate into the tensor network's details. This was later used in [367] to argue for a Nielsen-type interpretation of the Liouville action in terms of an appropriate choice of the cost function on the complexity geometry. As opposed to the developments on Nielsen's complexity discussed in Sec. 5, the work [367] utilized necessarily circuits that contained both unitary and Hermitian gates associated with components of the energy-momentum tensor operator. This is similar in spirit to the results [320] discussed in Sec. 7.5.1 and has the same origin: Euclidean time evolution is an efficient and common theoretical way of preparing relevant states. This points towards a mathematical generalization of the Nielsen's complexity that involves both unitary and Hermitian exponents of the generators.

Finally, the results in Ref. [367] pointed out that a general cost function for path integral optimization will also contain positive powers of the cut-off ϵ associated with higher derivatives of

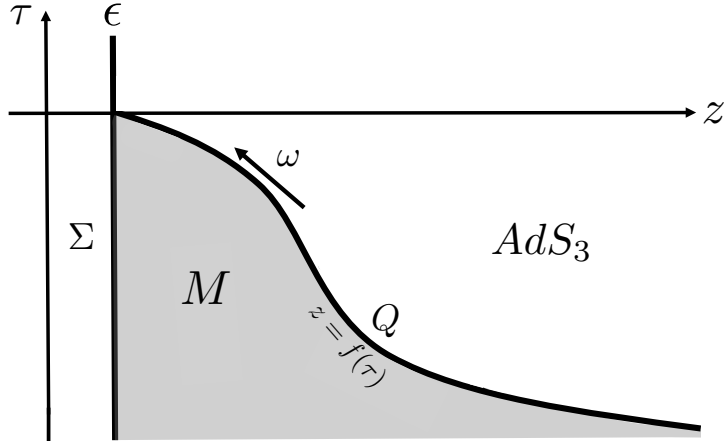


Figure 14: Holographic proposal for the gravity dual of the path-integral optimization, adapted from [368].

ϕ in the spirit of an effective field theory. However, the solutions of Eq. (134) acquire derivatives that are themselves of the order of $1/\epsilon$. This breaks the hierarchy within these more general cost functions that left the contribution (133) as the dominant term and calls for a systematic inclusion of the UV cut-off ϵ . This moves us directly to the subject of the next section.

8.2. Holographic path-integral optimization

The optimization process described above starts with a CFT path integral in a flat geometry, and effectively places it on a particular hyperbolic metric. After an appropriate identification of the Euclidean time with a radial coordinate, this metric can be interpreted as a slice of AdS spacetime. It is then natural to ask whether this procedure, when applied to holographic CFTs, could have a dual geometric interpretation within the AdS/CFT correspondence. If successful, this embedding in holography could shed new light on the interpretation of the gravity dual of the Liouville action in terms of path-integral complexity of a CFT state.

With this motivation, references [368, 369] first proposed a holographic dual of the path-integral optimization procedure. Their construction was very closely related to the framework of Anti-de Sitter/Boundary Conformal Field Theory (AdS/BCFT) [336]. The main idea was to propose as the geometrical dual the maximization of Hartle-Hawking (HH) wave functions in gravity. We consider a boundary cut-off surface Σ located at $z = \epsilon$ (where z is the radial coordinate of the AdS spacetime), and a generic spacelike surface Q parametrized by $z = f(\tau)$. Referring to Fig. 14, the HH wave functions were computed using Eq. (130) inside the shaded region M bounded by Σ and Q . The wave functions need to be maximized with respect to the induced metric h_{ab} on the time-slice Q , described by the metric (with an appropriate choice of gauge)

$$ds^2 = e^{2\phi(\omega)}(d\omega^2 + dx^2). \quad (136)$$

Then, to the leading order in $1/G_N$, the HH wave function can be semiclassically computed as the exponent of the gravitational action. The latter is composed by the Einstein-Hilbert bulk term, plus appropriate boundary contributions: the Gibbons-Hawking term, and a codimension-one brane term with tension T . As a result, the maximization in gravity is equivalent to imposing the Neumann

boundary conditions on Q (indeed in complete analogy with AdS/BCFT)

$$K_{ab} - Kh_{ab} = -Th_{ab}, \quad (137)$$

where K is the trace of extrinsic curvature K_{ab} on Q . Interestingly, performing the optimization of HH wave functions in AdS₃ spacetimes as well in the BTZ black hole background, reproduces metrics identical to those in the CFT optimization (131), after the following identifications:

$$\tau = \omega, \quad \frac{c}{3} = \frac{2l}{G_N} \quad \mu = 1 - \frac{T^2}{(d-1)^2}. \quad (138)$$

One key insight from this construction was the UV completion of the Liouville action, which could be interpreted as the leading $1/\epsilon$ contribution to path-integral complexity (see also the discussion in [367] and its summary in the preceding section). Specifically, [368, 369] argued that the gravity action in region M (see Fig. 14), supplemented with appropriate boundary and Hayward corner terms, provided a finite-cutoff completion of the Liouville action. As a consistency check, taking the "boundary" limit of the gravity action reproduced both the Liouville action (133), and its higher-dimensional generalization [29].

A closely related setup was later explored in [370] as an approach to holographic tensor networks in holographic CFTs. It was demonstrated that the CFT on the slices Q could be explicitly constructed using $T\bar{T}$ deformation with a coupling that depended on Euclidean time³¹, and could be described within finite cut-off holography [372]. Parallel works [31, 33] also argued for $T\bar{T}$ -like interpretation of path integral complexity in holographic CFTs.

The key distinction between references [368, 369] and the work [370] was the way in which partition functions of holographic CFTs deformed by $T\bar{T}$ were computed. Namely, in the $T\bar{T}$ context, the on-shell action was evaluated in the bulk region from the interior up to Q ; whereas in the holographic path-integral optimization context, the action was evaluated in the region M attached to the boundary. In both cases, HH wave functions give rise to identical, constant mean curvature slices of AdS₃ spacetime. Interestingly, slices of AdS spacetime with constant extrinsic curvature also appear naturally in the context of tensor networks. Reference [338] used the same kind of slices to match the volume of the ERB in three-dimensional black hole geometries with a boundary notion of Nielsen complexity.

Concluding, path integral optimization has a great advantage: it defines complexity as a partition function, which is central for a precise holographic map between quantum and gravitational observables. It would be interesting to further push this notion of complexity to find a precise holographic map to geometric observables in AdS spacetime.

³¹This deformation later became the starting point of the "Cauchy-slice holography" [371].

9. Quantum complexity in quantum information theory and many-body physics

Quantum information (QI) theory and complexity inform each other in many ways. We focus on three. First, QI theory shows that complexity governs a resource consumed in operational tasks (Sec. 9.1). Second, complexity distinguishes topological phases (Sec. 9.2). Third, a QI-theoretic quantity—entanglement entropy—bounds complexity under certain conditions (Sec. 9.3).³² Finally, the output of probability distributions also serves as a tool to bound complexity (Sec. 9.4). We chose these topics because holographers called for the resource theory, entropy is the workhorse of QI theory, and the topological application predated holographic applications of complexity. Other QI-complexity intersections lie outside this review’s scope. Examples include the bounding of complexity with the quantum Wasserstein distance [373], the relationship between complexity and quantum circuits’ expressivity [374], and applications of complexity to quantum machine learning [375].

9.1. Operationalism and resource theory

Brown and Susskind suggested that complexity controls a resource useful in operational tasks [44]. Let ρ denote an arbitrary quantum state of a system S ; $\mathcal{C}(\rho)$, the complexity of ρ ; and \mathcal{C}_{\max} , the greatest possible complexity of S . Define the *uncomplexity* of ρ as the gap $\mathcal{C}_{\max} - \mathcal{C}(\rho)$. Uncomplexity serves as a resource in quantum computation: consider running a quantum computation on an n -qubit register. The optimal input state is the zero-complexity state $|0\rangle^{\otimes n}$. It serves analogously to clean scrap paper on which we write scratchwork when performing classical computations.

Brown and Susskind conjectured that one can define a resource theory for quantum uncomplexity [44]. A *resource theory* is a simple, information-theoretic model for any context in which agents are restricted to perform only certain operations. For example, in the resource theory of entanglement, agents can perform only local operations and classical communications (LOCC). The allowed operations are called *free*, being modeled as costing nothing. Anything not free is a *resource*; it may be consumed to enable an operational task. In the entanglement theory, for instance, entangled states are resources. Agents may consume a maximally entangled pair of qubits to teleport quantum information, using LOCC.

Yunger Halpern *et al.* defined a resource theory of quantum uncomplexity in [376]. For simplicity, suppose that an agent in the resource theory has n qubits (the setting can be generalized). The free operations are called *fuzzy operations*: the agent can attempt to perform any two-qubit gate U (the setting can be generalized to k -qubit gates, for any $k \leq n$, and to gates in a particular set). However, noise corrupts every gate implementation. Hence the gate \tilde{U} realized is chosen randomly from an ϵ -ball (a small open set) about U . \tilde{U} is called a *fuzzy gate*. The compositions of all fuzzy gates are the fuzzy operations. Every agent will have a personal tolerance for how fuzzy, or unknown, the state can become. This tolerance limits how many fuzzy gates the agent is willing to perform—and so curtails the complexities of the operations performed on the system.

Resource theories can be used to formulate operational tasks and to quantify the tasks’ optimal efficiencies. An example is *uncomplexity extraction* [376]: let $\delta \geq 0$ denote an error tolerance; and ρ , an arbitrary n -qubit state. One extracts uncomplexity from ρ by distilling a state δ -close to $|0\rangle^{\otimes k}$ in trace distance. How large a k is achievable? The answer depends on the *complexity entropy*.

³²We already discussed another connection between complexity and entanglement in the context of Nielsen’s complexity in section 5.4. There, we saw that very special definitions of complexity are completely fixed by the entanglement and Rényi entropies.

The complexity entropy quantifies how random ρ looks to an agent who can perform only computationally restricted measurements [376, 377]. In QI theory, a measurement is modeled with a *positive-operator-valued measure* $\{Q_\alpha\}$ [10]. The *measurement operators* Q_α are positive-semidefinite, $Q_\alpha \geq 0$, and normalized as $\sum_\alpha Q_\alpha = \mathbb{1}$. Define as a *zero-complexity measurement operator* any Q_α that acts on each qubit either (i) as the identity or (ii) by projecting the qubit onto $|0\rangle\langle 0|$: $\bigotimes_{j=1}^n (|0\rangle\langle 0|)^{\alpha_j}$, if $\alpha_j \in \{0, 1\}$, and $(|0\rangle\langle 0|)^0 := \mathbb{1}$. Let $r \in \mathbb{Z}_{\geq 0}$ denote a fixed integer. Consider performing $\leq r$ gates and then a zero-complexity measurement operator. This process effects a *complexity- r measurement operator*, the set of which we denote by M_r . We apply these definitions as follows. Consider performing a binary hypothesis test between ρ and $\mathbb{1}/2^n$: we receive one of the two states and must guess which we received. We perform a measurement $\{Q, \mathbb{1} - Q\}$. If the Q outcome obtains, we guess that we received ρ ; and, if the $\mathbb{1} - Q$ outcome, then $\mathbb{1}/2^n$. A type I error occurs if, upon receiving ρ , we wrongfully guess $\mathbb{1}/2^n$. Let $1 - \eta$ upper-bound the maximum allowable type I-error probability: $\text{Tr}(Q\rho) \geq \eta$. A type II error occurs if, upon receiving $\mathbb{1}/2^n$, we wrongfully guess ρ . The minimal type II-error probability $\text{Tr}(Q\mathbb{1})/2^n$, subject to the type I constraint, forms the *complexity entropy's* essence:

$$H_c^{r,\eta}(\rho) := \min_{\substack{Q \in M_r, \\ \text{Tr}(Q\rho) \geq \eta}} \{\log_2(\text{Tr}(Q))\}. \quad (139)$$

The complexity entropy controls the number of uncomplex qubits extractable from ρ via fuzzy operations [376]. Let ϵ quantify the gates' fuzziness, and let the tolerance $\delta \geq r\epsilon$. For every parameter value $\eta \in [1 - (\delta - r\epsilon)^2, 1]$, one can extract $k = n - H_c^{r,\eta}(\rho)$ qubits δ -close to $|0\rangle^{\otimes n}$, using fuzzy operations. Conversely, one can extract at most $n - H_c^{r,1-\delta}$ qubits. These results follow a pattern common in QI theory: entropies quantify the optimal efficiencies with which operational tasks can be performed.

Entropies are the workhorses of QI theory. That an entropy can quantify complexity, however, was far from obvious, before [376]. For example, consider an n -qubit system prepared in a pure tensor-product state $\rho(0) = |\psi(0)\rangle\langle\psi(0)|$. Under a nonintegrable Hamiltonian, the state evolves to $\rho(t) = |\psi(t)\rangle\langle\psi(t)|$ in a time t . The state's complexity grows, yet the von Neumann entropy $S_{\text{vN}}(\rho(t)) = -\text{Tr}(\rho(t) \log_2 \rho(t))$ remains zero. Every subsystem's reduced state has an S_{vN} that likely grows, but such entropies saturate long before $\rho(t)$'s complexity does. Hence commonly used entropies do not track complexity. Avoiding this pitfall, the complexity entropy (139) quantifies how random $\rho(t)$ *appears* to a computationally restricted observer. The observer-centric approach was pioneered in [378], through a metric called the strong complexity. Other precursors to the complexity entropy include [379, 380], motivated by pseudorandomness and cryptography. Reference [377] introduces variations on $H_c^{r,\eta}(\rho)$. These variations quantify the optimal efficiencies of more information-processing and thermodynamic tasks, including erasure and decoupling.

These results offer hope that complexity entropies might quantify holographic tasks' operational efficiencies. For example, consider an agent Alice falling into a black hole [44]. A firewall is expected to consume her if the horizon is dual to a CFT whose complexity is decreasing. Tossing a qubit into the black hole doubles the CFT state's uncomplexity, enabling the complexity to return to decreasing—and saving Alice. This story might be generalized beyond qubits with help from $H_c^{r,\eta}$.

9.2. Circuit complexity and topological order

Phases of matter characterize how large numbers of particles can organize. This includes the solid, liquid and gas phases. In this section, we will briefly explain how topological order and quantum circuit complexity are related.

Up until the early 80s it was thought that all phases of matter fit into Landau’s framework of symmetry breaking [381, 382]. Roughly, Landau’s theory asserts that a phase transition can only occur when a symmetry is broken, like the spontaneous change from a continuous symmetry in a chaotic/liquid phase to a discrete symmetry in a solid phase. Here, every phase is described by a pair of symmetry groups G_H and G_ψ , where G_H are all symmetry operations of the Hamiltonian and $G_\psi \subseteq G_H$ is the symmetry group of the ground state ψ . A phase transition then occurs if the symmetry group G_ψ changes under an order parameter (such as the strength of a magnetic field).

Starting with a plethora of inequivalent chiral spin states all satisfying the same symmetries, it was discovered that quantum Hamiltonians exhibit an even richer theory of phase transitions. For an extensive review about topological phases, we refer to Wen [383]. Since then an entire “zoo of topological phases” was discovered [384]. Topological phases refer to gapped ground states that show vast differences in their entanglement structure but are otherwise seemingly featureless (and therefore indistinguishable by symmetry groups).

In the following we will show how quantum circuit complexity is related to the concept of topological order. States exhibiting topological order are gapped ground states of local Hamiltonians that cannot be reduced to a product state continuously without the gap closing. In particular, they are in a topological phase distinct from all product state, also called the trivial phase. More precisely, consider a gapped local Hamiltonian H_0 with a unique ground state $|\psi\rangle$. $|\psi\rangle$ can always be transformed into a product state via a continuous path consisting of local Hamiltonians $H(s)$ for $s \in [0, 1]$ with $H(0) = H_0$: For H_0 acting on n qubits we simply define $H(s) = (1-s)H_0 + s \sum_{i=1}^n Z_i$, where Z_i denotes the Pauli Z matrix acting on the i th qubit/spin. Clearly, the unique ground state of $H(1)$ is $|0^n\rangle$ and $H(1)$ is gapped. However, it is very likely that at least one of the $H(s)$ has a degenerate ground state, and thus closes the gap. A state is in the trivial phase if such a continuous path exists such that the gap above the unique ground state $|\psi(s)\rangle$ is uniformly lower bounded by a positive constant along the path. A state is topologically ordered if no such path exists. A continuous path of Hamiltonians with a uniformly lower bounded spectral gap is called *adiabatic*.

How does this relate to quantum circuit complexity? It was observed in Ref. [385] that the above definition of topological order in terms of the absence of adiabatic paths is equivalent to superconstant lower bounds on the quantum circuit complexity. It turns out that the existence of an adiabatic path is equivalent to the existence of a *local unitary transformation* [385]:

$$|\psi(s)\rangle = \mathcal{T} \left(e^{-i \int_0^s \tilde{H}(r) dr} \right) |\psi(0)\rangle, \quad (140)$$

where $\tilde{H}(r)$ is a local Hamiltonian and \mathcal{T} denotes the path-ordering operator. On the other hand, the existence of such a local unitary transformation implies the existence of an adiabatic path via³³

$$H(s) := U(s) H U^\dagger(s), \quad U(s) = \mathcal{T} \left(e^{-i \int_0^s \tilde{H}(r) dr} \right). \quad (141)$$

³³The notation in Eq. (141) is analogous to Eq. (18), which defined a trajectory implementing a unitary operator in the complexity geometry.

It is easy to see that the Hamiltonians $H(s)$ are all gapped and the unitaries $U(s)$ preserve the spectrum of H and therefore the spectral gap as well. The relation to circuit complexity now follows from the fact that the operator $U(1)$ can be approximated by a constant depth quantum circuit via Trotterization. Trotterization proceeds by splitting the time evolution (here the integral $\int_0^1 ds \tilde{H}(s)$) into small pieces, which are approximately local. The error this approximation introduces can be made arbitrarily small by increasing the circuit depth. In other words, the existence of a constant depth quantum circuit preparing the ground state of a gapped quantum Hamiltonian is equivalent to the state being topologically ordered.

9.3. Bounding complexity growth with entanglement

Quantum circuit complexity of a state quantifies the elementary resources necessary to prepare said state from a product state. Therefore, complexity also quantifies the resources necessary to transform the state back into a product state. Clearly, complexity can be viewed as a measure of entanglement, which is ultimately the failure of a state to be product. As such, we can compare it to the entanglement entropy, arguably the most prominent measure of entanglement. A high entanglement entropy along a bipartite cut does not imply a high circuit complexity: the maximally entangled state between two systems each consisting of n qubits can be prepared on a quantum computer with a constant depth quantum circuit. Even if we consider the maximum entanglement entropy over all bipartite cuts of the qubits, we find that it saturates trivially at a maximum value of n , whereas the circuit complexity grows for an exponentially long time eventually reaching values of $\Omega(2^n/n)$ (compare Section 4.3). On the other hand, we can easily show the existence of quantum circuits with superpolynomial circuit complexity but no entanglement between some parts of the system. E.g., simply apply a Haar random unitary to $\log^{1+\varepsilon}(n)$ many qubits and leave all other qubits untouched. So if these two notions are not equivalent, what can we say about their relationship?

Entanglement growth implies early-time bounds on complexity during chaotic evolutions. More precisely, it turns out that entanglement *does* imply non-trivial circuit lower bounds, but entanglement needs to be present along any bipartite cut. The reason behind this is that the Schmidt rank along any bipartite cut can only be increased by a constant factor. In particular, if a state $|\psi\rangle$ has a Schmidt rank of SR_i for a bipartite cut of all qubits into two sets $A = \{1, \dots, i\}$ and $B = \{i+1, \dots, n\}$, then we know that at least $c \log(\text{SR}_i)$ gates (each acting on a qubit in A and a qubit in B) are required to prepare $|\psi\rangle$. Suppose that we only want to lower bound the size of any geometrically local circuit that approximates the state $|\psi\rangle$. However, a geometrically local circuit can only apply gates to neighbouring qubits $(i, i+1)$. Then, any gate that acts on A and B necessarily acts on $(i, i+1)$. We can thus apply the above argument for all n Schmidt ranks SR_i without overcounting and find:

$$\min_{\text{geom. loc. circuits}} \# \text{gates} \geq \sum_{i=1}^n c \log(\text{SR}_i). \quad (142)$$

A version of this argument was applied in Ref. [106] to lower bound the circuit cost by the entanglement cost, which is closer to the more natural entanglement entropy than the Schmidt rank we used for the argument above. This bound can never produce a superpolynomial lower bound on the circuit complexity $\log(\text{SR}) = O(n)$.

Finally, let us mention a relation between circuit complexity and the so-called *embezzlement of entanglement*. The latter terminology refers to a process in which entanglement is approximately extracted from a resource system by using local unitary operators, with no detectable change to the resource's state [386]. References [387, 388] argued that any state of a relativistic QFT could serve as a resource for the process, where the error of the approximation can be made arbitrarily small. Recently, the author of [389] showed that circuit complexity is lower-bounded by a quantity proportional to the inverse of the error. In other words, circuit complexity acts as an obstruction to perfect embezzlement.

9.4. Bounding complexity via concentration

Another way to bound the circuit complexity of a state and, in particular, the *depth* necessary to prepare it is via correlations in the output probability distributions. Let $|\psi\rangle = U|0^n\rangle$ be a state on n qubits prepared by a constant depth quantum circuit U . The state $|\psi\rangle$ can be used to define a probability distribution over the bitstrings $x \in \{0, 1\}^n$ via the Born rule $p_x := |\langle x|\psi\rangle|^2$. We can show that the probability distribution is concentrated in the Boolean cube. To make this more precise, we can define the orthogonal projector

$$\Pi_{\substack{>k \\ <k}} := \sum_{\substack{x \in \{0,1\}^n \\ |x| \gtrless k}} |x\rangle\langle x|, \quad (143)$$

where $|x|$ denotes the Hamming weight of x , i.e. the number of 1s in the bitstring. Then, we can show that

$$\langle \psi | \Pi_{>(1-c)n} | \psi \rangle \langle \psi | \Pi_{<cn} | \psi \rangle \approx 0 \quad (144)$$

for a constant $c > 0$. In other words, the mass of the output probability distribution cannot be in two far away regions.

We briefly sketch a proof of the concentration explained above, where we follow the argument presented in Ref. [390]. Readers that are only interested in how to apply such a statement to circuit complexity can skip this paragraph. $|\psi\rangle$ is the unique ground state of the commuting, gapped and l -local Hamiltonian $H = \sum_i \mathbb{1} - U \mathbb{1}_{i-1} \otimes |0_i\rangle\langle 0_i| \otimes \mathbb{1}_{n-i} U^\dagger$, where $l \leq 2^{\text{depth of } U}$. We can use that Chebyshev polynomials C_m (of the first kind) satisfy $C_m(x) \leq e^{-m\sqrt{1-h}}$ for $x \in [0, h]$ and $C_r(1) = 1$. Using that the spectral gap of H is 1, we find

$$\left\| |\psi\rangle\langle\psi| - C_m \left(\mathbb{1} - \frac{H}{n} \right) \right\|_\infty \leq e^{-m/\sqrt{n}}. \quad (145)$$

Choosing $m = c'n$ for another constant $c' > 0$ makes this small. However, we can notice that the operator $C_m \left(\mathbb{1} - \frac{H}{n} \right)$ is a sum over $lc'n$ -local terms. In particular, for a string of Hamming weight $< cn$, we have that each bitstring that has overlap with $C_m \left(\mathbb{1} - \frac{H}{n} \right) |x\rangle$ has Hamming weight at most $(c + lc')n$. Combining this limitation on the increase in Hamming weight with the approximation (145) yields

$$\langle \psi | \Pi_{>(1-c)n} | \psi \rangle \langle \psi | \Pi_{<cn} | \psi \rangle \approx \langle \psi | C_m \left(\mathbb{1} - \frac{H}{n} \right) \Pi_{>cn} | \psi \rangle \approx 0. \quad (146)$$

Why does this property allow us to prove lower bounds on the depth necessary to prepare a

state? Consider for an extreme example the GHZ state $|\text{GHZ}\rangle = \frac{1}{\sqrt{2}}(|0^n\rangle + |1^n\rangle)$. Clearly, the output probability distribution p_x is a fair coin toss between 0^n and 1^n and

$$\langle \text{GHZ} | \Pi_{>(1-c)n} | \text{GHZ} \rangle \langle \text{GHZ} | \Pi_{<cn} | \text{GHZ} \rangle = \frac{1}{4}, \quad (147)$$

for any $c > 0$, which is in direct contradiction to the concentration property Eq. (144). But Eq. (144) is a direct consequence of the assumption that $|\text{GHZ}\rangle$ was prepared by a constant depth circuit. We conclude that $|\text{GHZ}\rangle$ requires a superconstant quantum circuit to prepare.

This strategy based on concentration in output probability distributions, was used in the proof of Freedman and Hasting's NLTS conjecture [391] due to Anshu, Breuckmann and Nirkhe [392]. The NLTS theorem asserts that Hamiltonians exist such that any state with an energy density below some constant threshold is topologically ordered in the sense of Section 9.2. More precisely, there is a family of k -local Hamiltonians $H_n = \sum_{i=1}^m h_i$ acting on n qubits with $m = O(n)$ and a $\varepsilon > 0$ such that all states $|\psi\rangle$ with $\langle \psi | H | \psi \rangle / n \leq \varepsilon$ are topologically ordered. In particular, this result shows that topological order can persist at constant temperatures.

The techniques discussed in this subsection can only produce polynomial lower bounds on the circuit complexity of a state. More precisely, the parent Hamiltonian $H = \sum_i \mathbb{1} - U \mathbb{1}_{i-1} \otimes |0_i\rangle\langle 0_i| \otimes \mathbb{1}_{n-i} U^\dagger$ will be of locality $\sim n$, which does not result in a contradiction with concentration as $\Pi_{>(1-c)n} H \Pi_{<cn} \neq 0$.

10. Epilogue

We conclude this review by summarizing the main results and open problems. The summary assumes the form of a dialogue, in the spirit of Sec. 3. Sofia, Sagredo, and Complexio have now read the rest of the review and are discussing their takeaways, as at a journal club.

Sagredo: I have been impatiently awaiting your arrival, as I need guidance to identify the major opportunities in quantum-complexity research. Also, it would be helpful if Sofia could summarize the main achievements obtained so far.

Sofia: I am happy to overview the main findings. The review explored multiple notions of complexity in quantum contexts: exact and approximate circuit complexities, Nielsen’s geometric approach, notions based on operator and state spreading, and definitions inspired by tensor networks. These notions have deepened our understanding of quantum systems’ evolution, including thermalization and the chaos-integrability boundary. Within the AdS/CFT correspondence, complexity is related to gravitational observables, which can elucidate the region behind a black hole’s horizon.

Complexio: The gravitational quantities seem related to complexity only qualitatively. Is it worth spending so much research effort on hand waving?

Sofia: As a matter of fact, Refs. [26, 27, 316, 320] identified a quantitative relationship recently. Section 7.5.1 described this breakthrough: a double-scaled SYK model’s spread complexity is dual to the size of an ERB in two-dimensional theories of gravity. The duality, being exact, is a major achievement.

Complexio: Still, the result has a narrow range of validity. In two bulk dimensions, the graviton is not even dynamical. Should we truly regard this result as a success?

Sofia: The duality is simplest in two bulk dimensions, and this simplicity facilitated the proof. Yet Ref. [27] reinterprets the matching in a language that should enable a generalization to higher dimensions. Additionally, insight into two-dimensional theories has advanced long-standing problems, famously including the black-hole-information paradox [393–396]. The similar insight here will hopefully enable similar advancements.

Complexio: Those opportunities sound appealing. Still, what if nobody proves a duality between spread complexity and ERB volume in higher-dimensional theories?

Sofia: Regardless of the holographic duality, studying complexity benefits the quantum-information and quantum-gravity communities. As the review showed, quantum complexity can help us simulate time evolutions, identify quantum chaos, and more. In gravitational systems, geometric observables can illuminate the black-hole interior, black-hole evaporation, and causal properties of a spacetime.

Sagredo: You mentioned chaos. Do I recall correctly from Sec. 6.3.3 that Krylov and spread complexities diagnose chaos?

Sofia: They do to an extent. Consider an ensemble of theories, such as the SYK model, distinguished by random values of one or more parameters. The Krylov and spread complexities’ variances diagnose chaos [126, 165]. Whether Krylov complexity distinguishes chaotic from integrable QFTs remains an open question [186, 187]. Recent advances appear in Ref. [188, 189], which leverage von Neumann algebras and algebraic QFTs.

Complexio: Do other notions of complexity that we have heard about—apart from Krylov complexity—diagnose chaos?

Sofia: Yes, Sec. 5.3 illustrated with a finite-dimensional quantum system: as a quantum state evolves under a chaotic Hamiltonian, it follows a geodesic in Nielsen’s complexity geometry. This result depends on the geometry’s—that is, on the unitary manifold’s—having a negative average-sectional-curvature [37, 39, 86, 96]. References [14, 82] highlighted complexity geometries that satisfy this requirement. Conveniently, we can address those geometries analytically, since their curvatures are modest.

Complexio: So we can learn about chaos from quantum complexity. Can we similarly learn from complexity about the holographic dictionary?

Sofia: Certainly—we have known for years that quantum information theory can reveal which part of the bulk encodes which feature of the boundary theory. This research program relates to the claim that slices of AdS geometry naturally arise in tensor networks [4]. The claim inspired notions of complexity discussed in Sec. 8.1. These notions may help us identify holographically dual quantities.

Sagredo: As your response highlights, researchers have devoted substantial work to AdS spacetimes. However, we live in an expanding universe. Can complexity help us understand quantum-gravity theories for expanding universes, such as our universe and de Sitter space?

Sofia: I believe so. Whether de Sitter spacetime has a quantum dual remains an open question. If the answer is yes, then the AdS/CFT duality ports over to de Sitter spacetime, perhaps with some modifications. Consequently, we can translate quantum-gravity questions into conceptually simpler questions about quantum systems. For now, people are conjecturing such a translation, as well as conjecturing about duals of complexity [173, 258–309, 311, 312, 397, 398]. Hopefully, exploring holographic complexity in de Sitter spacetime will indicate which properties the spacetime’s quantum dual should have, if it exists.

Such a development would unlock a further opportunity for future work: researchers expect the quantum dual to be an open quantum system [173, 174]. Therefore, we may learn about open quantum systems’ complexities through de Sitter holography. Several works have already begun unpacking open quantum systems’ complexities [376, 399–405].

Complexio: Also on the topic of holography, according to the review, holographers called for the development of quantum-information-theoretic tools, including a resource theory for quantum complexity (see Sec. 9.1). Quantum information theorists defined the resource theory in [376]. In turn, the resource theory led to new entropic measures of complexity [376, 377]. Can these made-to-order tools now benefit holography?

Sofia: I hope so. For example, holographers have imagined an observer Alice falling into a black hole and fearing that she will hit a firewall. If Bob throws a maximally mixed qubit into the black hole, holographers have noted, the qubit will alleviate Alice’s danger to an extent. We can now progress beyond that simple qubit. What if Bob throws a quantum system, of arbitrary dimensionality, in an arbitrary state? How much will he alleviate Alice’s danger? Our new quantum-information-theoretic tools should enable general, quantitative answers.

Complexio: The partnership between quantum information theorists and high-energy physicists is promising. However, I heard that computer scientists have been suspicious of the duality proposed between volume and quantum complexity in the AdS/CFT correspondence.

Sofia: You heard correctly. This skepticism led to the research topic that debuted in [345]: the holographic dictionary’s complexity. According to Sec. 7.6, translating between complexity and volume takes time unless quantum gravity allows for more computational power than a quantum computer. Computer scientists have proposed that the holographic dictionary might be highly

complex. Their argument extends beyond the complexity=volume conjecture to other holographic complexity conjectures. Followup work focused on the duality between area and entanglement entropy [348]. Still, we are not certain for which entries the holographic dictionary is complex. Ramifications will include our ability to study quantum gravity through quantum computing.

Sagredo: These holographic concerns bring to mind your earlier claim that, even in the absence of any duality, quantum complexity merits studying within quantum information theory. Sofia has already pointed out some open quantum-information-theoretic problems centered on quantum complexity. Can you list more?

Sofia: Certainly; I have three in mind. According to Sec. 4, physicists do not know how random quantum circuits can realize the switchback effect. Such a realization would strengthen the relationship between quantum chaos and random quantum circuits.

Second, we should lower-bound the circuit complexities of states in families that we can describe efficiently. We already have a lower bound $\sim \log(n)n$ as discussed in Sec. 9.4. Such an endeavor may encounter obstacles that classical computer scientists face. More precisely, pseudorandom functions could hinder the establishment of these circuit-complexity lower bounds. The reason, roughly, is the following: imagine a quantity that distinguishes low-complexity-functions from high-complexity-functions. This quantity must, itself, be hard to compute. Otherwise, one could easily use the quantity to distinguish pseudorandom functions (low complexity) from random functions (high complexity). The resulting obstacles for lower-bounding circuit complexity, we call *natural proof barriers* [58]. We might quantize these natural proof barriers by strengthening a recent construction of pseudorandom unitaries [347].

Third, researchers expect that some local Hamiltonians' low-energy states have superpolynomial circuit complexities. However, proving an unconditional superpolynomial lower bound would come close to separating the complexity classes QMA (quantum Merlin-Arthur) and QCMA (quantum-classical Merlin-Arthur) [406]. QMA contains decision problems that one can verify with a quantum proof; and QCMA, decision problems that a quantum computer can verify with a classical proof. Unconditionally separating QMA and QCMA, one would achieve a monumental breakthrough in theoretical computer science by also separating the classes P and PSPACE. Compare Ref. [407] for details. A more modest goal is to separate QMA from QCMA "relative to an oracle". An oracle is a black box that solves a powerful problem in one step. Often, unconditional statements about complexity classes can be made if all Turing machines are given access to such an oracle. The problem of separating QMA from QCMA relative to increasingly weaker oracles was subject to significant efforts in the past years [406, 408–414].

Let me mention, as an aside, that the mathematics community has studied problems related to circuit optimization. They have focused on the minimum number of steps required to reach all the points on certain group manifolds. We can recognize this number as a type of complexity. Finding gates that minimize this complexity amounts to solving the *golden-gates problem* [415–417]. That problem, in turn, relates to the famous mathematical problem of sphere packing. So complexity is really everywhere!

Sagredo: And let this conclude today's discussion. Clearly, many opportunities await us. I look forward to reading a future review that satisfies our curiosity about them!

Acknowledgments

We would like to thank Brian Swingle and Beni Yoshida for their involvement in the early stages of this review. We are grateful to our collaborators on the topic of quantum complexity who significantly contributed to both the knowledge development described here, as well as to our viewpoints on open questions in this area. Furthermore, we thank Igal Arav, Javier Magan, and Tim Schuhmann for valuable discussions during the writing process. We especially thank Saskia Demulder, Damian Galante, Tim Schuhmann, Tal Schwartzman and Zixi Wei for insightful discussions and comments on the draft. The authors gratefully acknowledge the organizers and participants of the workshop “EuroStrings 2024” in Southampton, United Kingdom, where part of this work was carried out. The work of S. B. was supported by the INFN grant “Gauge Theories and Strings” (GAST), via a research grant on “Holographic dualities, quantum information and gravity.” V. B. is supported in part by the DOE through DE-SC0013528 and QuantISED grant DE-SC0020360, and in part by the Eastman Professorship at Balliol College, University of Oxford. The work of S. B. and S. C. was supported by the Israel Science Foundation (grant No. 1417/21), by the German Research Foundation through the German-Israeli Project Cooperation (DIP) grant “Holography and the Swampland,” by Carole and Marcus Weinstein through the BGU Presidential Faculty Recruitment Fund, and by the ISF Center of Excellence for theoretical high-energy physics. S. C. is also supported by the ERC starting Grant dSHologQI (project number 101117338). P. C. is supported by NCN Sonata Bis 9 2019/34/E/ST2/00123 grant and by an ERC Consolidator grant (number: 101125449/acronym: QComplexity). Views and opinions expressed are, however, those of the authors only and do not necessarily reflect those of the European Union or the European Research Council. Neither the European Union nor the granting authority can be held responsible for them. N. Y. H. received support from the National Science Foundation (QLCI grant OMA-2120757). J. H. is supported by the Harvard Quantum Initiative (HQI). M. P. H. has received support from the European Research Council (ERC) under the European Union’s Horizon 2020 research and innovation programme (grant number: 101089093 / project acronym: High-TheQ).

Appendix A. Guide to acronyms

Acronym	Full form
AdS	anti-de Sitter
\mathcal{BC}	binding complexity
BCFT	boundary conformal field theory
CA	complexity=action
CAny	complexity=anything
CFT	conformal field theory
cMERA	continuous multiscale entanglement renormalization ansatz
CV	complexity=volume
CV2.0	complexity=volume 2.0
DSSYK	double-scaled Sachdev-Ye-Kitaev

EOW	end-of-the-world
ERB	Einstein-Rosen bridge
EW	entanglement wedge
FS	Fubini-Study
GHZ	Greenberger-Horne-Zeilinger
GUE	Gaussian unitary ensemble
HRT	Hubeny-Rangamani-Takayanagi
IR	infrared
JT	Jackiw-Teitelboim
LOCC	local operations and classical communication
MERA	multiscale entanglement renormalization ansatz
NLTS	no low-energy trivial state
OTOC	out-of-time-ordered correlator
QCMA	quantum classical Merlin-Arthur
QFT	quantum field theory
QM	quantum mechanics
QMA	quantum Merlin-Arthur
RMT	random matrix theory
SFF	spectral form factor
SYK	Sachdev-Ye-Kitaev
TFD	thermofield-double
TN	tensor network
UV	ultraviolet
WDW	Wheeler-De Witt

References

- [1] L. Susskind, Three Lectures on Complexity and Black Holes (10 2018). [arXiv:1810.11563](https://arxiv.org/abs/1810.11563), [doi:10.1007/978-3-030-45109-7](https://doi.org/10.1007/978-3-030-45109-7).
- [2] S. Chapman, G. Policastro, Quantum computational complexity from quantum information to black holes and back, *Eur. Phys. J. C* 82 (2) (2022) 128. [arXiv:2110.14672](https://arxiv.org/abs/2110.14672), [doi:10.1140/epjc/s10052-022-10037-1](https://doi.org/10.1140/epjc/s10052-022-10037-1).
- [3] P. Nandy, A. S. Matsoukas-Roubeas, P. Martínez-Azcona, A. Dymarsky, A. del Campo, Quantum Dynamics in Krylov Space: Methods and Applications (5 2024). [arXiv:2405.09628](https://arxiv.org/abs/2405.09628).
- [4] B. Swingle, Entanglement Renormalization and Holography, *Phys. Rev. D* 86 (2012) 065007. [arXiv:0905.1317](https://arxiv.org/abs/0905.1317), [doi:10.1103/PhysRevD.86.065007](https://doi.org/10.1103/PhysRevD.86.065007).

- [5] J. Maldacena, S. H. Shenker, D. Stanford, A bound on chaos, JHEP 08 (2016) 106. [arXiv:1503.01409](#), [doi:10.1007/JHEP08\(2016\)106](#).
- [6] T. G. Mertens, G. J. Turiaci, Solvable models of quantum black holes: a review on Jackiw–Teitelboim gravity, Living Rev. Rel. 26 (1) (2023) 4. [arXiv:2210.10846](#), [doi:10.1007/s41114-023-00046-1](#).
- [7] F. Haake, Quantum Signatures of Chaos, 3rd Edition, Springer, 2010. [doi:https://doi.org/10.1007/978-3-642-05428-0](#).
- [8] A. P. Luca D’Alessio, Yariv Kafri, M. Rigol, From quantum chaos and eigenstate thermalization to statistical mechanics and thermodynamics, Advances in Physics 65 (3) (2016) 239–362. [doi:10.1080/00018732.2016.1198134](#).
- [9] C. Gogolin, J. Eisert, Equilibration, thermalisation, and the emergence of statistical mechanics in closed quantum systems, Reports on Progress in Physics 79 (5) (2016) 056001. [doi:10.1088/0034-4885/79/5/056001](#).
- [10] M. A. Nielsen, I. L. Chuang, Quantum Computation and Quantum Information: 10th Anniversary Edition, Cambridge University Press, 2010. [doi:10.1017/CB09780511976667](#).
- [11] J. I. Cirac, D. Perez-Garcia, N. Schuch, F. Verstraete, Matrix product states and projected entangled pair states: Concepts, symmetries, theorems, Rev. Mod. Phys. 93 (4) (2021) 045003. [arXiv:2011.12127](#), [doi:10.1103/RevModPhys.93.045003](#).
- [12] G. Vidal, Entanglement Renormalization, Phys. Rev. Lett. 99 (22) (2007) 220405. [arXiv:cond-mat/0512165](#), [doi:10.1103/PhysRevLett.99.220405](#).
- [13] J. Haegeman, T. J. Osborne, H. Verschelde, F. Verstraete, Entanglement Renormalization for Quantum Fields in Real Space, Phys. Rev. Lett. 110 (10) (2013) 100402. [arXiv:1102.5524](#), [doi:10.1103/PhysRevLett.110.100402](#).
- [14] A. R. Brown, Polynomial Equivalence of Complexity Geometries, Quantum 8 (2024) 1391. [arXiv:2205.04485](#), [doi:10.22331/q-2024-07-02-1391](#).
- [15] A. N. Kolmogorov, On tables of random numbers, Sankhyā: The Indian Journal of Statistics, Series A (1961-2002) 25 (4) (1963) 369–376.
- [16] D. E. Parker, X. Cao, A. Avdoshkin, T. Scaffidi, E. Altman, A Universal Operator Growth Hypothesis, Phys. Rev. X 9 (4) (2019) 041017. [arXiv:1812.08657](#), [doi:10.1103/PhysRevX.9.041017](#).
- [17] V. Balasubramanian, P. Caputa, J. M. Magan, Q. Wu, Quantum chaos and the complexity of spread of states, Phys. Rev. D 106 (4) (2022) 046007. [arXiv:2202.06957](#), [doi:10.1103/PhysRevD.106.046007](#).
- [18] L. Susskind, Entanglement is not enough, Fortsch. Phys. 64 (2016) 49–71. [arXiv:1411.0690](#), [doi:10.1002/prop.201500095](#).

- [19] D. Stanford, L. Susskind, Complexity and Shock Wave Geometries, *Phys. Rev. D* 90 (12) (2014) 126007. [arXiv:1406.2678](#), [doi:10.1103/PhysRevD.90.126007](#).
- [20] A. R. Brown, D. A. Roberts, L. Susskind, B. Swingle, Y. Zhao, Holographic Complexity Equals Bulk Action?, *Phys. Rev. Lett.* 116 (19) (2016) 191301. [arXiv:1509.07876](#), [doi:10.1103/PhysRevLett.116.191301](#).
- [21] A. R. Brown, D. A. Roberts, L. Susskind, B. Swingle, Y. Zhao, Complexity, action, and black holes, *Phys. Rev. D* 93 (8) (2016) 086006. [arXiv:1512.04993](#), [doi:10.1103/PhysRevD.93.086006](#).
- [22] J. Couch, W. Fischler, P. H. Nguyen, Noether charge, black hole volume, and complexity, *JHEP* 03 (2017) 119. [arXiv:1610.02038](#), [doi:10.1007/JHEP03\(2017\)119](#).
- [23] A. Belin, R. C. Myers, S.-M. Ruan, G. Sárosi, A. J. Speranza, Does Complexity Equal Anything?, *Phys. Rev. Lett.* 128 (8) (2022) 081602. [arXiv:2111.02429](#), [doi:10.1103/PhysRevLett.128.081602](#).
- [24] A. Belin, R. C. Myers, S.-M. Ruan, G. Sárosi, A. J. Speranza, Complexity equals anything II, *JHEP* 01 (2023) 154. [arXiv:2210.09647](#), [doi:10.1007/JHEP01\(2023\)154](#).
- [25] L. V. Iliesiu, M. Mezei, G. Sárosi, The volume of the black hole interior at late times, *JHEP* 07 (2022) 073. [arXiv:2107.06286](#), [doi:10.1007/JHEP07\(2022\)073](#).
- [26] E. Rabinovici, A. Sánchez-Garrido, R. Shir, J. Sonner, A bulk manifestation of Krylov complexity, *JHEP* 08 (2023) 213. [arXiv:2305.04355](#), [doi:10.1007/JHEP08\(2023\)213](#).
- [27] V. Balasubramanian, J. M. Magan, P. Nandi, Q. Wu, Spread complexity and the saturation of wormhole size (12 2024). [arXiv:2412.02038](#).
- [28] P. Caputa, N. Kundu, M. Miyaji, T. Takayanagi, K. Watanabe, Anti-de Sitter Space from Optimization of Path Integrals in Conformal Field Theories, *Phys. Rev. Lett.* 119 (7) (2017) 071602. [arXiv:1703.00456](#), [doi:10.1103/PhysRevLett.119.071602](#).
- [29] P. Caputa, N. Kundu, M. Miyaji, T. Takayanagi, K. Watanabe, Liouville Action as Path-Integral Complexity: From Continuous Tensor Networks to AdS/CFT, *JHEP* 11 (2017) 097. [arXiv:1706.07056](#), [doi:10.1007/JHEP11\(2017\)097](#).
- [30] P. Caputa, J. M. Magan, Quantum Computation as Gravity, *Phys. Rev. Lett.* 122 (23) (2019) 231302. [arXiv:1807.04422](#), [doi:10.1103/PhysRevLett.122.231302](#).
- [31] A. R. Chandra, J. de Boer, M. Flory, M. P. Heller, S. Hörtner, A. Rolph, Spacetime as a quantum circuit, *JHEP* 21 (2021) 207. [arXiv:2101.01185](#), [doi:10.1007/JHEP04\(2021\)207](#).
- [32] N. Chagnet, S. Chapman, J. de Boer, C. Zukowski, Complexity for Conformal Field Theories in General Dimensions, *Phys. Rev. Lett.* 128 (5) (2022) 051601. [arXiv:2103.06920](#), [doi:10.1103/PhysRevLett.128.051601](#).

- [33] A. R. Chandra, J. de Boer, M. Flory, M. P. Heller, S. Hörtner, A. Rolph, Cost of holographic path integrals, *SciPost Phys.* 14 (4) (2023) 061. [arXiv:2203.08842](#), [doi:10.21468/SciPostPhys.14.4.061](#).
- [34] J. Erdmenger, A.-L. Weigel, M. Gerbershagen, M. P. Heller, From complexity geometry to holographic spacetime, *Phys. Rev. D* 108 (10) (2023) 106020. [arXiv:2212.00043](#), [doi:10.1103/PhysRevD.108.106020](#).
- [35] E. Jørstad, R. C. Myers, S.-M. Ruan, Complexity=anything: singularity probes, *JHEP* 07 (2023) 223. [arXiv:2304.05453](#), [doi:10.1007/JHEP07\(2023\)223](#).
- [36] A. Belin, A. Lewkowycz, G. Sárosi, Complexity and the bulk volume, a new York time story, *JHEP* 03 (2019) 044. [arXiv:1811.03097](#), [doi:10.1007/JHEP03\(2019\)044](#).
- [37] A. R. Brown, L. Susskind, Complexity geometry of a single qubit, *Phys. Rev. D* 100 (4) (2019) 046020. [arXiv:1903.12621](#), [doi:10.1103/PhysRevD.100.046020](#).
- [38] L. Susskind, Y. Zhao, Switchbacks and the Bridge to Nowhere (8 2014). [arXiv:1408.2823](#).
- [39] A. R. Brown, L. Susskind, Y. Zhao, Quantum Complexity and Negative Curvature, *Phys. Rev. D* 95 (4) (2017) 045010. [arXiv:1608.02612](#), [doi:10.1103/PhysRevD.95.045010](#).
- [40] L. Susskind, Addendum to Fast Scramblers (1 2011). [arXiv:1101.6048](#).
- [41] N. Lashkari, D. Stanford, M. Hastings, T. Osborne, P. Hayden, Towards the Fast Scrambling Conjecture, *JHEP* 04 (2013) 022. [arXiv:1111.6580](#), [doi:10.1007/JHEP04\(2013\)022](#).
- [42] L. Susskind, Black Holes and Complexity Classes (2 2018). [arXiv:1802.02175](#).
- [43] S. Chapman, H. Marrochio, R. C. Myers, Holographic complexity in Vaidya spacetimes. Part II, *JHEP* 06 (2018) 114. [arXiv:1805.07262](#), [doi:10.1007/JHEP06\(2018\)114](#).
- [44] A. R. Brown, L. Susskind, Second law of quantum complexity, *Phys. Rev. D* 97 (8) (2018) 086015. [arXiv:1701.01107](#), [doi:10.1103/PhysRevD.97.086015](#).
- [45] B. Swingle, Unscrambling the physics of out-of-time-order correlators, *Nature Phys.* 14 (10) (2018) 988–990. [doi:10.1038/s41567-018-0295-5](#).
- [46] F. J. Dyson, Statistical Theory of the Energy Levels of Complex Systems. III, *J. Math. Phys.* 3 (1) (1962) 166. [doi:10.1063/1.1703775](#).
- [47] L. Leviandier, M. Lombardi, R. Jost, J. P. Pique, Fourier Transform: A Tool to Measure Statistical Level Properties in Very Complex Spectra, *Phys. Rev. Lett.* 56 (23) (1986) 2449. [doi:10.1103/PhysRevLett.56.2449](#).
- [48] E. Brézin, S. Hikami, Spectral form factor in a random matrix theory, *Phys. Rev. E* 55 (1997) 4067–4083. [doi:10.1103/PhysRevE.55.4067](#).
- [49] C. Murthy, A. Babakhani, F. Iniguez, M. Srednicki, N. Y. Halpern, Non-Abelian Eigenstate Thermalization Hypothesis, *Phys. Rev. Lett.* 130 (14) (2023) 140402. [arXiv:2206.05310](#), [doi:10.1103/PhysRevLett.130.140402](#).

- [50] E. H. Lieb, D. W. Robinson, The finite group velocity of quantum spin systems, *Commun. Math. Phys.* 28 (1972) 251–257. [doi:10.1007/BF01645779](https://doi.org/10.1007/BF01645779).
- [51] A. I. Larkin, Y. N. Ovchinnikov, Quasiclassical Method in the Theory of Superconductivity, *Soviet Journal of Experimental and Theoretical Physics* 28 (1969) 1200.
- [52] I. L. Aleiner, A. I. Larkin, Divergence of classical trajectories and weak localization, *Phys. Rev. B* 54 (1996) 14423–14444. [doi:10.1103/PhysRevB.54.14423](https://doi.org/10.1103/PhysRevB.54.14423).
- [53] H. Schomerus, P. Jacquod, Quantum-to-classical correspondence in open chaotic systems, *Journal of Physics A: Mathematical and General* 38 (49) (2005) 10663. [doi:10.1088/0305-4470/38/49/013](https://doi.org/10.1088/0305-4470/38/49/013).
- [54] P. Kos, M. Ljubotina, T. c. v. Prosen, Many-body quantum chaos: Analytic connection to random matrix theory, *Phys. Rev. X* 8 (2018) 021062. [doi:10.1103/PhysRevX.8.021062](https://doi.org/10.1103/PhysRevX.8.021062).
- [55] M. H. Winer, Spectral Statistics, Hydrodynamics, and Quantum Chaos, Ph.D. thesis, Maryland U., College Park (2024). [arXiv:2407.07692](https://arxiv.org/abs/2407.07692).
- [56] N. R. Hunter-Jones, Chaos and randomness in strongly-interacting quantum systems, Ph.D. thesis, California Institute of Technology (2018). [doi:doi:10.7907/BHZ5-HV76](https://doi.org/10.7907/BHZ5-HV76).
- [57] B. Bhattacharjee, A. Andreanov, S. Flach, Thermalization slowing down of weakly nonintegrable quantum spin dynamics (5 2024). [arXiv:2405.00786](https://arxiv.org/abs/2405.00786).
- [58] A. A. Razborov, Feasible proofs and computations: Partnership and fusion, in: *International Colloquium on Automata, Languages, and Programming*, Springer, 2004, pp. 8–14.
- [59] T. Gowers, Razborov and rudich’s natural proofs argument, [blog entry](#).
- [60] S. Arora, B. Barak, *Computational complexity: a modern approach*, Cambridge University Press, 2009.
- [61] C. E. Shannon, The synthesis of two-terminal switching circuits, *The Bell System Technical Journal* 28 (1) (1949) 59–98. [doi:10.1002/j.1538-7305.1949.tb03624.x](https://doi.org/10.1002/j.1538-7305.1949.tb03624.x).
- [62] J. Preskill, Lecture notes for physics 229: Quantum information and computation, *California institute of technology* 16 (1) (1998) 1–8.
- [63] J. Haferkamp, P. Faist, N. B. T. Kothakonda, J. Eisert, N. Yunger Halpern, Linear growth of quantum circuit complexity (2021). [arXiv:2106.05305](https://arxiv.org/abs/2106.05305).
- [64] Z. Li, Short Proofs of Linear Growth of Quantum Circuit Complexity (5 2022). [arXiv:2205.05668](https://arxiv.org/abs/2205.05668).
- [65] C. Dankert, Efficient Simulation of Random Quantum States and Operators (12 2005). [arXiv:quant-ph/0512217](https://arxiv.org/abs/quant-ph/0512217).
- [66] D. Gross, K. Audenaert, J. Eisert, Evenly distributed unitaries: On the structure of unitary designs, *Journal of Mathematical Physics* 48 (5). [doi:10.1063/1.2716992](https://doi.org/10.1063/1.2716992).

- [67] R. A. Low, Pseudo-randomness and Learning in Quantum Computation, Ph.D. thesis, Bristol U. (2009). [arXiv:1006.5227](#).
- [68] F. G. Brandão, W. Chemissany, N. Hunter-Jones, R. Kueng, J. Preskill, Models of quantum complexity growth, PRX Quantum 2 (2021) 030316. [doi:10.1103/PRXQuantum.2.030316](#).
- [69] F. G. S. L. Brandão, A. W. Harrow, M. Horodecki, Local Random Quantum Circuits are Approximate Polynomial-Designs, Commun. Math. Phys. 346 (2) (2016) 397–434. [arXiv:1208.0692](#), [doi:10.1007/s00220-016-2706-8](#).
- [70] D. A. Roberts, B. Yoshida, Chaos and complexity by design, JHEP 04 (2017) 121. [arXiv:1610.04903](#), [doi:10.1007/JHEP04\(2017\)121](#).
- [71] W. G. Brown, L. Viola, Convergence rates for arbitrary statistical moments of random quantum circuits, Phys. Rev. Lett. 104 (2010) 250501. [doi:10.1103/PhysRevLett.104.250501](#).
- [72] C.-F. Chen, J. Haah, J. Haferkamp, Y. Liu, T. Metger, X. Tan, Incompressibility and spectral gaps of random circuits (6 2024). [arXiv:2406.07478](#).
- [73] J. Haferkamp, Random quantum circuits are approximate unitary t -designs in depth $O(nt^{5+o(1)})$, Quantum 6 (2022) 795. [arXiv:2203.16571](#), [doi:10.22331/q-2022-09-08-795](#).
- [74] F. G. S. L. Brandão, A. W. Harrow, M. Horodecki, Efficient quantum pseudorandomness, Phys. Rev. Lett. 116 (2016) 170502. [doi:10.1103/PhysRevLett.116.170502](#).
- [75] E. Onorati, O. Buerschaper, M. Kliesch, W. Brown, A. H. Werner, J. Eisert, Mixing properties of stochastic quantum Hamiltonians, Commun. Math. Phys. 355 (3) (2017) 905–947. [arXiv:1606.01914](#), [doi:10.1007/s00220-017-2950-6](#).
- [76] S.-K. Jian, G. Bentsen, B. Swingle, Linear growth of circuit complexity from Brownian dynamics, JHEP 08 (2023) 190. [arXiv:2206.14205](#), [doi:10.1007/JHEP08\(2023\)190](#).
- [77] M. Oszmaniec, M. Kotowski, M. Horodecki, N. Hunter-Jones, Saturation and Recurrence of Quantum Complexity in Random Local Quantum Dynamics, Phys. Rev. X 14 (4) (2024) 041068. [arXiv:2205.09734](#), [doi:10.1103/PhysRevX.14.041068](#).
- [78] M. A. Nielsen, A geometric approach to quantum circuit lower bounds (2005). [arXiv:quant-ph/0502070](#).
- [79] M. A. Nielsen, M. R. Dowling, M. Gu, A. C. Doherty, Quantum computation as geometry, Science 311 (5764) (2006) 1133–1135. [arXiv:quant-ph/0603161](#), [doi:10.1126/science.1121541](#).
- [80] M. R. Dowling, M. A. Nielsen, The geometry of quantum computation (2006). [arXiv:quant-ph/0701004](#).
- [81] S. Lloyd, Universal quantum simulators, Science 273 (5278) (1996) 1073–1078. [doi:10.1126/science.273.5278.1073](#).

- [82] A. R. Brown, M. H. Freedman, H. W. Lin, L. Susskind, Universality in long-distance geometry and quantum complexity, *Nature* 622 (7981) (2023) 58–62. [arXiv:2111.12700](#), [doi:10.1038/s41586-023-06460-3](#).
- [83] M. Nozaki, S. Ryu, T. Takayanagi, Holographic Geometry of Entanglement Renormalization in Quantum Field Theories, *JHEP* 10 (2012) 193. [arXiv:1208.3469](#), [doi:10.1007/JHEP10\(2012\)193](#).
- [84] R. Jefferson, R. C. Myers, Circuit complexity in quantum field theory, *JHEP* 10 (2017) 107. [arXiv:1707.08570](#), [doi:10.1007/JHEP10\(2017\)107](#).
- [85] S. Chapman, M. P. Heller, H. Marrochio, F. Pastawski, Toward a Definition of Complexity for Quantum Field Theory States, *Phys. Rev. Lett.* 120 (12) (2018) 121602. [arXiv:1707.08582](#), [doi:10.1103/PhysRevLett.120.121602](#).
- [86] R. Auzzi, S. Baiguera, G. B. De Luca, A. Legramandi, G. Nardelli, N. Zenoni, Geometry of quantum complexity, *Phys. Rev. D* 103 (10) (2021) 106021. [arXiv:2011.07601](#), [doi:10.1103/PhysRevD.103.106021](#).
- [87] P. Petersen, *Riemannian geometry*, Vol. 171, Springer, 2016.
- [88] R. Khan, C. Krishnan, S. Sharma, Circuit Complexity in Fermionic Field Theory, *Phys. Rev. D* 98 (12) (2018) 126001. [arXiv:1801.07620](#), [doi:10.1103/PhysRevD.98.126001](#).
- [89] L. Hackl, R. C. Myers, Circuit complexity for free fermions, *JHEP* 07 (2018) 139. [arXiv:1803.10638](#), [doi:10.1007/JHEP07\(2018\)139](#).
- [90] S. Chapman, J. Eisert, L. Hackl, M. P. Heller, R. Jefferson, H. Marrochio, R. C. Myers, Complexity and entanglement for thermofield double states, *SciPost Phys.* 6 (3) (2019) 034. [arXiv:1810.05151](#), [doi:10.21468/SciPostPhys.6.3.034](#).
- [91] A. Bhattacharyya, A. Shekar, A. Sinha, Circuit complexity in interacting QFTs and RG flows, *JHEP* 10 (2018) 140. [arXiv:1808.03105](#), [doi:10.1007/JHEP10\(2018\)140](#).
- [92] M. Guo, J. Hernandez, R. C. Myers, S.-M. Ruan, Circuit Complexity for Coherent States, *JHEP* 10 (2018) 011. [arXiv:1807.07677](#), [doi:10.1007/JHEP10\(2018\)011](#).
- [93] A. Bernamonti, F. Galli, J. Hernandez, R. C. Myers, S.-M. Ruan, J. Simón, First Law of Holographic Complexity, *Phys. Rev. Lett.* 123 (8) (2019) 081601. [arXiv:1903.04511](#), [doi:10.1103/PhysRevLett.123.081601](#).
- [94] E. Caceres, S. Chapman, J. D. Couch, J. P. Hernandez, R. C. Myers, S.-M. Ruan, Complexity of Mixed States in QFT and Holography, *JHEP* 03 (2020) 012. [arXiv:1909.10557](#), [doi:10.1007/JHEP03\(2020\)012](#).
- [95] V. Balasubramanian, M. DeCross, A. Kar, O. Parrikar, Binding Complexity and Multiparty Entanglement, *JHEP* 02 (2019) 069. [arXiv:1811.04085](#), [doi:10.1007/JHEP02\(2019\)069](#).

- [96] V. Balasubramanian, M. Decross, A. Kar, O. Parrikar, Quantum Complexity of Time Evolution with Chaotic Hamiltonians, JHEP 01 (2020) 134. [arXiv:1905.05765](#), [doi:10.1007/JHEP01\(2020\)134](#).
- [97] P. Basteiro, J. Erdmenger, P. Fries, F. Goth, I. Matthaikakakis, R. Meyer, Quantum complexity as hydrodynamics, Phys. Rev. D 106 (6) (2022) 065016. [arXiv:2109.01152](#), [doi:10.1103/PhysRevD.106.065016](#).
- [98] V. Balasubramanian, M. DeCross, A. Kar, Y. C. Li, O. Parrikar, Complexity growth in integrable and chaotic models, JHEP 07 (2021) 011. [arXiv:2101.02209](#), [doi:10.1007/JHEP07\(2021\)011](#).
- [99] S. Baiguera, S. Chapman, G. Policastro, T. Schwartzman, The Complexity of Being Entangled, Quantum 8 (2024) 1472. [arXiv:2311.04277](#), [doi:10.22331/q-2024-09-12-1472](#).
- [100] B. O'Neill, The fundamental equations of a submersion., Michigan Mathematical Journal 13 (4) (1966) 459–469.
- [101] J. Milnor, Curvatures of left invariant metrics on lie groups, Advances in Mathematics 21 (3) (1976) 293–329. [doi:https://doi.org/10.1016/S0001-8708\(76\)80002-3](#).
- [102] R. J. Caginalp, S. Leutheusser, Complexity in One- and Two-Qubit Systems (10 2020). [arXiv:2010.15099](#).
- [103] S. Bravyi, Upper bounds on entangling rates of bipartite hamiltonians, Phys. Rev. A 76 (2007) 052319. [doi:10.1103/PhysRevA.76.052319](#).
- [104] K. Van Acoleyen, M. Mariën, F. Verstraete, Entanglement rates and area laws, Phys. Rev. Lett. 111 (2013) 170501. [doi:10.1103/PhysRevLett.111.170501](#).
- [105] M. Mariën, K. M. R. Audenaert, K. Van Acoleyen, F. Verstraete, Entanglement rates and the stability of the area law for the entanglement entropy, Communications in Mathematical Physics 346 (1) (2016) 35–73. [arXiv:1411.0680](#).
- [106] J. Eisert, Entangling power and quantum circuit complexity, Phys. Rev. Lett. 127 (2021) 020501. [doi:10.1103/PhysRevLett.127.020501](#).
- [107] J. Cotler, M. R. Mohammadi Mozaffar, A. Mollabashi, A. Naseh, Renormalization Group Circuits for Weakly Interacting Continuum Field Theories, Fortsch. Phys. 67 (10) (2019) 1900038. [arXiv:1806.02831](#), [doi:10.1002/prop.201900038](#).
- [108] H. A. Camargo, L. Hackl, M. P. Heller, A. Jahn, T. Takayanagi, B. Windt, Entanglement and complexity of purification in (1+1)-dimensional free conformal field theories, Phys. Rev. Res. 3 (1) (2021) 013248. [arXiv:2009.11881](#), [doi:10.1103/PhysRevResearch.3.013248](#).
- [109] K. Hashimoto, N. Iizuka, S. Sugishita, Time evolution of complexity in Abelian gauge theories, Phys. Rev. D 96 (12) (2017) 126001. [arXiv:1707.03840](#), [doi:10.1103/PhysRevD.96.126001](#).

- [110] S. Chapman, H. Z. Chen, Charged Complexity and the Thermofield Double State, JHEP 02 (2021) 187. [arXiv:1910.07508](#), [doi:10.1007/JHEP02\(2021\)187](#).
- [111] D. Ge, G. Policastro, Circuit Complexity and 2D Bosonisation, JHEP 10 (2019) 276. [arXiv:1904.03003](#), [doi:10.1007/JHEP10\(2019\)276](#).
- [112] H. A. Camargo, P. Caputa, D. Das, M. P. Heller, R. Jefferson, Complexity as a novel probe of quantum quenches: universal scalings and purifications, Phys. Rev. Lett. 122 (8) (2019) 081601. [arXiv:1807.07075](#), [doi:10.1103/PhysRevLett.122.081601](#).
- [113] J. Erdmenger, M. Flory, M. Gerbershagen, M. P. Heller, A.-L. Weigel, Exact Gravity Duals for Simple Quantum Circuits, SciPost Phys. 13 (3) (2022) 061. [arXiv:2112.12158](#), [doi:10.21468/SciPostPhys.13.3.061](#).
- [114] J. Erdmenger, M. Gerbershagen, A.-L. Weigel, Complexity measures from geometric actions on Virasoro and Kac-Moody orbits, JHEP 11 (2020) 003. [arXiv:2004.03619](#), [doi:10.1007/JHEP11\(2020\)003](#).
- [115] M. Flory, M. P. Heller, Geometry of Complexity in Conformal Field Theory, Phys. Rev. Res. 2 (4) (2020) 043438. [arXiv:2005.02415](#), [doi:10.1103/PhysRevResearch.2.043438](#).
- [116] J. de Boer, V. Godet, J. Kastikainen, E. Keski-Vakkuri, Quantum information geometry of driven CFTs, JHEP 09 (2023) 087. [arXiv:2306.00099](#), [doi:10.1007/JHEP09\(2023\)087](#).
- [117] M. Flory, M. P. Heller, Conformal field theory complexity from Euler-Arnold equations, JHEP 12 (2020) 091. [arXiv:2007.11555](#), [doi:10.1007/JHEP12\(2020\)091](#).
- [118] M. Flory, N. Miekley, Complexity change under conformal transformations in AdS₃/CFT₂, JHEP 05 (2019) 003. [arXiv:1806.08376](#), [doi:10.1007/JHEP05\(2019\)003](#).
- [119] J. Erdmenger, J. Kastikainen, T. Schuhmann, Towards complexity of primary-deformed Virasoro circuits (9 2024). [arXiv:2409.08319](#).
- [120] J. M. Magán, Black holes, complexity and quantum chaos, JHEP 09 (2018) 043. [arXiv:1805.05839](#), [doi:10.1007/JHEP09\(2018\)043](#).
- [121] S. Baiguera, N. Chagnet, S. Chapman, O. Shoval, CFT complexity and penalty factors, to appear.
- [122] C. Lanczos, An iteration method for the solution of the eigenvalue problem of linear differential and integral operators, J. Res. Natl. Bur. Stand. B 45 (1950) 255–282. [doi:10.6028/jres.045.026](#).
- [123] T. Guhr, A. Muller-Groeling, H. A. Weidenmuller, Random matrix theories in quantum physics: Common concepts, Phys. Rept. 299 (1998) 189–425. [arXiv:cond-mat/9707301](#), [doi:10.1016/S0370-1573\(97\)00088-4](#).
- [124] J. S. Cotler, G. Gur-Ari, M. Hanada, J. Polchinski, P. Saad, S. H. Shenker, D. Stanford, A. Streicher, M. Tezuka, Black Holes and Random Matrices, JHEP 05 (2017) 118. [arXiv:1611.04650](#), [doi:10.1007/JHEP05\(2017\)118](#).

- [125] A. del Campo, J. Molina-Vilaplana, J. Sonner, Scrambling the spectral form factor: unitarity constraints and exact results, *Phys. Rev. D* 95 (12) (2017) 126008. [arXiv:1702.04350](#), [doi:10.1103/PhysRevD.95.126008](#).
- [126] V. Balasubramanian, J. M. Magan, Q. Wu, Tridiagonalizing random matrices, *Phys. Rev. D* 107 (12) (2023) 126001. [arXiv:2208.08452](#), [doi:10.1103/PhysRevD.107.126001](#).
- [127] P. Calabrese, J. Cardy, Entanglement entropy and conformal field theory, *J. Phys. A* 42 (2009) 504005. [arXiv:0905.4013](#), [doi:10.1088/1751-8113/42/50/504005](#).
- [128] J. Abajo-Arrastia, J. Aparicio, E. Lopez, Holographic Evolution of Entanglement Entropy, *JHEP* 11 (2010) 149. [arXiv:1006.4090](#), [doi:10.1007/JHEP11\(2010\)149](#).
- [129] V. Balasubramanian, A. Bernamonti, J. de Boer, N. Copland, B. Craps, E. Keski-Vakkuri, B. Muller, A. Schafer, M. Shigemori, W. Staessens, Holographic Thermalization, *Phys. Rev. D* 84 (2011) 026010. [arXiv:1103.2683](#), [doi:10.1103/PhysRevD.84.026010](#).
- [130] V. Balasubramanian, A. Bernamonti, J. de Boer, N. Copland, B. Craps, E. Keski-Vakkuri, B. Muller, A. Schafer, M. Shigemori, W. Staessens, Thermalization of Strongly Coupled Field Theories, *Phys. Rev. Lett.* 106 (2011) 191601. [arXiv:1012.4753](#), [doi:10.1103/PhysRevLett.106.191601](#).
- [131] H. Liu, S. J. Suh, Entanglement growth during thermalization in holographic systems, *Phys. Rev. D* 89 (6) (2014) 066012. [arXiv:1311.1200](#), [doi:10.1103/PhysRevD.89.066012](#).
- [132] P. Caputa, S. Datta, Operator growth in 2d CFT, *JHEP* 12 (2021) 188. [arXiv:2110.10519](#), [doi:10.1007/JHEP12\(2021\)188](#).
- [133] J. L. F. Barbón, E. Rabinovici, R. Shir, R. Sinha, On The Evolution Of Operator Complexity Beyond Scrambling, *JHEP* 10 (2019) 264. [arXiv:1907.05393](#), [doi:10.1007/JHEP10\(2019\)264](#).
- [134] P. Caputa, J. M. Magan, D. Patramanis, Geometry of Krylov complexity, *Phys. Rev. Res.* 4 (1) (2022) 013041. [arXiv:2109.03824](#), [doi:10.1103/PhysRevResearch.4.013041](#).
- [135] D. Patramanis, Probing the entanglement of operator growth, *PTEP* 2022 (6) (2022) 063A01. [arXiv:2111.03424](#), [doi:10.1093/ptep/ptac081](#).
- [136] P. Caputa, G. Di Giulio, Local Quenches from a Krylov Perspective (2 2025). [arXiv:2502.19485](#).
- [137] R. Basu, A. Ganguly, S. Nath, O. Parrikar, Complexity growth and the Krylov-Wigner function, *JHEP* 05 (2024) 264. [arXiv:2402.13694](#), [doi:10.1007/JHEP05\(2024\)264](#).
- [138] K. Hashimoto, K. Murata, N. Tanahashi, R. Watanabe, Krylov complexity and chaos in quantum mechanics, *JHEP* 11 (2023) 040. [arXiv:2305.16669](#), [doi:10.1007/JHEP11\(2023\)040](#).

- [139] H. A. Camargo, V. Jahnke, H.-S. Jeong, K.-Y. Kim, M. Nishida, Spectral and Krylov complexity in billiard systems, *Phys. Rev. D* 109 (4) (2024) 046017. [arXiv:2306.11632](https://arxiv.org/abs/2306.11632), [doi:10.1103/PhysRevD.109.046017](https://doi.org/10.1103/PhysRevD.109.046017).
- [140] V. Balasubramanian, R. N. Das, J. Erdmenger, Z.-Y. Xian, Chaos and integrability in triangular billiards (7 2024). [arXiv:2407.11114](https://arxiv.org/abs/2407.11114).
- [141] M. Alishahiha, S. Banerjee, A universal approach to Krylov state and operator complexities, *SciPost Phys.* 15 (3) (2023) 080. [arXiv:2212.10583](https://arxiv.org/abs/2212.10583), [doi:10.21468/SciPostPhys.15.3.080](https://doi.org/10.21468/SciPostPhys.15.3.080).
- [142] P. Caputa, H.-S. Jeong, S. Liu, J. F. Pedraza, L.-C. Qu, Krylov complexity of density matrix operators, *JHEP* 05 (2024) 337. [arXiv:2402.09522](https://arxiv.org/abs/2402.09522), [doi:10.1007/JHEP05\(2024\)337](https://doi.org/10.1007/JHEP05(2024)337).
- [143] D. A. Roberts, D. Stanford, L. Susskind, Localized shocks, *JHEP* 03 (2015) 051. [arXiv:1409.8180](https://arxiv.org/abs/1409.8180), [doi:10.1007/JHEP03\(2015\)051](https://doi.org/10.1007/JHEP03(2015)051).
- [144] J. M. Magan, Decoherence and microscopic diffusion at the Sachdev-Ye-Kitaev model, *Phys. Rev. D* 98 (2) (2018) 026015. [arXiv:1612.06765](https://arxiv.org/abs/1612.06765), [doi:10.1103/PhysRevD.98.026015](https://doi.org/10.1103/PhysRevD.98.026015).
- [145] D. A. Roberts, D. Stanford, A. Streicher, Operator growth in the SYK model, *JHEP* 06 (2018) 122. [arXiv:1802.02633](https://arxiv.org/abs/1802.02633), [doi:10.1007/JHEP06\(2018\)122](https://doi.org/10.1007/JHEP06(2018)122).
- [146] X.-L. Qi, A. Streicher, Quantum Epidemiology: Operator Growth, Thermal Effects, and SYK, *JHEP* 08 (2019) 012. [arXiv:1810.11958](https://arxiv.org/abs/1810.11958), [doi:10.1007/JHEP08\(2019\)012](https://doi.org/10.1007/JHEP08(2019)012).
- [147] J. M. Magán, J. Simón, On operator growth and emergent Poincaré symmetries, *JHEP* 05 (2020) 071. [arXiv:2002.03865](https://arxiv.org/abs/2002.03865), [doi:10.1007/JHEP05\(2020\)071](https://doi.org/10.1007/JHEP05(2020)071).
- [148] A. Jamiołkowski, Linear transformations which preserve trace and positive semidefiniteness of operators, *Reports on Mathematical Physics* 3 (4) (1972) 275–278. [doi:https://doi.org/10.1016/0034-4877\(72\)90011-0](https://doi.org/10.1016/0034-4877(72)90011-0).
- [149] M.-D. Choi, Completely positive linear maps on complex matrices, *Linear Algebra and its Applications* 10 (3) (1975) 285–290. [doi:https://doi.org/10.1016/0024-3795\(75\)90075-0](https://doi.org/10.1016/0024-3795(75)90075-0).
- [150] E. Rabinovici, A. Sánchez-Garrido, R. Shir, J. Sonner, Operator complexity: a journey to the edge of Krylov space, *JHEP* 06 (2021) 062. [arXiv:2009.01862](https://arxiv.org/abs/2009.01862), [doi:10.1007/JHEP06\(2021\)062](https://doi.org/10.1007/JHEP06(2021)062).
- [151] A. Dymarsky, A. Gorsky, Quantum chaos as delocalization in Krylov space, *Phys. Rev. B* 102 (8) (2020) 085137. [arXiv:1912.12227](https://arxiv.org/abs/1912.12227), [doi:10.1103/PhysRevB.102.085137](https://doi.org/10.1103/PhysRevB.102.085137).
- [152] W. Mück, Y. Yang, Krylov complexity and orthogonal polynomials, *Nucl. Phys. B* 984 (2022) 115948. [arXiv:2205.12815](https://arxiv.org/abs/2205.12815), [doi:10.1016/j.nuclphysb.2022.115948](https://doi.org/10.1016/j.nuclphysb.2022.115948).
- [153] N. Hörnedal, N. Carabba, A. S. Matsoukas-Roubeas, A. del Campo, Ultimate Speed Limits to the Growth of Operator Complexity, *Commun. Phys.* 5 (2022) 207. [arXiv:2202.05006](https://arxiv.org/abs/2202.05006), [doi:10.1038/s42005-022-00985-1](https://doi.org/10.1038/s42005-022-00985-1).

- [154] E. Rabinovici, A. Sánchez-Garrido, R. Shir, J. Sonner, Krylov localization and suppression of complexity, JHEP 03 (2022) 211. [arXiv:2112.12128](#), [doi:10.1007/JHEP03\(2022\)211](#).
- [155] E. Rabinovici, A. Sánchez-Garrido, R. Shir, J. Sonner, Krylov complexity from integrability to chaos, JHEP 07 (2022) 151. [arXiv:2207.07701](#), [doi:10.1007/JHEP07\(2022\)151](#).
- [156] V. Balasubramanian, J. M. Magan, Q. Wu, Quantum chaos, integrability, and late times in the Krylov basis, Phys. Rev. E 111 (1) (2025) 014218. [arXiv:2312.03848](#), [doi:10.1103/PhysRevE.111.014218](#).
- [157] A. Avdoshkin, A. Dymarsky, Euclidean operator growth and quantum chaos, Phys. Rev. Res. 2 (4) (2020) 043234. [arXiv:1911.09672](#), [doi:10.1103/PhysRevResearch.2.043234](#).
- [158] Y. Gu, A. Kitaev, P. Zhang, A two-way approach to out-of-time-order correlators, JHEP 03 (2022) 133. [arXiv:2111.12007](#), [doi:10.1007/JHEP03\(2022\)133](#).
- [159] S. Sachdev, J. Ye, Gapless spin fluid ground state in a random, quantum Heisenberg magnet, Phys. Rev. Lett. 70 (1993) 3339. [arXiv:cond-mat/9212030](#), [doi:10.1103/PhysRevLett.70.3339](#).
- [160] A. Kitaev, A simple model of quantum holography, talk at KITP, <http://online.kitp.ucsb.edu/online/entangled15/kitaev/>, University of California, Santa Barbara, CA, U.S.A., 7 April 2015.
- [161] J. Maldacena, D. Stanford, Remarks on the Sachdev-Ye-Kitaev model, Phys. Rev. D 94 (10) (2016) 106002. [arXiv:1604.07818](#), [doi:10.1103/PhysRevD.94.106002](#).
- [162] G. Sárosi, AdS₂ holography and the SYK model, PoS Modave2017 (2018) 001. [arXiv:1711.08482](#), [doi:10.22323/1.323.0001](#).
- [163] V. Rosenhaus, An introduction to the SYK model, J. Phys. A 52 (2019) 323001. [arXiv:1807.03334](#), [doi:10.1088/1751-8121/ab2ce1](#).
- [164] D. Chowdhury, A. Georges, O. Parcollet, S. Sachdev, Sachdev-Ye-Kitaev models and beyond: Window into non-Fermi liquids, Rev. Mod. Phys. 94 (3) (2022) 035004. [arXiv:2109.05037](#), [doi:10.1103/RevModPhys.94.035004](#).
- [165] S. Chapman, S. Demulder, D. A. Galante, S. U. Sheorey, O. Shoval, Krylov complexity and chaos in deformed Sachdev-Ye-Kitaev models, Phys. Rev. B 111 (3) (2025) 035141. [arXiv:2407.09604](#), [doi:10.1103/PhysRevB.111.035141](#).
- [166] A. M. García-García, B. Loureiro, A. Romero-Bermúdez, M. Tezuka, Chaotic-Integrable Transition in the Sachdev-Ye-Kitaev Model, Phys. Rev. Lett. 120 (24) (2018) 241603. [arXiv:1707.02197](#), [doi:10.1103/PhysRevLett.120.241603](#).
- [167] J. Kim, X. Cao, Comment on "Chaotic-Integrable Transition in the Sachdev-Ye-Kitaev Model", Phys. Rev. Lett. 126 (10) (2021) 109101. [arXiv:2004.05313](#), [doi:10.1103/PhysRevLett.126.109101](#).

- [168] A. M. García-García, B. Loureiro, A. Romero-Bermúdez, M. Tezuka, Reply to Comment on "Chaotic-Integrable Transition in the Sachdev-Ye-Kitaev Model", *Phys. Rev. Lett.* 126 (10) (2021) 109102. [arXiv:2007.06121](https://arxiv.org/abs/2007.06121), [doi:10.1103/PhysRevLett.126.109102](https://doi.org/10.1103/PhysRevLett.126.109102).
- [169] A. V. Lunkin, A. Y. Kitaev, M. V. Feigel'man, Perturbed Sachdev-Ye-Kitaev Model: A Polaron in the Hyperbolic Plane, *Phys. Rev. Lett.* 125 (19) (2020) 196602. [arXiv:2006.14535](https://arxiv.org/abs/2006.14535), [doi:10.1103/PhysRevLett.125.196602](https://doi.org/10.1103/PhysRevLett.125.196602).
- [170] D. K. Nandy, T. Cadez, B. Dietz, A. Andreanov, D. Rosa, Delayed thermalization in the mass-deformed Sachdev-Ye-Kitaev model, *Phys. Rev. B* 106 (24) (2022) 245147. [arXiv:2206.08599](https://arxiv.org/abs/2206.08599), [doi:10.1103/PhysRevB.106.245147](https://doi.org/10.1103/PhysRevB.106.245147).
- [171] H. G. Menzler, R. Jha, Krylov delocalization/localization across ergodicity breaking, *Phys. Rev. B* 110 (12) (2024) 125137. [arXiv:2403.14384](https://arxiv.org/abs/2403.14384), [doi:10.1103/PhysRevB.110.125137](https://doi.org/10.1103/PhysRevB.110.125137).
- [172] J. Jiang, Z. Yang, Thermodynamics and Many Body Chaos for generalized large q SYK models, *JHEP* 08 (2019) 019. [arXiv:1905.00811](https://arxiv.org/abs/1905.00811), [doi:10.1007/JHEP08\(2019\)019](https://doi.org/10.1007/JHEP08(2019)019).
- [173] D. Anninos, D. A. Galante, Constructing AdS_2 flow geometries, *JHEP* 02 (2021) 045. [arXiv:2011.01944](https://arxiv.org/abs/2011.01944), [doi:10.1007/JHEP02\(2021\)045](https://doi.org/10.1007/JHEP02(2021)045).
- [174] D. Anninos, D. A. Galante, S. U. Sheorey, Renormalisation group flows of deformed SYK models, *JHEP* 11 (2023) 197. [arXiv:2212.04944](https://arxiv.org/abs/2212.04944), [doi:10.1007/JHEP11\(2023\)197](https://doi.org/10.1007/JHEP11(2023)197).
- [175] J. C. Louw, L. M. van Manen, R. Jha, Thermodynamics and dynamics of coupled complex SYK models, *J. Phys. Condens. Matter* 36 (49) (2024) 495601. [arXiv:2312.14644](https://arxiv.org/abs/2312.14644), [doi:10.1088/1361-648X/ad743a](https://doi.org/10.1088/1361-648X/ad743a).
- [176] I. Dumitriu, A. Edelman, Matrix models for beta ensembles, *Journal of Mathematical Physics* 43 (11) (2002) 5830–5847. [doi:10.1063/1.1507823](https://doi.org/10.1063/1.1507823).
- [177] O. Bohigas, M. J. Giannoni, C. Schmit, Characterization of chaotic quantum spectra and universality of level fluctuation laws, *Phys. Rev. Lett.* 52 (1984) 1–4. [doi:10.1103/PhysRevLett.52.1](https://doi.org/10.1103/PhysRevLett.52.1).
- [178] M. C. Bañuls, J. I. Cirac, M. B. Hastings, Strong and weak thermalization of infinite nonintegrable quantum systems, *Physical Review Letters* 106 (5). [doi:10.1103/physrevlett.106.050405](https://doi.org/10.1103/physrevlett.106.050405).
- [179] J. Erdmenger, S.-K. Jian, Z.-Y. Xian, Universal chaotic dynamics from Krylov space, *JHEP* 08 (2023) 176. [arXiv:2303.12151](https://arxiv.org/abs/2303.12151), [doi:10.1007/JHEP08\(2023\)176](https://doi.org/10.1007/JHEP08(2023)176).
- [180] M. Baggioli, K.-B. Huh, H.-S. Jeong, K.-Y. Kim, J. F. Pedraza, Krylov complexity as an order parameter for quantum chaotic-integrable transitions (7 2024). [arXiv:2407.17054](https://arxiv.org/abs/2407.17054).
- [181] M. Alishahiha, S. Banerjee, M. J. Vasli, Krylov Complexity as a Probe for Chaos (8 2024). [arXiv:2408.10194](https://arxiv.org/abs/2408.10194).
- [182] B. Bhattacharjee, X. Cao, P. Nandy, T. Pathak, Krylov complexity in saddle-dominated scrambling, *JHEP* 05 (2022) 174. [arXiv:2203.03534](https://arxiv.org/abs/2203.03534), [doi:10.1007/JHEP05\(2022\)174](https://doi.org/10.1007/JHEP05(2022)174).

- [183] K.-B. Huh, H.-S. Jeong, J. F. Pedraza, Spread complexity in saddle-dominated scrambling, JHEP 05 (2024) 137. [arXiv:2312.12593](#), [doi:10.1007/JHEP05\(2024\)137](#).
- [184] T. Xu, T. Scaffidi, X. Cao, Does scrambling equal chaos?, Phys. Rev. Lett. 124 (14) (2020) 140602. [arXiv:1912.11063](#), [doi:10.1103/PhysRevLett.124.140602](#).
- [185] A. Dymarsky, M. Smolkin, Krylov complexity in conformal field theory (2021). [arXiv:2104.09514](#).
- [186] A. Avdoshkin, A. Dymarsky, M. Smolkin, Krylov complexity in quantum field theory, and beyond, JHEP 06 (2024) 066. [arXiv:2212.14429](#), [doi:10.1007/JHEP06\(2024\)066](#).
- [187] H. A. Camargo, V. Jahnke, K.-Y. Kim, M. Nishida, Krylov complexity in free and interacting scalar field theories with bounded power spectrum, JHEP 05 (2023) 226. [arXiv:2212.14702](#), [doi:10.1007/JHEP05\(2023\)226](#).
- [188] S. Ouseph, K. Furuya, N. Lashkari, K. L. Leung, M. Moosa, Local Poincaré algebra from quantum chaos, JHEP 01 (2024) 112. [arXiv:2310.13736](#), [doi:10.1007/JHEP01\(2024\)112](#).
- [189] E. Gesteau, Emergent spacetime and the ergodic hierarchy, Phys. Rev. D 110 (10) (2024) 106005. [arXiv:2310.13733](#), [doi:10.1103/PhysRevD.110.106005](#).
- [190] A. Kar, L. Lamprou, M. Rozali, J. Sully, Random matrix theory for complexity growth and black hole interiors, JHEP 01 (2022) 016. [arXiv:2106.02046](#), [doi:10.1007/JHEP01\(2022\)016](#).
- [191] C. Lv, R. Zhang, Q. Zhou, Building Krylov complexity from circuit complexity, Phys. Rev. Res. 6 (4) (2024) L042001. [arXiv:2303.07343](#), [doi:10.1103/PhysRevResearch.6.L042001](#).
- [192] S. E. Aguilar-Gutierrez, A. Rolph, Krylov complexity is not a measure of distance between states or operators, Phys. Rev. D 109 (8) (2024) L081701. [arXiv:2311.04093](#), [doi:10.1103/PhysRevD.109.L081701](#).
- [193] B. Craps, O. Evnin, G. Pascuzzi, A Relation between Krylov and Nielsen Complexity, Phys. Rev. Lett. 132 (16) (2024) 160402. [arXiv:2311.18401](#), [doi:10.1103/PhysRevLett.132.160402](#).
- [194] K. Takahashi, A. del Campo, Krylov Subspace Methods for Quantum Dynamics with Time-Dependent Generators, Phys. Rev. Lett. 134 (3) (2025) 030401. [arXiv:2408.08383](#), [doi:10.1103/PhysRevLett.134.030401](#).
- [195] P. Caputa, S. Liu, Quantum complexity and topological phases of matter, Phys. Rev. B 106 (19) (2022) 195125. [arXiv:2205.05688](#), [doi:10.1103/PhysRevB.106.195125](#).
- [196] C. Agon, V. Balasubramanian, S. Kasko, A. Lawrence, Coarse Grained Quantum Dynamics, Phys. Rev. D 98 (2) (2018) 025019. [arXiv:1412.3148](#), [doi:10.1103/PhysRevD.98.025019](#).
- [197] M. Block, Y. Bao, S. Choi, E. Altman, N. Y. Yao, Measurement-induced transition in long-range interacting quantum circuits, Physical Review Letters 128 (1) (2022) 010604.

- [198] M. Guica, T. Hartman, W. Song, A. Strominger, The Kerr/CFT Correspondence, *Phys. Rev. D* 80 (2009) 124008. [arXiv:0809.4266](#), [doi:10.1103/PhysRevD.80.124008](#).
- [199] V. Balasubramanian, A. Naqvi, J. Simon, A Multiboundary AdS orbifold and DLCQ holography: A Universal holographic description of extremal black hole horizons, *JHEP* 08 (2004) 023. [arXiv:hep-th/0311237](#), [doi:10.1088/1126-6708/2004/08/023](#).
- [200] V. Balasubramanian, J. de Boer, M. M. Sheikh-Jabbari, J. Simon, What is a chiral 2d CFT? And what does it have to do with extremal black holes?, *JHEP* 02 (2010) 017. [arXiv:0906.3272](#), [doi:10.1007/JHEP02\(2010\)017](#).
- [201] T. Banks, W. Fischler, S. H. Shenker, L. Susskind, M theory as a matrix model: A conjecture, *Phys. Rev. D* 55 (1997) 5112–5128. [arXiv:hep-th/9610043](#), [doi:10.1201/9781482268737-37](#).
- [202] V. Balasubramanian, R. Gopakumar, F. Larsen, Gauge theory, geometry and the large N limit, *Nucl. Phys. B* 526 (1998) 415–431. [arXiv:hep-th/9712077](#), [doi:10.1016/S0550-3213\(98\)00377-0](#).
- [203] J. Polchinski, M theory and the light cone, *Prog. Theor. Phys. Suppl.* 134 (1999) 158–170. [arXiv:hep-th/9903165](#), [doi:10.1143/PTPS.134.158](#).
- [204] T. Hartman, J. Maldacena, Time Evolution of Entanglement Entropy from Black Hole Interiors, *JHEP* 05 (2013) 014. [arXiv:1303.1080](#), [doi:10.1007/JHEP05\(2013\)014](#).
- [205] J. Maldacena, L. Susskind, Cool horizons for entangled black holes, *Fortsch. Phys.* 61 (2013) 781–811. [arXiv:1306.0533](#), [doi:10.1002/prop.201300020](#).
- [206] L. Susskind, Computational Complexity and Black Hole Horizons, *Fortsch. Phys.* 64 (2016) 24–43, [Addendum: *Fortsch.Phys.* 64, 44–48 (2016)]. [arXiv:1403.5695](#), [doi:10.1002/prop.201500092](#).
- [207] L. Lehner, R. C. Myers, E. Poisson, R. D. Sorkin, Gravitational action with null boundaries, *Phys. Rev. D* 94 (8) (2016) 084046. [arXiv:1609.00207](#), [doi:10.1103/PhysRevD.94.084046](#).
- [208] D. Carmi, R. C. Myers, P. Rath, Comments on Holographic Complexity, *JHEP* 03 (2017) 118. [arXiv:1612.00433](#), [doi:10.1007/JHEP03\(2017\)118](#).
- [209] S. Chapman, H. Marrochio, R. C. Myers, Holographic complexity in Vaidya spacetimes. Part I, *JHEP* 06 (2018) 046. [arXiv:1804.07410](#), [doi:10.1007/JHEP06\(2018\)046](#).
- [210] S. H. Shenker, D. Stanford, Black holes and the butterfly effect, *JHEP* 03 (2014) 067. [arXiv:1306.0622](#), [doi:10.1007/JHEP03\(2014\)067](#).
- [211] S. H. Shenker, D. Stanford, Multiple Shocks, *JHEP* 12 (2014) 046. [arXiv:1312.3296](#), [doi:10.1007/JHEP12\(2014\)046](#).
- [212] S. Lloyd, Ultimate physical limits to computation, *Nature* 406 (6799) (2000) 1047–1054. [doi:10.1038/35023282](#).

- [213] D. Carmi, S. Chapman, H. Marrochio, R. C. Myers, S. Sugishita, On the Time Dependence of Holographic Complexity, JHEP 11 (2017) 188. [arXiv:1709.10184](#), [doi:10.1007/JHEP11\(2017\)188](#).
- [214] B. Swingle, Y. Wang, Holographic Complexity of Einstein-Maxwell-Dilaton Gravity, JHEP 09 (2018) 106. [arXiv:1712.09826](#), [doi:10.1007/JHEP09\(2018\)106](#).
- [215] R.-Q. Yang, C. Niu, C.-Y. Zhang, K.-Y. Kim, Comparison of holographic and field theoretic complexities for time dependent thermofield double states, JHEP 02 (2018) 082. [arXiv:1710.00600](#), [doi:10.1007/JHEP02\(2018\)082](#).
- [216] J. Couch, S. Eccles, W. Fischler, M.-L. Xiao, Holographic complexity and noncommutative gauge theory, JHEP 03 (2018) 108. [arXiv:1710.07833](#), [doi:10.1007/JHEP03\(2018\)108](#).
- [217] R. Auzzi, S. Baiguera, G. Nardelli, Volume and complexity for warped AdS black holes, JHEP 06 (2018) 063. [arXiv:1804.07521](#), [doi:10.1007/JHEP06\(2018\)063](#).
- [218] R. Auzzi, S. Baiguera, M. Grassi, G. Nardelli, N. Zenoni, Complexity and action for warped AdS black holes, JHEP 09 (2018) 013. [arXiv:1806.06216](#), [doi:10.1007/JHEP09\(2018\)013](#).
- [219] Y.-S. An, R.-H. Peng, Effect of the dilaton on holographic complexity growth, Phys. Rev. D 97 (6) (2018) 066022. [arXiv:1801.03638](#), [doi:10.1103/PhysRevD.97.066022](#).
- [220] M. Alishahiha, A. Faraji Astaneh, M. R. Mohammadi Mozaffar, A. Mollabashi, Complexity Growth with Lifshitz Scaling and Hyperscaling Violation, JHEP 07 (2018) 042. [arXiv:1802.06740](#), [doi:10.1007/JHEP07\(2018\)042](#).
- [221] A. Bernamonti, F. Bigazzi, D. Billo, L. Faggi, F. Galli, Holographic and QFT complexity with angular momentum, JHEP 11 (2021) 037. [arXiv:2108.09281](#), [doi:10.1007/JHEP11\(2021\)037](#).
- [222] Y. Wang, J. Ren, Holographic complexity of hyperbolic black holes, Phys. Rev. D 108 (4) (2023) 046006. [arXiv:2304.10454](#), [doi:10.1103/PhysRevD.108.046006](#).
- [223] S. E. Aguilar-Gutierrez, B. Craps, J. Hernandez, M. Khramtsov, M. Knysh, A. Shukla, Holographic complexity: braneworld gravity versus the Lloyd bound, JHEP 03 (2024) 173. [arXiv:2312.12349](#), [doi:10.1007/JHEP03\(2024\)173](#).
- [224] W. Cottrell, M. Montero, Complexity is simple!, JHEP 02 (2018) 039. [arXiv:1710.01175](#), [doi:10.1007/JHEP02\(2018\)039](#).
- [225] M. Miyaji, S.-M. Ruan, S. Shibuya, K. Yano, Non-perturbative Overlaps in JT Gravity: From Spectral Form Factor to Generating Functions of Complexity (2 2025). [arXiv:2502.12266](#).
- [226] T. Nishioka, S. Ryu, T. Takayanagi, Holographic entanglement entropy: an overview, Journal of Physics A Mathematical General 42 (50) (2009) 504008. [arXiv:0905.0932](#), [doi:10.1088/1751-8113/42/50/504008](#).

- [227] H. Casini, M. Huerta, Entanglement entropy in free quantum field theory, *Journal of Physics A Mathematical General* 42 (50) (2009) 504007. [arXiv:0905.2562](#), [doi:10.1088/1751-8113/42/50/504007](#).
- [228] D. Carmi, R. C. Myers, P. Rath, Comments on holographic complexity, *Journal of High Energy Physics* 2017 (3) (2017) 118. [arXiv:1612.00433](#), [doi:10.1007/JHEP03\(2017\)118](#).
- [229] S. Chapman, H. Marrochio, R. C. Myers, Complexity of Formation in Holography, *JHEP* 01 (2017) 062. [arXiv:1610.08063](#), [doi:10.1007/JHEP01\(2017\)062](#).
- [230] M. Alishahiha, Holographic Complexity, *Phys. Rev. D* 92 (12) (2015) 126009. [arXiv:1509.06614](#), [doi:10.1103/PhysRevD.92.126009](#).
- [231] D. Harlow, TASI Lectures on the Emergence of Bulk Physics in AdS/CFT, *PoS TASI2017* (2018) 002. [arXiv:1802.01040](#), [doi:10.22323/1.305.0002](#).
- [232] M. Headrick, V. E. Hubeny, A. Lawrence, M. Rangamani, Causality & holographic entanglement entropy, *JHEP* 12 (2014) 162. [arXiv:1408.6300](#), [doi:10.1007/JHEP12\(2014\)162](#).
- [233] C. A. Agón, M. Headrick, B. Swingle, Subsystem Complexity and Holography, *JHEP* 02 (2019) 145. [arXiv:1804.01561](#), [doi:10.1007/JHEP02\(2019\)145](#).
- [234] M. Alishahiha, K. Babaei Velni, M. R. Mohammadi Mozaffar, Black hole subregion action and complexity, *Phys. Rev. D* 99 (12) (2019) 126016. [arXiv:1809.06031](#), [doi:10.1103/PhysRevD.99.126016](#).
- [235] E. Cáceres, J. Couch, S. Eccles, W. Fischler, Holographic Purification Complexity, *Phys. Rev. D* 99 (8) (2019) 086016. [arXiv:1811.10650](#), [doi:10.1103/PhysRevD.99.086016](#).
- [236] R. Auzzi, S. Baiguera, A. Mitra, G. Nardelli, N. Zenoni, Subsystem complexity in warped AdS, *JHEP* 09 (2019) 114. [arXiv:1906.09345](#), [doi:10.1007/JHEP09\(2019\)114](#).
- [237] O. Ben-Ami, D. Carmi, On Volumes of Subregions in Holography and Complexity, *JHEP* 11 (2016) 129. [arXiv:1609.02514](#), [doi:10.1007/JHEP11\(2016\)129](#).
- [238] R. Abt, J. Erdmenger, H. Hinrichsen, C. M. Melby-Thompson, R. Meyer, C. Northe, I. A. Reyes, Topological Complexity in AdS_3/CFT_2 , *Fortsch. Phys.* 66 (6) (2018) 1800034. [arXiv:1710.01327](#), [doi:10.1002/prop.201800034](#).
- [239] P. Roy, T. Sarkar, Note on subregion holographic complexity, *Phys. Rev. D* 96 (2) (2017) 026022. [arXiv:1701.05489](#), [doi:10.1103/PhysRevD.96.026022](#).
- [240] P. Roy, T. Sarkar, Subregion holographic complexity and renormalization group flows, *Phys. Rev. D* 97 (8) (2018) 086018. [arXiv:1708.05313](#), [doi:10.1103/PhysRevD.97.086018](#).
- [241] E. Bakhshaei, A. Mollabashi, A. Shirzad, Holographic Subregion Complexity for Singular Surfaces, *Eur. Phys. J. C* 77 (10) (2017) 665. [arXiv:1703.03469](#), [doi:10.1140/epjc/s10052-017-5247-1](#).

- [242] E. Caceres, M.-L. Xiao, Complexity-action of subregions with corners, JHEP 03 (2019) 062. [arXiv:1809.09356](#), [doi:10.1007/JHEP03\(2019\)062](#).
- [243] R. Abt, J. Erdmenger, M. Gerbershagen, C. M. Melby-Thompson, C. Northe, Holographic Subregion Complexity from Kinematic Space, JHEP 01 (2019) 012. [arXiv:1805.10298](#), [doi:10.1007/JHEP01\(2019\)012](#).
- [244] B. Chen, W.-M. Li, R.-Q. Yang, C.-Y. Zhang, S.-J. Zhang, Holographic subregion complexity under a thermal quench, JHEP 07 (2018) 034. [arXiv:1803.06680](#), [doi:10.1007/JHEP07\(2018\)034](#).
- [245] A. Bhattacharya, K. T. Grosvenor, S. Roy, Entanglement Entropy and Subregion Complexity in Thermal Perturbations around Pure-AdS Spacetime, Phys. Rev. D 100 (12) (2019) 126004. [arXiv:1905.02220](#), [doi:10.1103/PhysRevD.100.126004](#).
- [246] R. Auzzi, S. Baiguera, A. Legramandi, G. Nardelli, P. Roy, N. Zenoni, On subregion action complexity in AdS₃ and in the BTZ black hole, JHEP 01 (2020) 066. [arXiv:1910.00526](#), [doi:10.1007/JHEP01\(2020\)066](#).
- [247] R. Auzzi, G. Nardelli, F. I. Schaposnik Massolo, G. Tallarita, N. Zenoni, On volume subregion complexity in Vaidya spacetime, JHEP 11 (2019) 098. [arXiv:1908.10832](#), [doi:10.1007/JHEP11\(2019\)098](#).
- [248] Y. Sato, Complexity in a moving mirror model, Phys. Rev. D 105 (8) (2022) 086016. [arXiv:2108.04637](#), [doi:10.1103/PhysRevD.105.086016](#).
- [249] S. Chapman, D. Ge, G. Policastro, Holographic Complexity for Defects Distinguishes Action from Volume, JHEP 05 (2019) 049. [arXiv:1811.12549](#), [doi:10.1007/JHEP05\(2019\)049](#).
- [250] P. Braccia, A. L. Cotrone, E. Tonni, Complexity in the presence of a boundary, JHEP 02 (2020) 051. [arXiv:1910.03489](#), [doi:10.1007/JHEP02\(2020\)051](#).
- [251] Y. Sato, K. Watanabe, Does Boundary Distinguish Complexities?, JHEP 11 (2019) 132. [arXiv:1908.11094](#), [doi:10.1007/JHEP11\(2019\)132](#).
- [252] R. Auzzi, S. Baiguera, S. Bonansea, G. Nardelli, K. Toccacelo, Volume complexity for Janus AdS₃ geometries, JHEP 08 (2021) 045. [arXiv:2105.08729](#), [doi:10.1007/JHEP08\(2021\)045](#).
- [253] R. Auzzi, S. Baiguera, S. Bonansea, G. Nardelli, Action complexity in the presence of defects and boundaries, JHEP 02 (2022) 118. [arXiv:2112.03290](#), [doi:10.1007/JHEP02\(2022\)118](#).
- [254] S. Baiguera, S. Bonansea, K. Toccacelo, Volume complexity for the nonsupersymmetric Janus AdS₅ geometry, Phys. Rev. D 104 (8) (2021) 086030. [arXiv:2105.12743](#), [doi:10.1103/PhysRevD.104.086030](#).
- [255] M. Spradlin, A. Strominger, A. Volovich, Les Houches lectures on de Sitter space, in: Les Houches Summer School: Session 76: Euro Summer School on Unity of Fundamental Physics: Gravity, Gauge Theory and Strings, 2001, pp. 423–453. [arXiv:hep-th/0110007](#).

- [256] D. Anninos, De Sitter Musings, *Int. J. Mod. Phys. A* 27 (2012) 1230013. [arXiv:1205.3855](#), [doi:10.1142/S0217751X1230013X](#).
- [257] D. A. Galante, Modave lectures on de Sitter space & holography, *PoS Modave2022* (2023) 003. [arXiv:2306.10141](#), [doi:10.22323/1.435.0003](#).
- [258] G. W. Gibbons, S. W. Hawking, Cosmological Event Horizons, Thermodynamics, and Particle Creation, *Phys. Rev. D* 15 (1977) 2738–2751. [doi:10.1103/PhysRevD.15.2738](#).
- [259] R. Bousso, The Holographic principle for general backgrounds, *Class. Quant. Grav.* 17 (2000) 997–1005. [arXiv:hep-th/9911002](#), [doi:10.1088/0264-9381/17/5/309](#).
- [260] T. Banks, Cosmological breaking of supersymmetry?, *Int. J. Mod. Phys. A* 16 (2001) 910–921. [arXiv:hep-th/0007146](#), [doi:10.1142/S0217751X01003998](#).
- [261] R. Bousso, Positive vacuum energy and the N bound, *JHEP* 11 (2000) 038. [arXiv:hep-th/0010252](#), [doi:10.1088/1126-6708/2000/11/038](#).
- [262] T. Banks, W. Fischler, M theory observables for cosmological space-times (2 2001). [arXiv:hep-th/0102077](#).
- [263] A. Strominger, The dS / CFT correspondence, *JHEP* 10 (2001) 034. [arXiv:hep-th/0106113](#), [doi:10.1088/1126-6708/2001/10/034](#).
- [264] T. Banks, W. Fischler, S. Paban, Recurrent nightmares? Measurement theory in de Sitter space, *JHEP* 12 (2002) 062. [arXiv:hep-th/0210160](#), [doi:10.1088/1126-6708/2002/12/062](#).
- [265] F. Leblond, D. Marolf, R. C. Myers, Tall tales from de Sitter space 1: Renormalization group flows, *JHEP* 06 (2002) 052. [arXiv:hep-th/0202094](#), [doi:10.1088/1126-6708/2002/06/052](#).
- [266] F. Leblond, D. Marolf, R. C. Myers, Tall tales from de Sitter space. 2. Field theory dualities, *JHEP* 01 (2003) 003. [arXiv:hep-th/0211025](#), [doi:10.1088/1126-6708/2003/01/003](#).
- [267] M. K. Parikh, I. Savonije, E. P. Verlinde, Elliptic de Sitter space: dS/Z(2), *Phys. Rev. D* 67 (2003) 064005. [arXiv:hep-th/0209120](#), [doi:10.1103/PhysRevD.67.064005](#).
- [268] L. Dyson, J. Lindesay, L. Susskind, Is there really a de Sitter/CFT duality?, *JHEP* 08 (2002) 045. [arXiv:hep-th/0202163](#), [doi:10.1088/1126-6708/2002/08/045](#).
- [269] L. Dyson, M. Kleban, L. Susskind, Disturbing implications of a cosmological constant, *JHEP* 10 (2002) 011. [arXiv:hep-th/0208013](#), [doi:10.1088/1126-6708/2002/10/011](#).
- [270] M. K. Parikh, E. P. Verlinde, De Sitter holography with a finite number of states, *JHEP* 01 (2005) 054. [arXiv:hep-th/0410227](#), [doi:10.1088/1126-6708/2005/01/054](#).
- [271] T. Banks, Some thoughts on the quantum theory of stable de Sitter space (3 2005). [arXiv:hep-th/0503066](#).

- [272] B. Freivogel, V. E. Hubeny, A. Maloney, R. C. Myers, M. Rangamani, S. Shenker, Inflation in AdS/CFT, JHEP 03 (2006) 007. [arXiv:hep-th/0510046](#), [doi:10.1088/1126-6708/2006/03/007](#).
- [273] T. Banks, B. Fiol, A. Morisse, Towards a quantum theory of de Sitter space, JHEP 12 (2006) 004. [arXiv:hep-th/0609062](#), [doi:10.1088/1126-6708/2006/12/004](#).
- [274] D. A. Lowe, S. Roy, Punctuated eternal inflation via AdS/CFT, Phys. Rev. D 82 (2010) 063508. [arXiv:1004.1402](#), [doi:10.1103/PhysRevD.82.063508](#).
- [275] D. Anninos, S. A. Hartnoll, D. M. Hofman, Static Patch Solipsism: Conformal Symmetry of the de Sitter Worldline, Class. Quant. Grav. 29 (2012) 075002. [arXiv:1109.4942](#), [doi:10.1088/0264-9381/29/7/075002](#).
- [276] S. Fischetti, D. Marolf, A. C. Wall, A paucity of bulk entangling surfaces: AdS wormholes with de Sitter interiors, Class. Quant. Grav. 32 (2015) 065011. [arXiv:1409.6754](#), [doi:10.1088/0264-9381/32/6/065011](#).
- [277] D. Anninos, D. M. Hofman, Infrared Realization of dS_2 in AdS_2 , Class. Quant. Grav. 35 (8) (2018) 085003. [arXiv:1703.04622](#), [doi:10.1088/1361-6382/aab143](#).
- [278] D. Anninos, D. A. Galante, D. M. Hofman, De Sitter horizons & holographic liquids, JHEP 07 (2019) 038. [arXiv:1811.08153](#), [doi:10.1007/JHEP07\(2019\)038](#).
- [279] T. Banks, W. Fischler, The holographic spacetime model of cosmology, Int. J. Mod. Phys. D 27 (14) (2018) 1846005. [arXiv:1806.01749](#), [doi:10.1142/S0218271818460057](#).
- [280] X. Dong, E. Silverstein, G. Torroba, De Sitter Holography and Entanglement Entropy, JHEP 07 (2018) 050. [arXiv:1804.08623](#), [doi:10.1007/JHEP07\(2018\)050](#).
- [281] A. Lewkowycz, J. Liu, E. Silverstein, G. Torroba, $T\bar{T}$ and EE, with implications for (A)dS subregion encodings, JHEP 04 (2020) 152. [arXiv:1909.13808](#), [doi:10.1007/JHEP04\(2020\)152](#).
- [282] T. Banks, W. Fischler, Holographic space-time, Newton's law, and the dynamics of horizons, Adv. Theor. Math. Phys. 27 (1) (2023) 65–86. [arXiv:2003.03637](#), [doi:10.4310/ATMP.2023.v27.n1.a3](#).
- [283] M. Mirbabayi, Uptunneling to de Sitter, JHEP 09 (2020) 070. [arXiv:2003.05460](#), [doi:10.1007/JHEP09\(2020\)070](#).
- [284] D. Anninos, F. Denef, Y. T. A. Law, Z. Sun, Quantum de Sitter horizon entropy from quasi-canonical bulk, edge, sphere and topological string partition functions, JHEP 01 (2022) 088. [arXiv:2009.12464](#), [doi:10.1007/JHEP01\(2022\)088](#).
- [285] L. Susskind, De Sitter Holography: Fluctuations, Anomalous Symmetry, and Wormholes, Universe 7 (12) (2021) 464. [arXiv:2106.03964](#), [doi:10.3390/universe7120464](#).
- [286] L. Susskind, Black Holes Hint towards De Sitter Matrix Theory, Universe 9 (8) (2023) 368. [arXiv:2109.01322](#), [doi:10.3390/universe9080368](#).

- [287] E. Coleman, E. A. Mazenc, V. Shyam, E. Silverstein, R. M. Soni, G. Torroba, S. Yang, De Sitter microstates from $T\bar{T} + \Lambda_2$ and the Hawking-Page transition, JHEP 07 (2022) 140. [arXiv:2110.14670](#), [doi:10.1007/JHEP07\(2022\)140](#).
- [288] L. Susskind, Entanglement and Chaos in De Sitter Space Holography: An SYK Example, JHAP 1 (1) (2021) 1–22. [arXiv:2109.14104](#), [doi:10.22128/jhap.2021.455.1005](#).
- [289] E. Shaghoulian, The central dogma and cosmological horizons, JHEP 01 (2022) 132. [arXiv:2110.13210](#), [doi:10.1007/JHEP01\(2022\)132](#).
- [290] E. Shaghoulian, L. Susskind, Entanglement in De Sitter space, JHEP 08 (2022) 198. [arXiv:2201.03603](#), [doi:10.1007/JHEP08\(2022\)198](#).
- [291] H. Lin, L. Susskind, Infinite Temperature’s Not So Hot (6 2022). [arXiv:2206.01083](#).
- [292] B. Banihashemi, T. Jacobson, A. Svesko, M. Visser, The minus sign in the first law of de Sitter horizons, JHEP 01 (2023) 054. [arXiv:2208.11706](#), [doi:10.1007/JHEP01\(2023\)054](#).
- [293] E. Silverstein, Black hole to cosmic horizon microstates in string/M theory: timelike boundaries and internal averaging, JHEP 05 (2023) 160. [arXiv:2212.00588](#), [doi:10.1007/JHEP05\(2023\)160](#).
- [294] V. Chandrasekaran, R. Longo, G. Penington, E. Witten, An algebra of observables for de Sitter space, JHEP 02 (2023) 082. [arXiv:2206.10780](#), [doi:10.1007/JHEP02\(2023\)082](#).
- [295] E. Witten, A background-independent algebra in quantum gravity, JHEP 03 (2024) 077. [arXiv:2308.03663](#), [doi:10.1007/JHEP03\(2024\)077](#).
- [296] E. Witten, Algebras, regions, and observers, Proc. Symp. Pure Math. 107 (2024) 247–276. [arXiv:2303.02837](#).
- [297] A. A. Rahman, L. Susskind, Comments on a Paper by Narovlansky and Verlinde (12 2023). [arXiv:2312.04097](#).
- [298] V. Narovlansky, H. Verlinde, Double-scaled SYK and de Sitter Holography (10 2023). [arXiv:2310.16994](#).
- [299] G. Batra, G. B. De Luca, E. Silverstein, G. Torroba, S. Yang, Bulk-local dS_3 holography: the matter with $T\bar{T} + \Lambda_2$, JHEP 10 (2024) 072. [arXiv:2403.01040](#), [doi:10.1007/JHEP10\(2024\)072](#).
- [300] H. Verlinde, Double-scaled SYK, Chords and de Sitter Gravity (2 2024). [arXiv:2402.00635](#).
- [301] H. Verlinde, M. Zhang, SYK Correlators from 2D Liouville-de Sitter Gravity (2 2024). [arXiv:2402.02584](#).
- [302] D. Tietto, H. Verlinde, A microscopic model of de Sitter spacetime with an observer (2 2025). [arXiv:2502.03869](#).

- [303] E. Jørstad, R. C. Myers, S.-M. Ruan, Holographic complexity in dS_{d+1} , JHEP 05 (2022) 119. [arXiv:2202.10684](#), [doi:10.1007/JHEP05\(2022\)119](#).
- [304] T. Anegawa, N. Iizuka, S. K. Sake, N. Zenoni, Is action complexity better for de Sitter space in Jackiw-Teitelboim gravity?, JHEP 06 (2023) 213. [arXiv:2303.05025](#), [doi:10.1007/JHEP06\(2023\)213](#).
- [305] R. Auzzi, G. Nardelli, G. P. Ungureanu, N. Zenoni, Volume complexity of dS bubbles, Phys. Rev. D 108 (2) (2023) 026006. [arXiv:2302.03584](#), [doi:10.1103/PhysRevD.108.026006](#).
- [306] S. E. Aguilar-Gutierrez, M. P. Heller, S. Van der Schueren, Complexity equals anything can grow forever in de Sitter space, Phys. Rev. D 110 (6) (2024) 066009. [arXiv:2305.11280](#), [doi:10.1103/PhysRevD.110.066009](#).
- [307] S. Chapman, D. A. Galante, E. D. Kramer, Holographic complexity and de Sitter space, JHEP 02 (2022) 198. [arXiv:2110.05522](#), [doi:10.1007/JHEP02\(2022\)198](#).
- [308] S. Baiguera, R. Berman, S. Chapman, R. C. Myers, The cosmological switchback effect, JHEP 07 (2023) 162. [arXiv:2304.15008](#), [doi:10.1007/JHEP07\(2023\)162](#).
- [309] S. Baiguera, R. Berman, The cosmological switchback effect. Part II, JHEP 08 (2024) 086. [arXiv:2406.04397](#), [doi:10.1007/JHEP08\(2024\)086](#).
- [310] S. Gao, R. M. Wald, Theorems on gravitational time delay and related issues, Class. Quant. Grav. 17 (2000) 4999–5008. [arXiv:gr-qc/0007021](#), [doi:10.1088/0264-9381/17/24/305](#).
- [311] T. Anegawa, N. Iizuka, Shock waves and delay of hyperfast growth in de Sitter complexity, JHEP 08 (2023) 115. [arXiv:2304.14620](#), [doi:10.1007/JHEP08\(2023\)115](#).
- [312] S. E. Aguilar-Gutierrez, C=Anything and the switchback effect in Schwarzschild-de Sitter space, JHEP 03 (2024) 062. [arXiv:2309.05848](#), [doi:10.1007/JHEP03\(2024\)062](#).
- [313] S. S. Gubser, I. R. Klebanov, A. M. Polyakov, Gauge theory correlators from noncritical string theory, Phys. Lett. B 428 (1998) 105–114. [arXiv:hep-th/9802109](#), [doi:10.1016/S0370-2693\(98\)00377-3](#).
- [314] E. Witten, Anti-de Sitter space and holography, Adv. Theor. Math. Phys. 2 (1998) 253–291. [arXiv:hep-th/9802150](#), [doi:10.4310/ATMP.1998.v2.n2.a2](#).
- [315] M. Berkooz, O. Mamroud, A cordial introduction to double scaled SYK, Rept. Prog. Phys. 88 (3) (2025) 036001. [arXiv:2407.09396](#), [doi:10.1088/1361-6633/ada889](#).
- [316] H. W. Lin, The bulk Hilbert space of double scaled SYK, JHEP 11 (2022) 060. [arXiv:2208.07032](#), [doi:10.1007/JHEP11\(2022\)060](#).
- [317] L. Erdős, D. Schröder, Phase Transition in the Density of States of Quantum Spin Glasses, Math. Phys. Anal. Geom. 17 (3-4) (2014) 441–464. [arXiv:1407.1552](#), [doi:10.1007/s11040-014-9164-3](#).

- [318] M. Berkooz, P. Narayan, J. Simon, Chord diagrams, exact correlators in spin glasses and black hole bulk reconstruction, JHEP 08 (2018) 192. [arXiv:1806.04380](#), [doi:10.1007/JHEP08\(2018\)192](#).
- [319] L. V. Iliesiu, A. Levine, H. W. Lin, H. Maxfield, M. Mezei, On the non-perturbative bulk Hilbert space of JT gravity, JHEP 10 (2024) 220. [arXiv:2403.08696](#), [doi:10.1007/JHEP10\(2024\)220](#).
- [320] M. P. Heller, J. Papalini, T. Schuhmann, Krylov spread complexity as holographic complexity beyond JT gravity (12 2024). [arXiv:2412.17785](#).
- [321] A. Blommaert, T. G. Mertens, J. Papalini, The dilaton gravity hologram of double-scaled SYK (4 2024). [arXiv:2404.03535](#).
- [322] S. Collier, L. Eberhardt, M. Zhang, Solving 3d gravity with Virasoro TQFT, SciPost Phys. 15 (4) (2023) 151. [arXiv:2304.13650](#), [doi:10.21468/SciPostPhys.15.4.151](#).
- [323] L. Susskind, Why do Things Fall? (2 2018). [arXiv:1802.01198](#).
- [324] L. Susskind, Complexity and Newton's Laws, Front. in Phys. 8 (2020) 262. [arXiv:1904.12819](#), [doi:10.3389/fphy.2020.00262](#).
- [325] H. W. Lin, L. Susskind, Complexity Geometry and Schwarzian Dynamics, JHEP 01 (2020) 087. [arXiv:1911.02603](#), [doi:10.1007/JHEP01\(2020\)087](#).
- [326] L. Susskind, Y. Zhao, Complexity and Momentum, JHEP 03 (2021) 239. [arXiv:2006.03019](#), [doi:10.1007/JHEP03\(2021\)239](#).
- [327] J. L. F. Barbon, J. Martín-García, M. Sasieta, A Generalized Momentum/Complexity Correspondence, JHEP 04 (2021) 250. [arXiv:2012.02603](#), [doi:10.1007/JHEP04\(2021\)250](#).
- [328] J. L. F. Barbon, J. Martín-García, M. Sasieta, Proof of a Momentum/Complexity Correspondence, Phys. Rev. D 102 (10) (2020) 101901. [arXiv:2006.06607](#), [doi:10.1103/PhysRevD.102.101901](#).
- [329] J. L. F. Barbón, J. Martín-García, M. Sasieta, Momentum/Complexity Duality and the Black Hole Interior, JHEP 07 (2020) 169. [arXiv:1912.05996](#), [doi:10.1007/JHEP07\(2020\)169](#).
- [330] H. W. Lin, J. Maldacena, Y. Zhao, Symmetries Near the Horizon, JHEP 08 (2019) 049. [arXiv:1904.12820](#), [doi:10.1007/JHEP08\(2019\)049](#).
- [331] A. R. Brown, H. Gharibyan, A. Streicher, L. Susskind, L. Thorlacius, Y. Zhao, Falling Toward Charged Black Holes, Phys. Rev. D 98 (12) (2018) 126016. [arXiv:1804.04156](#), [doi:10.1103/PhysRevD.98.126016](#).
- [332] P. Caputa, B. Chen, R. W. McDonald, J. Simón, B. Strittmatter, Spread Complexity Rate as Proper Momentum (10 2024). [arXiv:2410.23334](#).
- [333] Z.-Y. Fan, Momentum-Krylov complexity correspondence (11 2024). [arXiv:2411.04492](#).

- [334] P.-Z. He, Revisit the relationship between spread complexity rate and radial momentum (11 2024). [arXiv:2411.19172](#).
- [335] M. Dodelson, Black holes from chaos (1 2025). [arXiv:2501.06170](#).
- [336] T. Takayanagi, Holographic Dual of BCFT, *Phys. Rev. Lett.* 107 (2011) 101602. [arXiv:1105.5165](#), [doi:10.1103/PhysRevLett.107.101602](#).
- [337] S. Ryu, T. Takayanagi, Holographic derivation of entanglement entropy from AdS/CFT, *Phys. Rev. Lett.* 96 (2006) 181602. [arXiv:hep-th/0603001](#), [doi:10.1103/PhysRevLett.96.181602](#).
- [338] A. Belin, A. Lewkowycz, G. Sárosi, The boundary dual of the bulk symplectic form, *Phys. Lett. B* 789 (2019) 71–75. [arXiv:1806.10144](#), [doi:10.1016/j.physletb.2018.10.071](#).
- [339] M. Flory, WdW-patches in AdS₃ and complexity change under conformal transformations II, *JHEP* 05 (2019) 086. [arXiv:1902.06499](#), [doi:10.1007/JHEP05\(2019\)086](#).
- [340] K. Skenderis, B. C. van Rees, Real-time gauge/gravity duality, *Phys. Rev. Lett.* 101 (2008) 081601. [arXiv:0805.0150](#), [doi:10.1103/PhysRevLett.101.081601](#).
- [341] K. Skenderis, B. C. van Rees, Real-time gauge/gravity duality: Prescription, Renormalization and Examples, *JHEP* 05 (2009) 085. [arXiv:0812.2909](#), [doi:10.1088/1126-6708/2009/05/085](#).
- [342] B. Czech, L. Lamprou, S. McCandlish, J. Sully, Integral Geometry and Holography, *JHEP* 10 (2015) 175. [arXiv:1505.05515](#), [doi:10.1007/JHEP10\(2015\)175](#).
- [343] B. Czech, L. Lamprou, S. McCandlish, B. Mosk, J. Sully, A Stereoscopic Look into the Bulk, *JHEP* 07 (2016) 129. [arXiv:1604.03110](#), [doi:10.1007/JHEP07\(2016\)129](#).
- [344] J. de Boer, F. M. Haehl, M. P. Heller, R. C. Myers, Entanglement, holography and causal diamonds, *JHEP* 08 (2016) 162. [arXiv:1606.03307](#), [doi:10.1007/JHEP08\(2016\)162](#).
- [345] A. Bouland, B. Fefferman, U. Vazirani, Computational pseudorandomness, the wormhole growth paradox, and constraints on the AdS/CFT duality (10 2019). [arXiv:1910.14646](#).
- [346] Z. Ji, Y.-K. Liu, F. Song, Pseudorandom quantum states (2018). [doi:10.1007/978-3-319-96878-0_5](#).
- [347] F. Ma, H.-Y. Huang, How to Construct Random Unitaries (10 2024). [arXiv:2410.10116](#).
- [348] C. Akers, A. Bouland, L. Chen, T. Kohler, T. Metger, U. Vazirani, Holographic pseudoentanglement and the complexity of the AdS/CFT dictionary (11 2024). [arXiv:2411.04978](#).
- [349] N. Bao, S. Nezami, H. Ooguri, B. Stoica, J. Sully, M. Walter, The Holographic Entropy Cone, *JHEP* 09 (2015) 130. [arXiv:1505.07839](#), [doi:10.1007/JHEP09\(2015\)130](#).
- [350] A. Hamilton, D. N. Kabat, G. Lifschytz, D. A. Lowe, Local bulk operators in AdS/CFT: A Boundary view of horizons and locality, *Phys. Rev. D* 73 (2006) 086003. [arXiv:hep-th/0506118](#), [doi:10.1103/PhysRevD.73.086003](#).

- [351] A. Hamilton, D. N. Kabat, G. Lifschytz, D. A. Lowe, Holographic representation of local bulk operators, *Phys. Rev. D* 74 (2006) 066009. [arXiv:hep-th/0606141](#), [doi:10.1103/PhysRevD.74.066009](#).
- [352] A. Hamilton, D. N. Kabat, G. Lifschytz, D. A. Lowe, Local bulk operators in AdS/CFT: A Holographic description of the black hole interior, *Phys. Rev. D* 75 (2007) 106001. [arXiv:hep-th/0612053](#), [doi:10.1103/PhysRevD.75.106001](#).
- [353] A. Hamilton, D. N. Kabat, G. Lifschytz, D. A. Lowe, Local bulk operators in AdS/CFT and the fate of the BTZ singularity, *AMS/IP Stud. Adv. Math.* 44 (2008) 85–100. [arXiv:0710.4334](#).
- [354] D. Kabat, G. Lifschytz, D. A. Lowe, Constructing local bulk observables in interacting AdS/CFT, *Phys. Rev. D* 83 (2011) 106009. [arXiv:1102.2910](#), [doi:10.1103/PhysRevD.83.106009](#).
- [355] S. Aaronson, A. Bouland, B. Fefferman, S. Ghosh, U. Vazirani, C. Zhang, Z. Zhou, Quantum Pseudoentanglement, *Leibniz Int. Proc. Inf.* 287 (2024) 2:1–2:21. [arXiv:2211.00747](#), [doi:10.4230/LIPIcs.ITCS.2024.2](#).
- [356] A. Gheorghiu, M. J. Hoban, On estimating the entropy of shallow circuit outputs, arXiv preprint [arXiv:2002.12814](#).
- [357] T. Schuster, J. Haferkamp, H.-Y. Huang, Random unitaries in extremely low depth (7 2024). [arXiv:2407.07754](#).
- [358] L. Susskind, Horizons protect church-turing, arXiv preprint [arXiv:2003.01807](#).
- [359] A. R. Brown, H. Gharibyan, G. Penington, L. Susskind, The Python’s Lunch: geometric obstructions to decoding Hawking radiation, *JHEP* 08 (2020) 121. [arXiv:1912.00228](#), [doi:10.1007/JHEP08\(2020\)121](#).
- [360] N. Engelhardt, G. Penington, A. Shahbazi-Moghaddam, Finding pythons in unexpected places, *Class. Quant. Grav.* 39 (9) (2022) 094002. [arXiv:2105.09316](#), [doi:10.1088/1361-6382/ac3e75](#).
- [361] G. Vidal, Class of Quantum Many-Body States That Can Be Efficiently Simulated, *Phys. Rev. Lett.* 101 (2008) 110501. [arXiv:quant-ph/0610099](#), [doi:10.1103/PhysRevLett.101.110501](#).
- [362] A. Bhattacharyya, P. Caputa, S. R. Das, N. Kundu, M. Miyaji, T. Takayanagi, Path-Integral Complexity for Perturbed CFTs, *JHEP* 07 (2018) 086. [arXiv:1804.01999](#), [doi:10.1007/JHEP07\(2018\)086](#).
- [363] P. Caputa, I. MacCormack, Geometry and Complexity of Path Integrals in Inhomogeneous CFTs, *JHEP* 01 (2021) 027. [arXiv:2004.04698](#), [doi:10.1007/JHEP01\(2021\)027](#).
- [364] B. Czech, Einstein Equations from Varying Complexity, *Phys. Rev. Lett.* 120 (3) (2018) 031601. [arXiv:1706.00965](#), [doi:10.1103/PhysRevLett.120.031601](#).

- [365] A. Milsted, G. Vidal, Tensor networks as path integral geometry (7 2018). [arXiv:1807.02501](#).
- [366] A. Milsted, G. Vidal, Geometric interpretation of the multi-scale entanglement renormalization ansatz (12 2018). [arXiv:1812.00529](#).
- [367] H. A. Camargo, M. P. Heller, R. Jefferson, J. Knaute, Path integral optimization as circuit complexity, Phys. Rev. Lett. 123 (1) (2019) 011601. [arXiv:1904.02713](#), [doi:10.1103/PhysRevLett.123.011601](#).
- [368] J. Boruch, P. Caputa, T. Takayanagi, Path-Integral Optimization from Hartle-Hawking Wave Function, Phys. Rev. D 103 (4) (2021) 046017. [arXiv:2011.08188](#), [doi:10.1103/PhysRevD.103.046017](#).
- [369] J. Boruch, P. Caputa, D. Ge, T. Takayanagi, Holographic path-integral optimization, JHEP 07 (2021) 016. [arXiv:2104.00010](#), [doi:10.1007/JHEP07\(2021\)016](#).
- [370] P. Caputa, J. Kruthoff, O. Parrikar, Building Tensor Networks for Holographic States, JHEP 05 (2021) 009. [arXiv:2012.05247](#), [doi:10.1007/JHEP05\(2021\)009](#).
- [371] G. Araujo-Regado, R. Khan, A. C. Wall, Cauchy slice holography: a new AdS/CFT dictionary, JHEP 03 (2023) 026. [arXiv:2204.00591](#), [doi:10.1007/JHEP03\(2023\)026](#).
- [372] L. McGough, M. Mezei, H. Verlinde, Moving the CFT into the bulk with $T\bar{T}$, JHEP 04 (2018) 010. [arXiv:1611.03470](#), [doi:10.1007/JHEP04\(2018\)010](#).
- [373] L. Li, K. Bu, D. Enshan Koh, A. Jaffe, S. Lloyd, Wasserstein Complexity of Quantum Circuits, arXiv e-prints (2022) arXiv:2208.06306 [arXiv:2208.06306](#), [doi:10.48550/arXiv.2208.06306](#).
- [374] T. Haug, K. Bharti, M. S. Kim, Capacity and Quantum Geometry of Parametrized Quantum Circuits, PRX Quantum 2 (4) (2021) 040309. [arXiv:2102.01659](#), [doi:10.1103/PRXQuantum.2.040309](#).
- [375] T. Haug, M. S. Kim, Generalization of quantum machine learning models using quantum fisher information metric, Phys. Rev. Lett. 133 (2024) 050603. [doi:10.1103/PhysRevLett.133.050603](#).
- [376] N. Yunger Halpern, N. B. T. Kothakonda, J. Haferkamp, A. Munson, J. Eisert, P. Faist, Resource theory of quantum uncomplexity, Phys. Rev. A 106 (2022) 062417. [doi:10.1103/PhysRevA.106.062417](#).
- [377] A. Munson, N. B. T. Kothakonda, J. Haferkamp, N. Yunger Halpern, J. Eisert, P. Faist, Complexity-constrained quantum thermodynamics, PRX Quantum 6 (2025) 010346. [doi:10.1103/PRXQuantum.6.010346](#).
- [378] F. G. S. L. Brandão, W. Chemissany, N. Hunter-Jones, R. Kueng, J. Preskill, Models of Quantum Complexity Growth, PRX Quantum 2 (3) (2021) 030316. [arXiv:1912.04297](#), [doi:10.1103/PRXQuantum.2.030316](#).

- [379] J. Håstad, R. Impagliazzo, L. A. Levin, M. Luby, A pseudorandom generator from any one-way function, *SIAM Journal on Computing* 28 (4) (1999) 1364–1396. [doi:10.1137/S0097539793244708](https://doi.org/10.1137/S0097539793244708).
- [380] Y.-H. Chen, K.-M. Chung, C.-Y. Lai, S. P. Vadhan, X. Wu, Computational notions of quantum min-entropy (2017). [arXiv:1704.07309](https://arxiv.org/abs/1704.07309).
- [381] L. Landau, G. Rumer, *Phys. z sowjetunion*, 11, TSS 26 (1937) 545.
- [382] V. L. Ginzburg, L. D. Landau, On the Theory of superconductivity, *Zh. Eksp. Teor. Fiz.* 20 (1950) 1064–1082. [doi:10.1016/b978-0-08-010586-4.50078-x](https://doi.org/10.1016/b978-0-08-010586-4.50078-x).
- [383] X.-G. Wen, Topological order: from long-range entangled quantum matter to an unification of light and electrons, *ISRN Cond. Matt. Phys.* 2013 (2013) 198710. [arXiv:1210.1281](https://arxiv.org/abs/1210.1281), [doi:10.1155/2013/198710](https://doi.org/10.1155/2013/198710).
- [384] X.-G. Wen, Colloquium: Zoo of quantum-topological phases of matter, *Rev. Mod. Phys.* 89 (2017) 041004. [doi:10.1103/RevModPhys.89.041004](https://doi.org/10.1103/RevModPhys.89.041004).
- [385] X. Chen, Z. C. Gu, X. G. Wen, Local unitary transformation, long-range quantum entanglement, wave function renormalization, and topological order, *Phys. Rev. B* 82 (2010) 155138. [arXiv:1004.3835](https://arxiv.org/abs/1004.3835), [doi:10.1103/PhysRevB.82.155138](https://doi.org/10.1103/PhysRevB.82.155138).
- [386] W. van Dam, P. Hayden, Universal entanglement transformations without communication, *Phys. Rev. A* 67 (2003) 060302. [doi:10.1103/PhysRevA.67.060302](https://doi.org/10.1103/PhysRevA.67.060302).
- [387] L. van Luijk, A. Stottmeister, R. F. Werner, H. Wilming, Embezzling entanglement from quantum fields (1 2024). [arXiv:2401.07292](https://arxiv.org/abs/2401.07292).
- [388] L. van Luijk, A. Stottmeister, R. F. Werner, H. Wilming, Embezzlement of entanglement, quantum fields, and the classification of von Neumann algebras (1 2024). [arXiv:2401.07299](https://arxiv.org/abs/2401.07299).
- [389] T. Schwartzman, The complexity of entanglement embezzlement (10 2024). [arXiv:2410.19051](https://arxiv.org/abs/2410.19051).
- [390] A. Anshu, T. Metger, Concentration bounds for quantum states and limitations on the QAOA from polynomial approximations, *Quantum* 7 (2023) 999. [arXiv:2209.02715](https://arxiv.org/abs/2209.02715), [doi:10.22331/q-2023-05-11-999](https://doi.org/10.22331/q-2023-05-11-999).
- [391] M. H. Freedman, M. B. Hastings, Quantum Systems on Non- k -Hyperfiniteness Complexes: A Generalization of Classical Statistical Mechanics on Expander Graphs (1 2013). [arXiv:1301.1363](https://arxiv.org/abs/1301.1363).
- [392] A. Anshu, N. P. Breuckmann, C. Nirkhe, NLTS Hamiltonians from Good Quantum Codes (6 2022). [arXiv:2206.13228](https://arxiv.org/abs/2206.13228), [doi:10.1145/3564246.3585114](https://doi.org/10.1145/3564246.3585114).
- [393] G. Penington, Entanglement Wedge Reconstruction and the Information Paradox, *JHEP* 09 (2020) 002. [arXiv:1905.08255](https://arxiv.org/abs/1905.08255), [doi:10.1007/JHEP09\(2020\)002](https://doi.org/10.1007/JHEP09(2020)002).

- [394] A. Almheiri, N. Engelhardt, D. Marolf, H. Maxfield, The entropy of bulk quantum fields and the entanglement wedge of an evaporating black hole, *JHEP* 12 (2019) 063. [arXiv:1905.08762](#), [doi:10.1007/JHEP12\(2019\)063](#).
- [395] A. Almheiri, R. Mahajan, J. Maldacena, Y. Zhao, The Page curve of Hawking radiation from semiclassical geometry, *JHEP* 03 (2020) 149. [arXiv:1908.10996](#), [doi:10.1007/JHEP03\(2020\)149](#).
- [396] A. Almheiri, T. Hartman, J. Maldacena, E. Shaghoulian, A. Tajdini, The entropy of Hawking radiation, *Rev. Mod. Phys.* 93 (3) (2021) 035002. [arXiv:2006.06872](#), [doi:10.1103/RevModPhys.93.035002](#).
- [397] S. E. Aguilar-Gutierrez, S. Baiguera, N. Zenoni, Holographic complexity of the extended Schwarzschild-de Sitter space, *JHEP* 05 (2024) 201. [arXiv:2402.01357](#), [doi:10.1007/JHEP05\(2024\)201](#).
- [398] S. E. Aguilar-Gutierrez, Towards complexity in de Sitter space from the doubled-scaled Sachdev-Ye-Kitaev model, *JHEP* 10 (2024) 107. [arXiv:2403.13186](#), [doi:10.1007/JHEP10\(2024\)107](#).
- [399] A. Bhattacharyya, T. Hanif, S. S. Haque, M. K. Rahman, Complexity for an open quantum system, *Phys. Rev. D* 105 (4) (2022) 046011. [arXiv:2112.03955](#), [doi:10.1103/PhysRevD.105.046011](#).
- [400] A. Bhattacharyya, T. Hanif, S. S. Haque, A. Paul, Decoherence, entanglement negativity, and circuit complexity for an open quantum system, *Phys. Rev. D* 107 (10) (2023) 106007. [arXiv:2210.09268](#), [doi:10.1103/PhysRevD.107.106007](#).
- [401] A. Bhattacharya, P. Nandy, P. P. Nath, H. Sahu, Operator growth and Krylov construction in dissipative open quantum systems, *JHEP* 12 (2022) 081. [arXiv:2207.05347](#), [doi:10.1007/JHEP12\(2022\)081](#).
- [402] C. Liu, H. Tang, H. Zhai, Krylov complexity in open quantum systems, *Phys. Rev. Res.* 5 (3) (2023) 033085. [arXiv:2207.13603](#), [doi:10.1103/PhysRevResearch.5.033085](#).
- [403] B. Bhattacharjee, X. Cao, P. Nandy, T. Pathak, Operator growth in open quantum systems: lessons from the dissipative SYK, *JHEP* 03 (2023) 054. [arXiv:2212.06180](#), [doi:10.1007/JHEP03\(2023\)054](#).
- [404] N. S. Srivatsa, C. von Keyserlingk, Operator growth hypothesis in open quantum systems, *Phys. Rev. B* 109 (12) (2024) 125149. [arXiv:2310.15376](#), [doi:10.1103/PhysRevB.109.125149](#).
- [405] A. Bhattacharyya, S. Brahma, S. S. Haque, J. S. Lund, A. Paul, The early universe as an open quantum system: complexity and decoherence, *JHEP* 05 (2024) 058. [arXiv:2401.12134](#), [doi:10.1007/JHEP05\(2024\)058](#).
- [406] S. Aaronson, G. Kuperberg, Quantum versus classical proofs and advice (2020). [arXiv:quant-ph/0604056](#).

- [407] S. Aaronson, $P \stackrel{?}{=} NP$ (07 2016). [doi:10.1007/978-3-319-32162-2_1](https://doi.org/10.1007/978-3-319-32162-2_1).
- [408] D. Aharonov, T. Naveh, Quantum NP - A Survey (10 2002). [arXiv:quant-ph/0210077](https://arxiv.org/abs/quant-ph/0210077).
- [409] B. Fefferman, S. Kimmel, Quantum vs classical proofs and subset verification (2018). [arXiv:1510.06750](https://arxiv.org/abs/1510.06750).
- [410] A. Natarajan, C. Nirkhe, A distribution testing oracle separation between QMA and QCMA, Quantum 8 (2024) 1377. [arXiv:2210.15380](https://arxiv.org/abs/2210.15380), [doi:10.22331/q-2024-06-17-1377](https://doi.org/10.22331/q-2024-06-17-1377).
- [411] X. Li, Q. Liu, A. Pelecanos, T. Yamakawa, Classical vs Quantum Advice and Proofs Under Classically-Accessible Oracle, Leibniz Int. Proc. Inf. 287 (2024) 72:1–72:19. [arXiv:2303.04298](https://arxiv.org/abs/2303.04298), [doi:10.4230/LIPIcs.ITCS.2024.72](https://doi.org/10.4230/LIPIcs.ITCS.2024.72).
- [412] Q. Liu, Non-uniformity and quantum advice in the quantum random oracle model., Lect. Notes Comput. Sci. 14004 (2023) 117. [arXiv:2210.06693](https://arxiv.org/abs/2210.06693), [doi:10.1007/978-3-031-30545-0_5](https://doi.org/10.1007/978-3-031-30545-0_5).
- [413] J. Liu, S. Mutreja, H. Yuen, QMA vs. QCMA and Pseudorandomness (11 2024). [arXiv:2411.14416](https://arxiv.org/abs/2411.14416).
- [414] M. Zhandry, Toward Separating QMA from QCMA with a Classical Oracle (11 2024). [arXiv:2411.01718](https://arxiv.org/abs/2411.01718).
- [415] O. Parzanchevski, P. Sarnak, Super-golden-gates for $pu(2)$, Advances in Mathematics 327 (2018) 869–901, special volume honoring David Kazhdan. [doi:https://doi.org/10.1016/j.aim.2017.06.022](https://doi.org/10.1016/j.aim.2017.06.022).
- [416] P. Sarnak, Letter to Aaronson and Pollington on the Solvay-Kitaev theorem and golden gates, 2015, URL: <http://publications.ias.edu/sarnak/paper/2637>.
- [417] S. Evra, O. Parzanchevski, Ramanujan complexes and golden gates in $pu(3)$, Geometric and Functional Analysis 32 (2) (2022) 193–235. [doi:10.1007/s00039-022-00593-9](https://doi.org/10.1007/s00039-022-00593-9).